# SENSORY ADAPTATION IN HAIR CELLS OF THE BULLFROG'S SACCULUS

Thesis by

Ruth Anne Eatock

In Partial Fulfillment of the Requirements

for the Degree of

Doctor of Philosophy

California Institute of Technology

Pasadena, California

1984

(Submitted June 13, 1983)

**Acknowledgements**

I would like to thank the members of my thesis committee: Jim Hudspeth, Mary Kennedy, Mark Konishi, Jerry Pine and David Van Essen, and two former members, Howard Berg and Jeremy Brockes, for the time and effort they have spent in my behalf. I am also grateful to Dr. Gordon Ross, and the Natural Sciences and Engineering Research Council of Canada, for their generous financial support. The research was funded by NIH research grant NS13154, and the Weigle Memorial Fund helped defray the costs of the thesis preparation.

I thank my advisor, Jim Hudspeth, for introducing me to exciting new experiments, and for sharing some of his exceptional expertise with me. I hope that in the future I will find that I have acquired some of his courage in approaching new research problems. I thank Jim, David Van Essen and Jeremy Brockes for teaching excellent and inspiring courses. I owe a great deal to David Corey for the generous and enthusiastic help and training he gave me during my first two years here. David and Jim made the original observations of hair cell adaptation, and suggested the project to me.

A number of people have helped me with the technical side of my thesis. I thank John Maunsell for setting up the local computer, without which I wouldn't be finishing even now, and for many helpful discussions. I am also indebted to John, and to Andy Moiseff, for writing averaging programs that I used extensively. John Power patiently developed and reworked to my capricious specifications an essential piece of equipment. Mike Walsh also has been very helpful. I am grateful to Tom Holton for expert technical help. I would like to thank Nancy Gill and Bill Lease, two people who have done so many big

and little things to make my life easier that I've lost track. I thank Candi Hochenedel, who has always been extraordinarily helpful, and Caren Oto for typing the thesis.

Richard Jacobs has helped me in my thesis work in innumerable ways, generously giving of his exceptional abilities. My fellow graduate student, Rich Lewis, has been an invaluable colleague and friend. I have benefitted greatly from his thoughtful attention to my scientific questions, and cannot adequately express my gratitude for his consistent support. I must also thank Rich, and Larry Katz, for their efforts to keep me laughing.

I have relied countless times on the generosity and affection of Carol and Sandy Shotwell, and have learned a great deal from both. I thank Herman Gordon for helpful discussions, critical reading of portions of this thesis, and a valuable friendship. Special thanks are due Isabel and David Van Essen for welcoming me into their wonderful home on so many occasions.

Finally, I thank Lori Jane, Brian, Mom and Dad for always being there when I call.

## Abstract

Hair cells in the bullfrog's sacculus, a vestibular organ sensitive to linear acceleration, show sensory adaptation: the response to a constant stimulus peaks near the stimulus onset, then decays. This has been studied in two different preparations. In an excised *in vitro* preparation of the saccular sensory epithelium, intracellular responses of hair cells to step deflections of their hair bundles were recorded. The second set of experiments was conducted *in vivo* using steps of vertical linear acceleration as stimuli. The hair cell response was recorded extracellularly in the form of the saccular microphonic potential. Both the intracellular response to direct hair bundle deflection and the extracellular response to acceleration adapted to a steady-state value within the first 100 ms following the step onset. In both cases, the response decline was largely due to a shift in the operating range of the cells in the direction of the constant stimulus. This shift occurred without significant change in dynamic range or in sensitivity within the operating range. Thus the hair cells appear to respond to static stimuli by resetting the bias point of the operating range in the direction of the stimulus.

The response of primary saccular neurons to acceleration steps also showed pronounced sensory adaptation. Comparison of the afferent activity and saccular microphonic potential suggests that adaptation of afferent responses to acceleration steps may be due largely to the adaptive operating range shift in the hair cell responses.

The adaptation of saccular neurons to acceleration steps may be explained by the following simple model. The acceleration step causes displacement of the saccular otolith and deflection of the underlying

hair bundles. The hair cells respond initially to the displacement, then adapt (as observed *in vitro*), and this information is faithfully translated postsynaptically into afferent spike rate. However, the possibility exists that the *in vitro* and *in vivo* adaptive shifts in operating range are not the same process. *In vivo*, one cannot distinguish an operating range shift within the hair cells from one due to mechanical adaptation of the stimulus to the hair bundles.

## Table of Contents

## Introduction

Sensory adaptation is a reversible decrease with time in a sensory response to a constant stimulus. The response may be of an entire sensory pathway or of any element within it, and the mechanisms by which sensory adaptation occurs are diverse. Despite their diversity, these processes represent the same fundamental and successful strategy for interacting with the environment, that of attending to changes. This thesis describes a kind of adaptation that occurs in the sensory cells--hair cells--of a vertebrate vestibular organ and attempts to relate this adaptation to the function of the organ. Since all inner ear organs have hair cells and many primary neurons innervating inner ear organs show prominent sensory adaptation, the localization of a sensory adaptation process within hair cells has potentially broad significance for the senses of the inner ear.

Inner ear organs fall into three functional classes: detectors of sound, linear acceleration, and angular acceleration, called, respectively, auditory organs, otolith organs, and semicircular canals. The otolith organs comprise the sacculus, utriculus and in some species, lagena. The present study investigates hair cells in the sacculus of the bullfrog. Otolith organs in different species are sensitive to linear accelerations ranging in frequency from 0 to several hundred hertz[1]. Normally, static stimuli are due to gravity, although experimentally they may be provided by constant centrifugal forces or forced paraboloid displacement of the substrate. Dynamic stimuli--changes in linear acceleration--ordinarily arise through the animal's own motion or

[1]The teleost sacculus is exceptional; morphologically it is an otolith organ, but it is sensitive to sounds in the frequency range 0.1-1 kHz as well as to vibratory stimuli below 100 Hz (Fay, 1978).

substrate vibrations. The amount of overlap in the frequency ranges subserved by the different otolith organs within an animal varies among species. In mammals which do not possess a lagena, the sacculus and utriculus appear to detect similar stimuli but in different planes (Fernandez and Goldberg, 1976a, b, and c). In frogs, sensitivity to static and very low-frequency linear accelerations (<1 Hz) derives from the utriculus and the lagena, while the sacculus detects linear accelerations over an approximate range of 1-250 Hz (Lewis et al., 1982, and personal observations).

An otolith organ is tuned in three-dimensional space as well as in the frequency domain, such that it is most sensitive to linear accelerations directed parallel to the plane of the sensory epithelium and virtually insensitive to accelerations orthogonal to the epithelium (Fernandez and Goldberg, 1976b). Because of this spatial selectivity, otolith afferents sensitive to static acceleration levels convey information about head position: as the head is tilted, the angle of the gravity vector with respect to the sensory epithelium changes, and the gravitational force sensed by the otolith organ changes accordingly. This information is essential for postural balance. For example, a unilateral ablation of the utriculus in a frog causes severe postural abnormalities, whereas bilateral destruction of the frog's sacculi has no obvious effect on its posture or righting abilities (McNally and Tait, 1925). These effects correlate well with the frequency selectivity of utricular and saccular afferents mentioned above.

Electrophysiological studies of the response behavior of primary neurons innervating the inner ear indicate that a large proportion of

them show some degree of adaptation to constant stimuli. Auditory neurons adapt during tone bursts (e.g., Furukawa and Matsuura, 1978; Smith, 1979; Megela and Capranica, 1981); semicircular canal afferents adapt to constant angular acceleration (e.g., Goldberg and Fernandez, 1971; Precht et al., 1971; Landolt and Correia, 1980); otolith neurons adapt to constant head position (Macadar et al., 1975; Blanks and Precht, 1976), to constant velocity change in head position (Caston et al., 1977), and to constant centrifugal force (equivalent to linear acceleration) (Fernandez and Goldberg, 1976a). The variety of stimuli listed for otolith afferents raises a possible source of confusion: clearly, if a neuron adapts to constant acceleration, it will adapt even more rapidly to a new level of velocity or to a new position. But it may respond tonically to "jerk", the rate of change of acceleration. In other words, tied up with the concept of sensory adaptation is that of the effective stimulus. Suppose a neuron's response to a change in acceleration decays to zero as the new level is maintained; one could say either that jerk is the effective stimulus for the neuron or that the neuron adapts fully to constant acceleration. In practice, people choose a stimulus and describe the response in terms of that stimulus. For reasons presented below, I chose to study the response of the bullfrog's sacculus to steps of constant acceleration and will describe the results in terms of adaptation to constant acceleration rather than sensitivity to jerk.

Vertebrate hair cells respond to deflection of their hair bundles (Flock, 1971; Hudspeth and Corey, 1977). In inner ear organs, the hair cells are located in specialized epithelia called maculae. The differences in modality among organs are largely determined by the accessory

structures that convey the external stimulus to the hair bundles. Otolith ("ear stone") organs are so-named because the accessory structure is a relatively dense deposit of calcium carbonate which loads the hair cells of the underlying macula. Except in teleosts, the otolith is not a single "stone" but rather a sticky aggregate of small, often crystalline, calcareous deposits called otoconia (Carlstrom, 1963). A schematic cross-section through the bullfrog's sacculus is shown in figure 1. The macula is about 1 mm wide and comprises supporting cells and about 3000 hair cells. The large otoconial mass is coupled to the hair bundles via an intervening otolithic membrane (figure 2). The entire structure shown in figure 1 is housed within a fluid-filled chamber bounded by the membranous labyrinth.

Briefly, otolith organs are thought to work in the following way. When the animal undegoes linear acceleration, the greater density of the otoconial mass relative to the surrounding fluid causes it to lag the motion of the underlying macula (Young, 1969; Correia and Guedry, 1978). Because the hair bundles are coupled to the otoconial mass, they are deflected when it moves relative to the macula. Thus, the mechanical response of the otolith organ transduces linear acceleration into hair bundle deflection.

In this study, the responses of saccular hair cells to constant stimuli were studied in two different kinds of experiments. In the first set of experiments, described in Chapter 1, the sacculus was excised and the otoconial mass and otolithic membrane removed in order to provide direct access to the hair cells. Using a glass probe, I deflected hair bundles individually and recorded the hair cells' responses intracellularly. Thus the constant stimulus of these

Figure 1. Schematic cross-section through the bullfrog's sacculus.

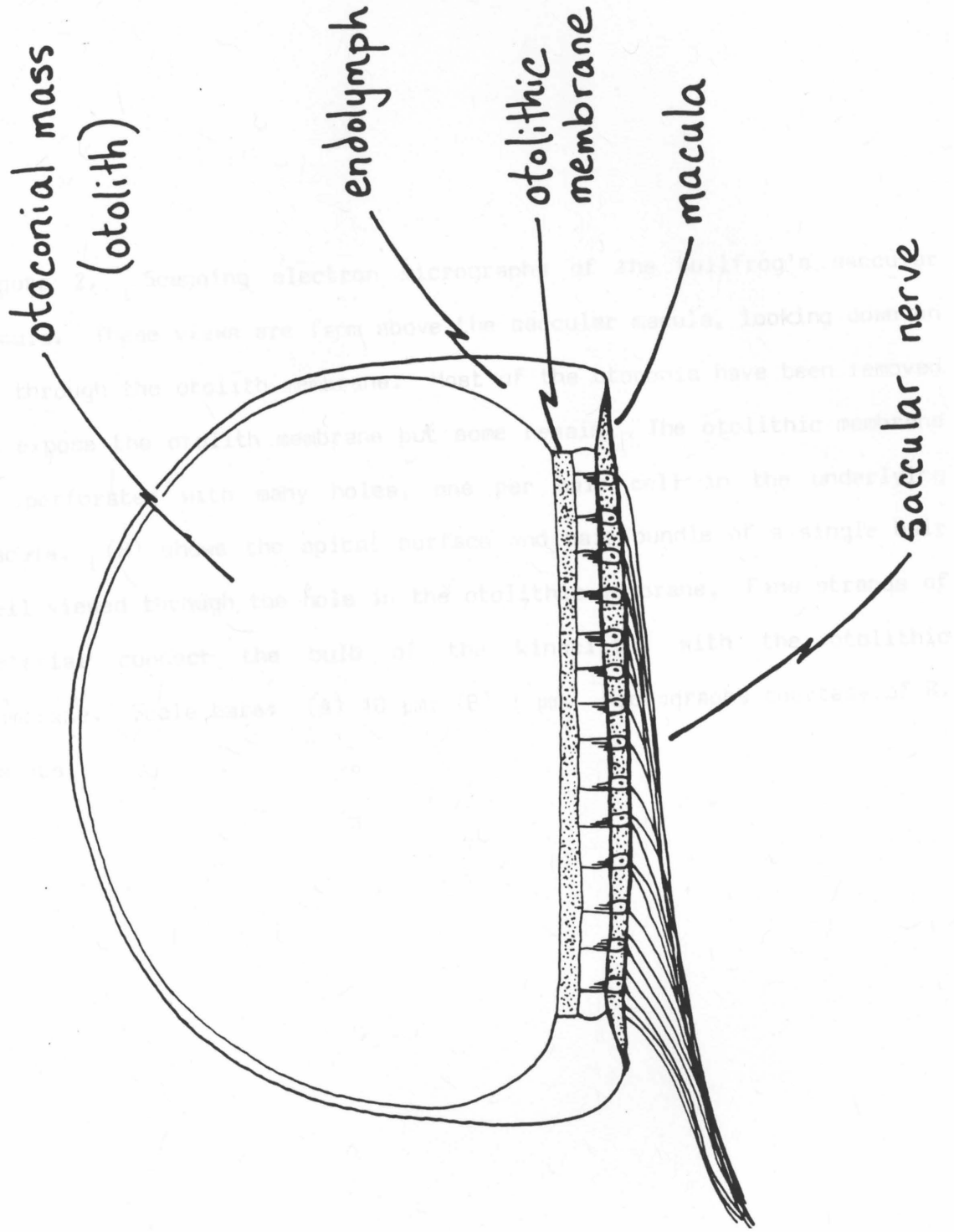
otoconial mass
(otolith)
endolymph
otolithic
membrane
macula
saccular nerve

Figure 2. Scanning electron micrographs of the bullfrog's saccular macula. These views are from above the saccular macula, looking down on it through the otolith membrane. Most of the otoconia have been removed to expose the otolith membrane but some remain. The otolithic membrane is perforated with many holes, one per hair cell in the underlying macula. (B) shows the apical surface and hair bundle of a single hair cell viewed through the hole in the otolithic membrane. Fine strands of material connect the bulb of the kinocilium with the otolithic membrane. Scale bars: (A) 10 µm; (B) 1 µm. Micrographs courtesy of R. Jacobs.

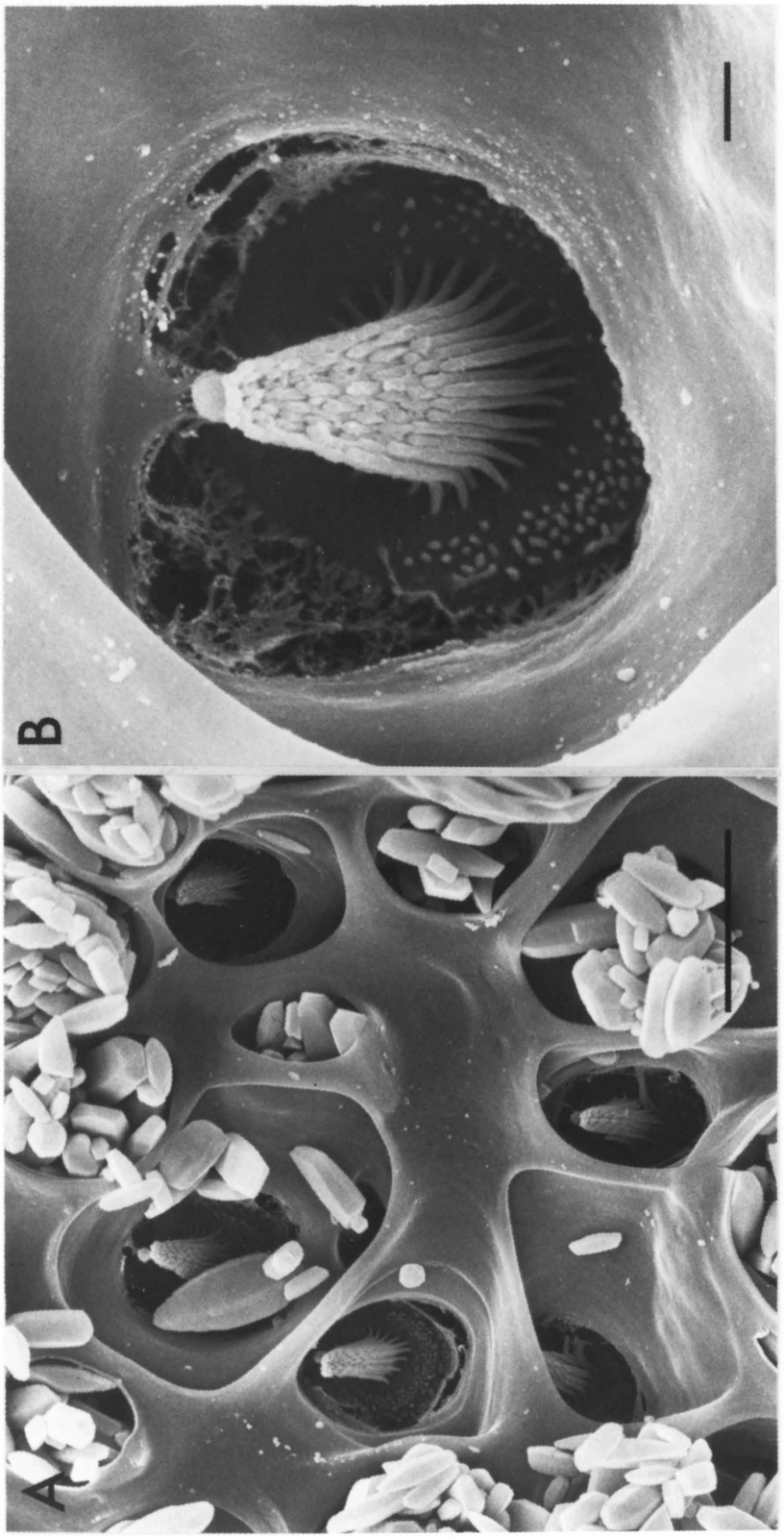
B
A

experiments was a maintained (step) deflection of an individual hair bundle. Chapter 2 describes the second set of experiments in which an acceleration stimulus was delivered to the whole frog, and the response was recorded from a surgically exposed sacculus. Either the extracellular response of the population of saccular hair cells or the activity of individual neurons in the saccular nerve was recorded. In these experiments, the constant stimulus took the form of a step of linear acceleration rather than direct deflection of the hair bundle. In both sets of experiments, the hair cell response showed sensory adaptation to the constant stimulus. The results from the excised, in vitro preparation indicate that adaptation is a property of the sensory cells in this organ. The in vivo results demonstrate sensory adaptation that is by several criteria similar to that described in vitro, and is an important feature of the output of the organ.

Several preliminary reports of these results have appeared (Eatock, Corey and Hudspeth, 1979; Eatock and Hudspeth, 1981; Eatock, 1983).

# CHAPTER 1

## Adaptation in Hair Cell Responses *In Vitro*

### Methods

Young American bullfrogs (*Rana catesbeiana*, 75-150 g) were kept in holding bins at about 20°C. Dissection, stimulation and recording techniques used in the *in vitro* experiments were largely developed by Hudspeth and Corey (Hudspeth and Corey, 1977, 1978; Corey and Hudspeth, 1979, 1980).

Prior to the dissection, the frog was "pithed" by inserting a needle in the spinal cord rostral to the scapulae and extending the needle up into the brain and down the cord. The head minus the lower jaw then was severed at a level about 1 cm caudal of the eardrums. While the sacculi were being removed, the head was kept moist with either (1) "artificial perilymph": 121.8 mM $Na^{++}$, 2 mM $K^{+}$, 1.36 mM $Ca^{++}$, 0.68 mM $Mg^{++}$, 128 mM $Cl^{-}$, 2.8 mM D-glucose, buffered to pH 7.3 with 5 mM Hepes, or (2) "high-$Ca^{++}$ perilymph", similar except that it contained 4 mM $Ca^{++}$ and 0 $Mg^{++}$. The dissections and experiments were done at room temperature, about 22°C.

The sacculus was exposed by cutting away the ventral wall of the otic capsule (figure 3). The membranous labyrinth was freed from the capsule wall and the saccular nerve transected several millimeters from the macula. Then the sacculus was transferred to a dish filled with artificial perilymph or high-$Ca^{++}$ perilymph. Extraneous tissue, including the outer membrane of the perilymphatic chamber surrounding the sacculus, was removed, leaving the structure illustrated schemati-

Figure 3. A ventral view of the bullfrog's sacculus and eighth nerve *in situ*. The otic capsule has been cut open in the horizontal plane to reveal a portion of the inner ear. From its medial to lateral edge, the saccular macula (sensory epithelium) is tilted ventrally and rostrally. The darkened area around the sacculus is the perilymphatic compartment of the inner ear: a fluid-filled chamber surrounding the inner ear organs and bounded by a membrane (the "membranous labyrinth", not shown).

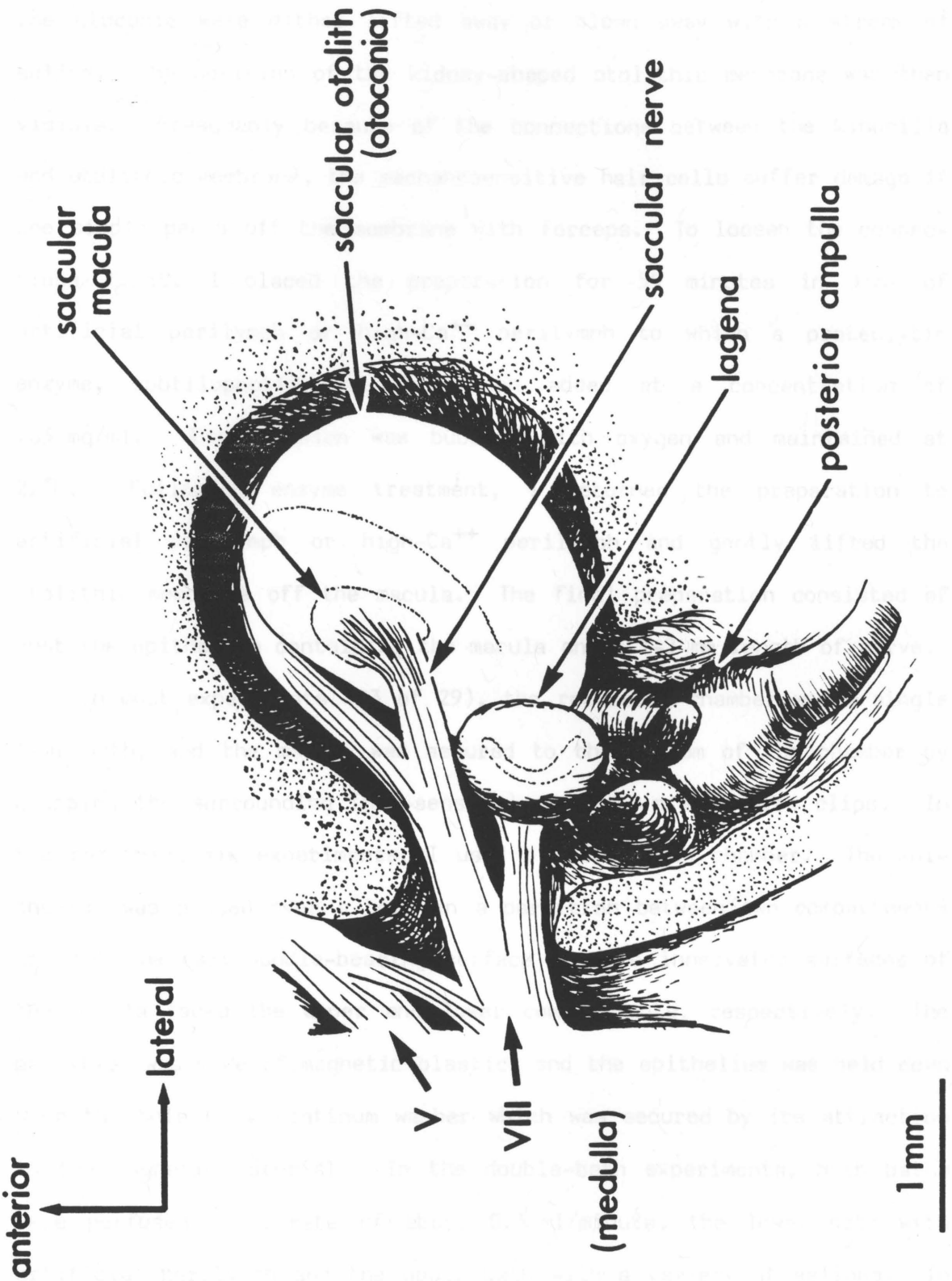
saccular macula
saccular otolith (otoconia)
saccular nerve
lagena
posterior ampulla
anterior
lateral
V
VIII
(medulla)
1 mm

cally in figure 2. The membrane enclosing the otoconia was slit, and the otoconia were either lifted away or blown away with a stream of saline. The position of the kidney-shaped otolithic membrane was then visible. Presumably because of the connections between the kinocilia and otolithic membrane, the mechanosensitive hair cells suffer damage if one simply peels off the membrane with forceps. To loosen the connections first, I placed the preparation for 55 minutes in 3 ml of artificial perilymph or high-$Ca^{++}$ perilymph to which a proteolytic enzyme, subtilopeptidase A, had been added at a concentration of .03 mg/ml. The solution was bubbled with oxygen and maintained at 22°C. Following enzyme treatment, I returned the preparation to artificial perilymph or high-$Ca^{++}$ perilymph and gently lifted the otolithic membrane off the macula. The final preparation consisted of just the epithelium containing the macula and a 1-2 mm length of nerve.

In most experiments (23 of 29), the recording chamber was a single 1-ml bath, and the macula was secured to the bottom of the chamber by clamping the surrounding (non-sensory) epithelium with wire clips. In the remaining six experiments, I used a double-bath chamber. The epithelium was placed over a hole in a partition between two compartments so that the hair-bundle-bearing surface and the innervated surfaces of the macula faced the upper and lower compartments, respectively. The partition was made of magnetic plastic, and the epithelium was held down over the hole by a platinum washer which was secured by its attraction to the magnetic material. In the double-bath experiments, both baths were perfused at a rate of about 0.3 ml/minute, the lower bath with artificial perilymph and the upper bath with a variety of salines. In three of the single-bath experiments, I exchanged the saline at

intervals of several minutes with a pipette. In the remaining 20 single-bath experiments, the chamber was perfused with an artificial saline at 0.3 ml/minute.

The recording chamber was mounted on the stage of a Zeiss WL compound microscope and viewed with Nomarski differential interference constrast optics through a 40x water-immersion lens with a numerical aperture of 0.75. The Nomarski optics allow one to resolve the kinocilia of individual hair bundles. The small working distance of the 40x lens (1.6 mm) necessitated that recording electrodes and probes for manipulating the hair bundles (stimulus probes) be bent near their tips so that the main axis of the electrode or probe could be brought in at a low angle, <30°, relative to the plane of the macula (Hudspeth and Corey, 1978). Microelectrodes were made from glass tubing (1.2 mm outer diameter, 0.9 or 0.6 mm inner diameter, Frederick Haer) containing a thin fiber to allow filling by capillary action. For experiments in which membrane potential was recorded, microelectrodes were pulled on a Brown-Flaming micropipette puller (Model P-77, Sutter Instrument Co.), filled with 3 M KCl, and had tip resistances of 150-300 MΩ. Membrane potential was recorded with a high-impedance preamplifier (W-P Instruments Model 701), then amplified and stored on tape (Hewlett-Packard FM tape recorder, Model 3968A; passband DC-1.25 kHz). To record trans-membrane current, I employed a two-electrode voltage clamp circuit designed by David Corey. The current-injecting and voltage-recording microelectrodes were made as described above, then bevelled by immersing the tips in a swirling solution of alumina powder in saline (5 g/l alumina powder in 120 mM KCl) until their resistances dropped to approximately 90 MΩ.

Stimulus probes were pulled from glass tubing, 1.2 mm in outer diameter, and bent using the same techniques as for microelectrodes. The probe holder and microelectrode holders were mounted on Leitz micromanipulators. Control of probe motion was achieved with an apparatus developed by Corey and Hudspeth (1980). Briefly, the glass probe was attached to a set of piezoelectric bimorph elements, each of which bends when a voltage is applied across it. With a set of three bimorph elements coupled to a mount so as to form a square, one can achieve controlled, small displacements of the stimulus probe in the two dimensions defined by the sides of the bimorph square. Good coupling between probe and hair bundle was achieved by bending the probe in two places near its tip so that the final segment could be inserted between the kinocilium and stereocilia (figure 4). Because the kinocilium is attached to the tallest stereocilia (A. J. Hudspeth, personal communication) and the stereocilia move as a unit, motion of a probe coupled in this way to the bundle causes reliable motion of the hair bundle. Stimulus amplitudes were in the range of ±2 μm, about the rest position of the hair bundle. For these experiments, the plane of the bimorph square was at a low angle (<20°), with respect to the surface of the macula, so that the stimulus probe would deflect the bundle laterally and exert minimal force along its vertical (long) axis. The bimorph square was driven by a step generator designed by David Corey or, for triangle-wave or sinusoidal stimuli, a Tektronix FG 501 function generator.

Probe motion, calibrated with an eyepiece micrometer, was a linear function of electronic input for the stimuli used. During experiments, the electronic driving signal was used as the stimulus monitor. With

Figure 4. The arrangement for recording receptor current from a hair cell. The hair bundle and apical surface of a cell are shown. The tip of a glass stimulus probe is inserted between the kinocilium and the adjacent stereocilia of the hair bundle. The kinociliary bulb at the top of the gently curving stalk that is the cilium proper is attached by fuzzy material to the tallest stereocilia. Thus a probe inserted as shown moves the entire bundle. Stimulation was always along the orientation axis of the bundle (arrows). Shown penetrating the cell's apical membrane behind the hair bundle are the voltage-recording and current-passing electrodes for voltage-clamping the cell membrane. Illustration courtesy of D. P. Corey.

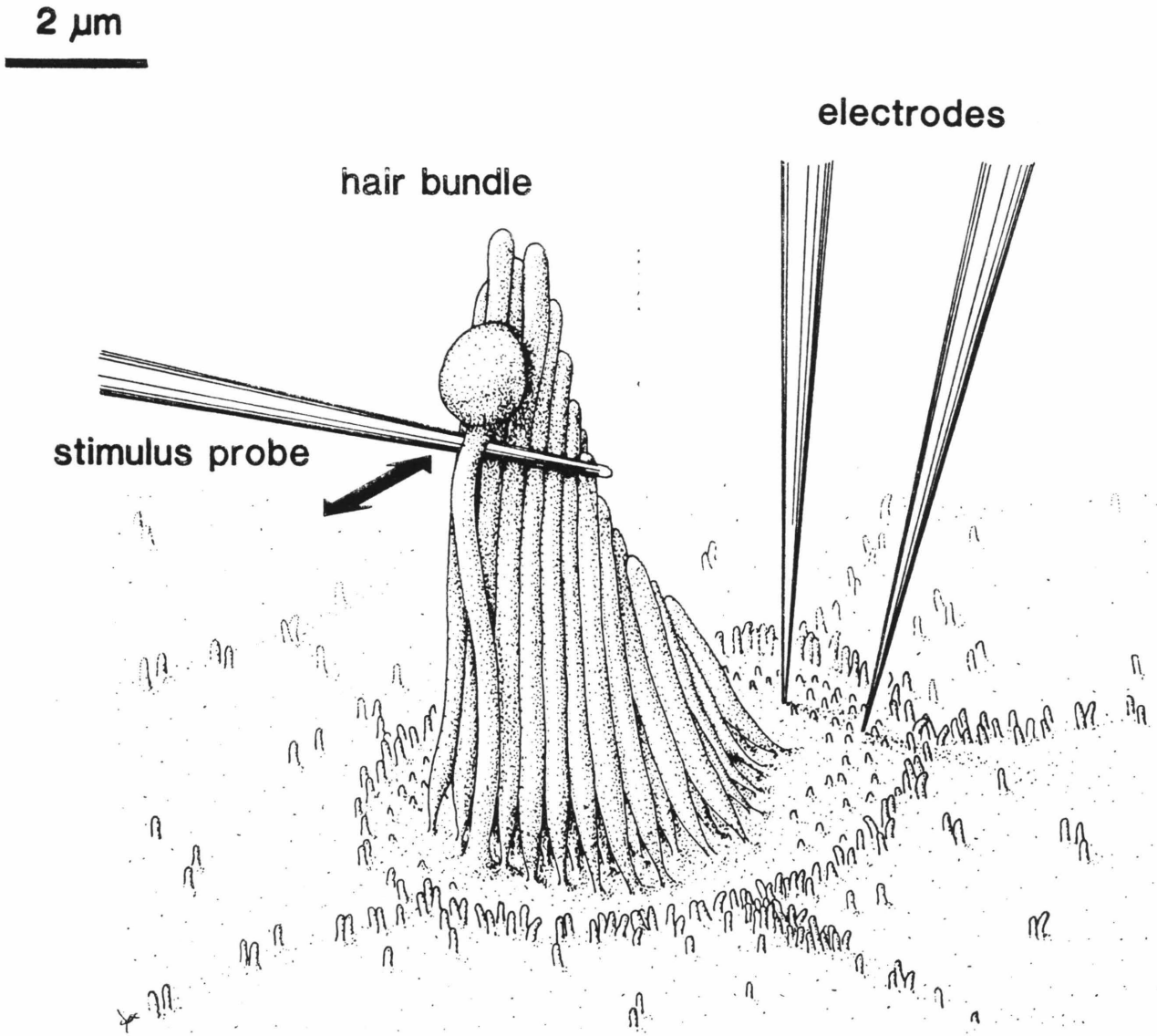
2 µm
electrodes
hair bundle
stimulus probe

good coupling between probe and bundle, displacement of the probe equals displacement of the hair bundle near its distal tip. Data were taken only when visual inspection indicated good coupling. Stimuli were (1) triangle-wave or sinusoidal displacements, which moved the hair bundle back and forth about its rest position, (2) maintained deflections, and (3) combinations of the preceding, presented either sequentially or simultaneously. Although I will refer to the maintained hair-bundle deflections used in these experiments as steps, they were not true steps in that the rising and falling phases were 5-10 ms long and sigmoidally shaped to avoid sharp transitions. These modifications were necessary because sharp transitions would cause ringing of the probe at its resonant frequency, near 300 Hz.

**Terminology**

The hair bundles of vertebrate hair cells have a morphological polarity which correlates with a functional polarity in the cells' responses. The morphological polarity is defined by a staircase arrangement of stereocilia heights (figures 1 and 4). The stereocilia occur in rows; height is constant within a row and decreases monotonically with distance from the kinocilium. A plane bisecting each row and normal to the macula also bisects the kinocilium; thus the bundle is bilaterally symmetric about this plane. The morphological polarity of a given cell is described by an "orientation vector" that is in the plane of bilateral symmetry, parallel to the macula and pointing toward the kinocilium. To a first approximation, the hair cell is sensitive to the component of a displacement stimulus that is parallel to its orientation vector (Shotwell *et al.*, 1981). In my experiments, probe motion was

approximately parallel to the orientation vector (arrows, figure 4). Our convention is that a displacement of zero means that the hair bundle is in its rest position and positive and negative displacements are in the direction of the orientation vector and opposite to it, respectively.

The hair cell's membrane can be divided into two regions or surfaces which in vivo are bathed in fluids of different ionic composition. The fluid separation is achieved with tight junctions which ring the cells just below the hair-bundle-bearing surface of the macula (A. J. Hudspeth, personal communication). We call the membrane on the hair-bundle side of the tight junctions the apical membrane, and the rest of the membrane the basal or basolateral membrane. The apical membrane includes the membrane of the stereocilia and kinocilium and in vivo faces a high-$K^+$, low-$Na^+$ saline called endolymph. The basolateral membrane includes presynaptic membrane of the afferent synapse and postsynaptic membrane of the efferent synapse. It is bathed in a saline that is similar to most extracellular fluid in having a high $Na^+$ and low $K^+$ content. The composition of endolymph and perilymph in the bullfrog sacculus has been studied with ion-selective electrodes (A. J. Hudspeth, R. Jacobs and J. H. R. Maunsell, unpublished data); the artificial perilymph described earlier is based on this study.

When a hair bundle is deflected in the direction of the cell's orientiation vector, the positive direction, a conductance in the apical cell membrane increases (Hudspeth, 1982). If the cell's membrane potential is clamped at resting potential, one records a net inward current due to the increased apical conductance (Corey and Hudspeth, 1979b). If the stimulus is in the negative direction, the conductance

decreases and one records a net outward current. We call the change in membrane current due to stimulation of the mechanosensitive apical conductance the receptor current. If the membrane potential is not clamped, the receptor current causes it to change. The cell depolarizes at the beginning of a positive stimulus and hyperpolarizes at the beginning of a negative stimulus. These initial changes in membrane potential affect voltage-sensitive conductances in the basolateral hair cell membrane causing more currents which feed back on membrane potential (Corey and Hudspeth, 1983a; Lewis and Hudspeth, 1983). Thus at a given time during a stimulus, the difference between membrane potential and resting potential, the receptor potential, is the net result of several currents. The term "receptor potential" is also used to refer to the envelope of the difference between resting and membrane potential throughout a stimulus.

The receptor potential data of this report are selected from a sample of 64 hair cells in 26 preparations. Voltage-clamp records of receptor current were obtained from five cells in three preparations.

**Results**

The major findings were that (1) sensory adaptation is an important feature of the cellular response, and (2) this cellular adaptation is largely due to a mechanism that extends the working range of the hair cells without reducing their dynamic sensitivity.

The simplest way to test for sensory adaptation is to present a constant stimulus. In these experiments, the tip of the hair bundle was stepped to a new position (displaced) and held there. Figure 5 shows the receptor potential recorded from a cell in response to a maintained

Figure 5. Adaptation of the hair cell receptor potential during a constant displacement of the tip of its hair bundle. This cell was in a single-bath recording chamber filled with high-$Ca^{++}$ perilymph. Both traces were averaged over three trials. The stimulus is displacement of the distal tip of the hair bundle in the plane parallel to the macula.

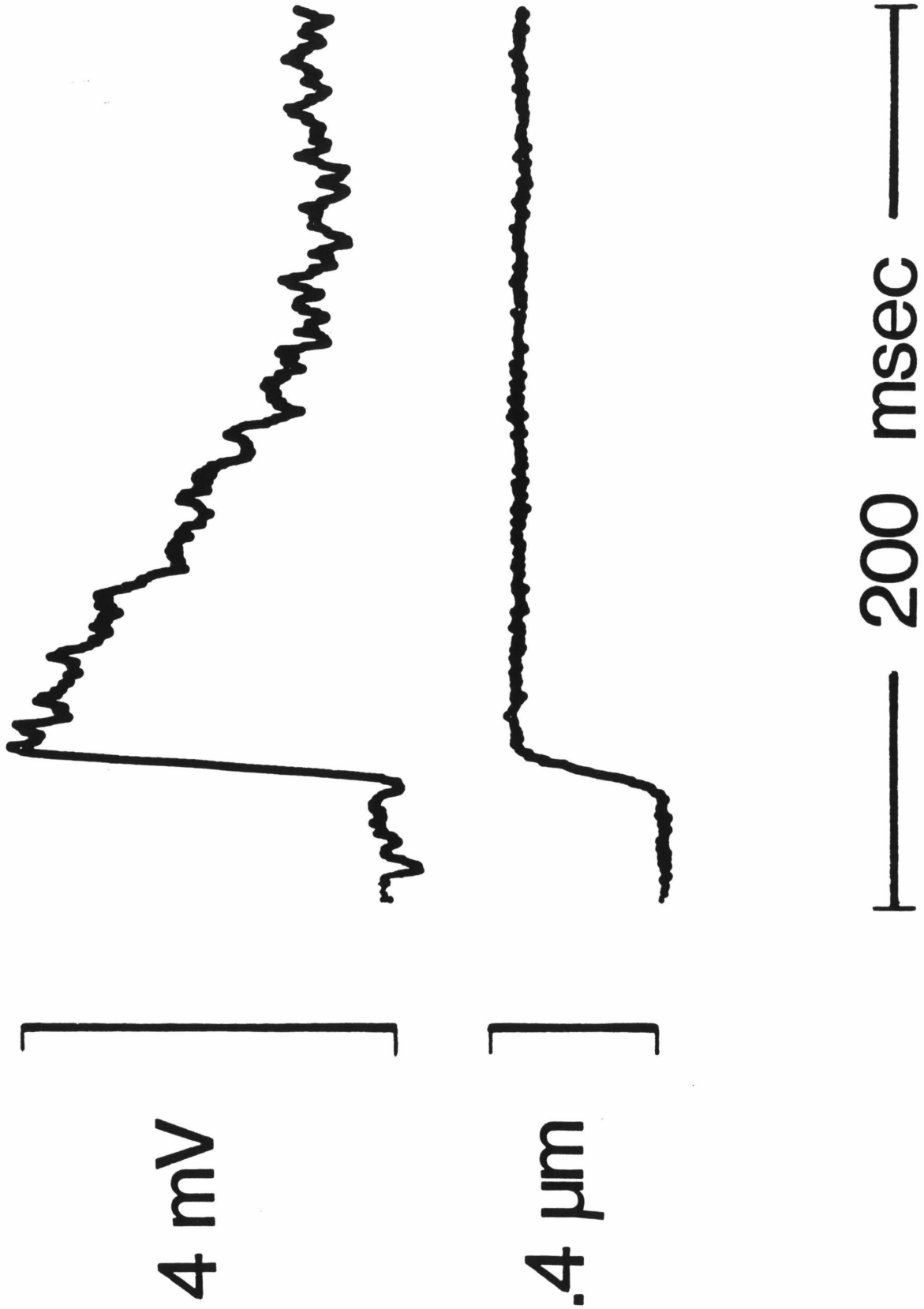
4 mV
.4 µm
200 msec

+0.35 μm displacement of its hair bundle. The cell depolarized rapidly at the beginning of the step, then more gradually repolarized. Since the depolarizing response decreased in the presence of a constant stimulus, this is an example of sensory adaptation. The adaptation was incomplete in that membrane potential did not return to its resting level during the displacement: 100 ms after the receptor potential peaked, it levelled off at 23% of its peak value. Of the 69 hair cells studied, 57 (83%) showed partial or complete adaptation to maintained stimuli. We do not know the nature of the processes leading to adaptation in these cells but can describe in an operational sense the kind of adaptation that is occurring.

Sensory adaptation of any kind constitutes a change in the relationship between stimulus and response for a sensory element. For a hair cell, this relationship is illustrated by a displacement-response curve, a graph of response vs. hair-bundle displacement. Our approach has been to investigate what happens to the displacement-response curve during adaptation. In this way, a third dimension, time, is added to the analysis of the relationship between stimulus and response. Before delving into the effects of adaptation on the displacement-response curves, what is known about them from "two-dimensional" analysis in which temporal affects are ignored or avoided?

The displacement-response curves of individual hair cells of the bullfrog sacculus share some fundamental features, illustrated schematically in figure 6(a). All cells respond approximately linearly to a narrow range of displacements, the operating range, and show saturation to displacements that extend outside this range. The curves of different cells show some variability in (1) sensitivity:

Figure 6. Possible mechanisms of adaptation. (A) A schematic displacement-response curve, representative of those obtained from bullfrog saccular hair cells. The origin of the graph indicates the resting position of the hair bundle and the resting level of membrane potential or current, depending on what is being monitored. If the hair bundle is stepped to a certain position (x-coordinate), the initial response is the corresponding y-coordinate on the curve (solid circle). With time, the response decays to a lower value (open circle). (B)-(D) show different mechanisms by which this decay might occur. In (B), the cell undergoes a general loss of sensitivity (solid line) which may be accompanied by a change in the width of the operating range--e.g., a broadening (dashed line). In (C), the cell's response range shifts to more hyperpolarized values (solid line) and may also change shape (dashed line). In (D), the operating range shifts in the direction of the stimulus. In a 100% operating-range shift, the bias point of the displacement-response curve, initially at the origin, would be reset to the stimulus position. The shift in (D) is 65% of the step displacement. Again, the displacement-response curve could shift without changing in any other way (solid line) or could be expanded or compressed along either axis (e.g., dashed line).

(a)

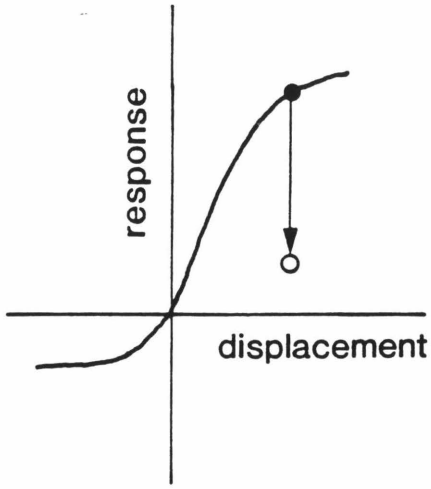


(b) desensitization

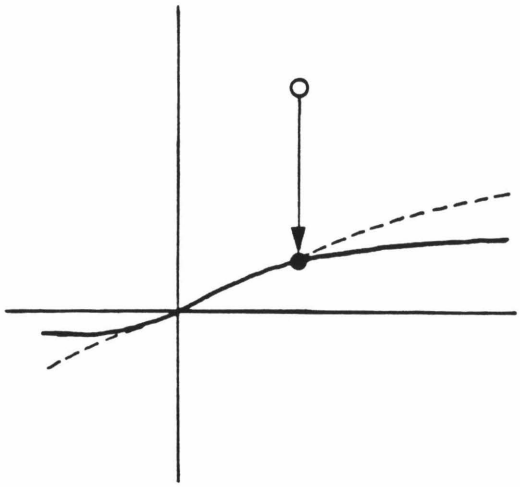

(c) response range shift

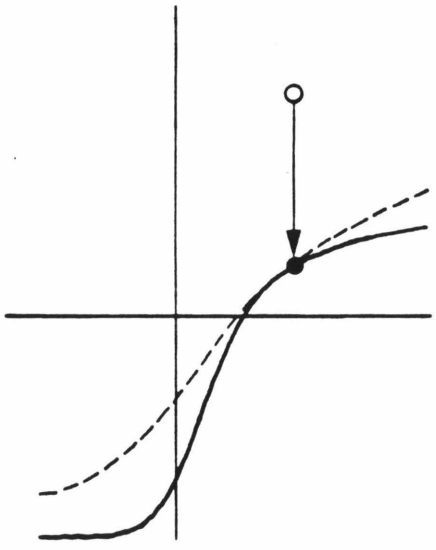

(d) operating range shift

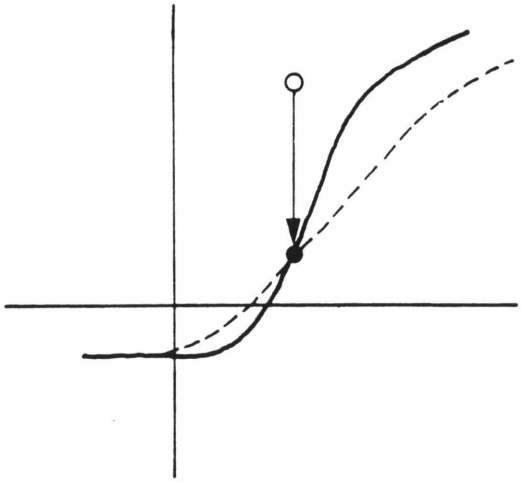

Δ(reponse)/Δ(displacement), (2) operating range and (3) response range: the range of membrane potentials corresponding to the operating range. Factors known to influence one or more of these features of the displacement-response curve include the health of the cells, the stimulus waveform, the divalent cation concentration in the medium bathing the apical surface (as will be illustrated later in this section, under "Calcium effects"), voltage-sensitive conductances and adaptation.

To investigate changes in the displacement-response curve during adaptation to a constant stimulus, one must superimpose "test" stimuli on the constant "adapting" step. To simplify interpretation, one would like to use test stimuli that do not themselves cause significant adaptation--i.e., fast stimuli or, in terms of frequency rather than time, high-frequency stimuli. In the frequency domain, any adaptation process acts like a high-pass filter, attenuating the response to low-frequency components of a stimulus. In the <u>in vitro</u> microphonic preparation, peak responses to sinusoidal stimuli were obtained in the frequency range of 75-200 Hz (Corey and Hudspeth, 1983). Below this range, response amplitude rolled off due to the adaptation process; the roll-off was adequately modelled with a single-pole, high-pass filter having a half-power frequency of 25 Hz. Based on these results, test stimuli ideally should have no frequency components below 75 Hz. A simple approach would be to use impulse displacements of different amplitudes to determine the displacement-response curve at a given time during an adapting step. This was not done for several reasons. First, the stimulus probe rang if driven with an impulse or square pulse. Second, high-frequency stimuli delivered by a probe in contact with the

hair bundle damaged it, at least in the amplitude range used in these experiments (0.1-1 μm). Third, intracellular responses to high frequencies are attenuated by the hair cell membrane which in healthy cells has a time constant on the order of 10 ms and therefore a half-power frequency of about 100 Hz. Finally, one must present a series of test impulses to obtain a single displacement-response curve. When each test impulse is superimposed on a relatively long adapting step, the process is time-consuming. For our purposes, a more convenient way of determining the displacement-response curve was to present a triangle-wave or sinusoidal displacement of sufficient amplitude; each half-cycle moves the hair bundle through a continuous series of displacements. (The major disadvantage of such stimuli is that the response to a given displacement during the cycle may be influenced by the response history, due to processes having a time dependence, notably adaptation and filtering by the cell membrane.) Triangle-wave or sinusoidal displacements between 20 and 30 Hz were used as test stimuli. Higher frequencies would have been preferable for studying adaptation, but triangle wave stimuli at fundamental frequencies as low as 50 Hz seemed to damage the cells possibly because of the higher harmonics present in the stimulus. The possibility that sinusoidal stimuli at frequencies above 30 Hz might not damage the cells was overlooked. The triangle waveform was chosen initially because it moves the hair bundle linearly through the operating range (Hudspeth and Corey, 1977). However, the high-frequency components of the stimulus, when filtered through the cell membrane, cause distortion of the receptor potential. Partly because of this and partly because other inner ear organs are typically studied using sinusoidal stimuli, I eventually switched to sine waves.

For the purposes of studying adaptation, the data obtained using the two kinds of stimuli can be pooled.

The schematic displacement-response curve of figure 6(a) is representative of receptor potential data recorded in response to 20-30 Hz sinusoidal or triangle-wave displacements, with high-$Ca^{++}$ saline bathing the apical surface of the cell. In terms of displacement of the tip of the hair bundle, the operating range is on the order of 0.2 μm. Since hair bundles are rigid and pivot at their bases, this displacement corresponds to an angular deflection of 1.4° for the average saccular hair bundle, 8 μm in height (A. J. Hudspeth, personal communication). Given a cell with such a displacement-response curve, if we step the hair bundle to a new positive position, the response will rise to the value corresponding to that position (displacement) on the curve. If the displacement is maintained, as in figure 1, the receptor potential will decay (adapt). Figures 6(b)-(d) show three different kinds of change in the displacement-response curve that would result in the observed decay. Figure 6(b) shows a mechanism that is sometimes called "desensitization": the response, $\Delta V$, to a given displacement, $\Delta x$, superimposed on the adapting step--i.e., the sensitivity, $\Delta v/\Delta x$--decreases with time after the onset of the step. Figure 6(c) demonstrates that a response decline would result from a shift in the displacement-response curve along the response axis in what could be called a "response-range shift". Figure 6(d) illustrates that a decline in receptor potential would occur if there were a shift in the operating range, that is, if the displacement-response curve shifted along the displacement axis in the direction of the imposed stimulus.

To monitor what happened to a hair cell's displacement-response curve during a step, I superimposed triangle-wave or sinusoidal displacements, "test" stimuli, on the "adapting" step. Figure 7 shows the results of such an experiment on the cell of figure 5. In 7(a) and (b), the adapting step was +0.3 μm but in (b) a 30-Hz sinusoidal displacement was superimposed. In (d), the same sine wave is superimposed on a +0.45 μm adapting step. In both (b) and (d), the responses to the sine wave became larger with time during the adapting step (this is less obvious in (b) because the sine wave response was fully developed by the first complete sinusoidal excursion, marked "2" on the figure). Therefore as the response to the step declined (a), the sensitivity to superimposed stimuli increased.

The data of (b) and (d), respectively, are replotted in 7(c) and (e) as series of displacement-response curves. To make each curve, the receptor potential was plotted against displacement over a window of time, and the curve was hand-drawn to fit the data points. Curve 1 in (c) and (e) is response vs. displacement during the rise of the step, labelled "1" in (b) and (d). Curves 2, 5 and 10 are graphs of response vs. displacement for the positive-going sweeps of the second, fifth and tenth sinusoidal cycles. (The rise time of the step was 8 ms, and the duration of each half-cycle 16.7 ms. Thus, although the curves were not "instantaneous", they did occur within time windows much shorter than the step, which lasted 360 ms.) Curve 1 is similar in (c) and (e) and indicates the cell's displacement-response curve at the onset of the step. At this time, the cell was linearly sensitive to displacement in the range +0.1 - +0.3 μm. Its sensitivity within this range was 1.22 mV/.1 μm in (c) and 1.25 mV/.1 μm in (e). The position of the

Figure 7. Changes in the displacement-response curve during a constant stimulus. The hair cell was the same as the cell in figure 5. (A) The receptor potential during a +0.3 μm, 360 ms adapting step. (B) A 30 Hz sine wave displacement was superimposed on the +0.3 μm adapting step. In (C), displacement-response curves were obtained from the data in (B) by plotting the response to the rise of the step (labelled 1 in B and C) and to a single positive-going half-cycle of the sine wave at the times makred 2, 5, and 10 (for the second, fifth and tenth cycles). Relative to the beginning of the step, time zero, the curves were obtained over the following time windows: (1) 0-8 ms; (2) 29-46 ms; (5) 162-179 ms; and (4) 329-346 ms. Curves have been fit by eye to the data points. (D) The same sine wave was superimposed on a +0.45 μm step. The data are replotted as displacement-response curves in (E) for the same time windows as in (B) and (C).

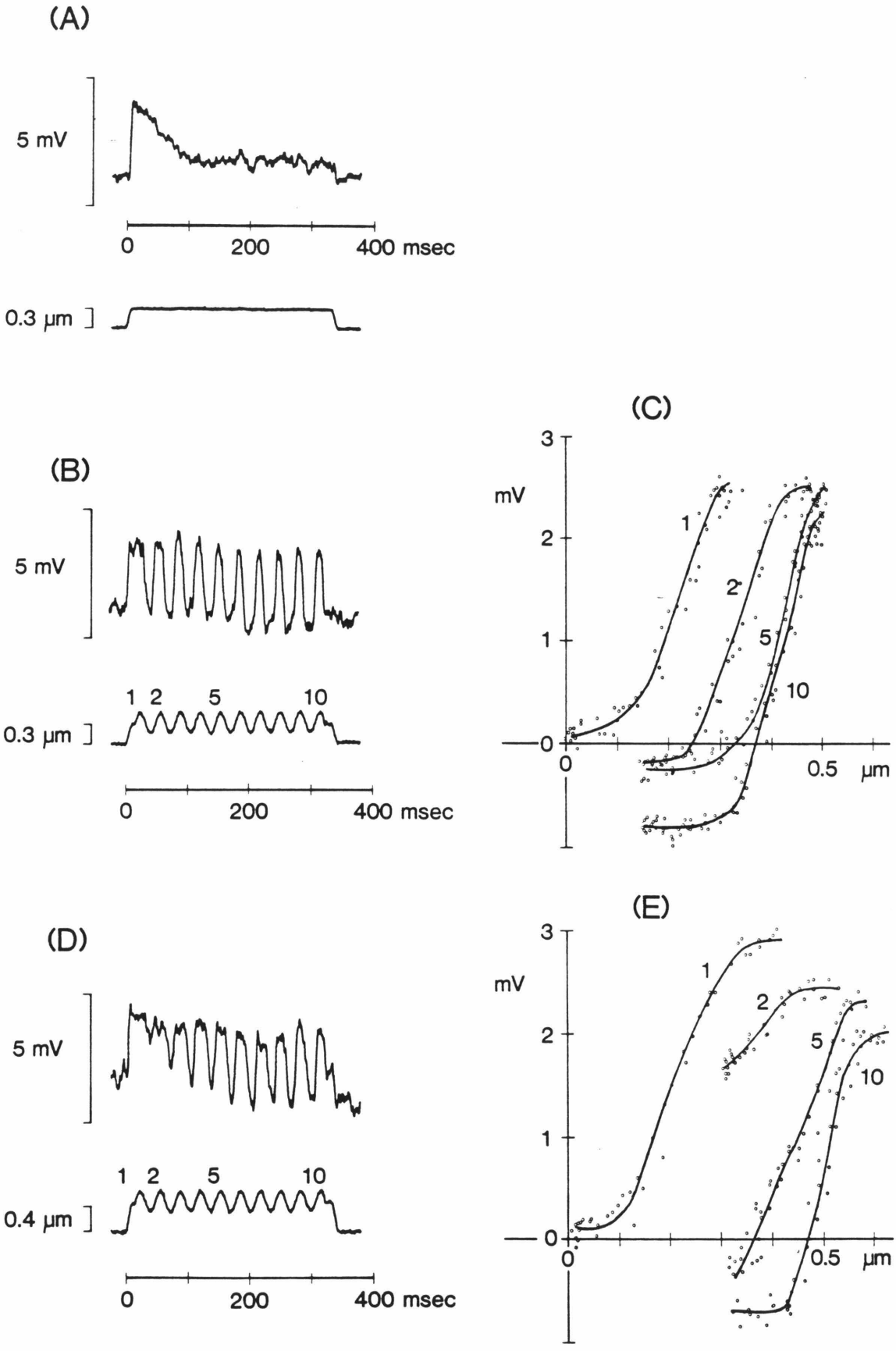
(A)
5 mV
0
200
400 msec
0.3 μm
(B)
5 mV
1 2 5 10
0.3 μm
0
200
400 msec
(C)
mV
3
2
1
0
1
2
5
10
0
0.5 μm
(D)
5 mV
1 2 5 10
0.4 μm
0
200
400 msec
(E)
mV
3
2
1
0
1
2
5
10
0
0.5 μm

operating range was more positive than usual (Hudspeth and Corey, 1977; see figure 6(a) for an illustration) which may be due to any of a variety of experimental factors[1] or may reflect a real variation in hair cell properties. For the present analysis, it is more important that during the step the cell's displacement-response curve underwent changes representative of the changes seen in all hair cells that showed adaptation.

The most dramatic and consistent change was a shift in the operating range in the direction of the step. In 7(c), the cell's operating range had shifted significantly by about 40 ms after the beginning of the step (curve 2) and even further by 170 ms (curve 5). A less consistent but still common effect was a change in the response range--the range of membrane potential corresponding to a saturated response. Between 170 ms and 340 ms (curve 10), the cell's operating range did not shift detectably, but its response range shifted in the hyperpolarizing direction, extending below the pre-step resting potential. During the +0.4 μm adapting step (e), the curve again shifted negatively along the voltage axis and positively along the displacement axis. Finally, the displacement-reponse curve did not appear to undergo consistent changes in shape--e.g., in the widths of either the operating or the response range, or in the slope sensitivity.

Figure 8 summarizes for the cell of figure 7 the time courses of the changes in the displacement-response curve during the +0.3 μm and +0.45 μm steps. Figures 8(a) and (c) show that slope sensitivity and

[1]Calcium affects the bias point of the operating range (Corey, 1980, and this chapter, p. 25). So one possibility is a local extracellular variation in $Ca^{++}$ level, or abnormal intracellular regulation of the ion.

Figure 8. Changes in the displacement-response curve during a constant stimulus. Different features of the displacement-response curves of figure 7 are plotted against time during the adapting steps. In (A), sensitivity within the operating range, Δ(response)/Δ(displacement), is plotted in mV per 0.1 μm. (B) plots the response range shift in mV, that is, the difference between membrane potential at either the positive or negative saturation level in curve 1 and the corresponding level in subsequent curves. (The choice of positive or negative saturation level depended on what was available--e.g., curves 2 and 5 in (E) show positive but not negative saturation.) The difference became more positive with time after the onset of the adapting step, indicating that the response range gradually hyperpolarized. In (C) and (D), operating range shift is plotted in μm and as percentage of the adapting step, respectively.

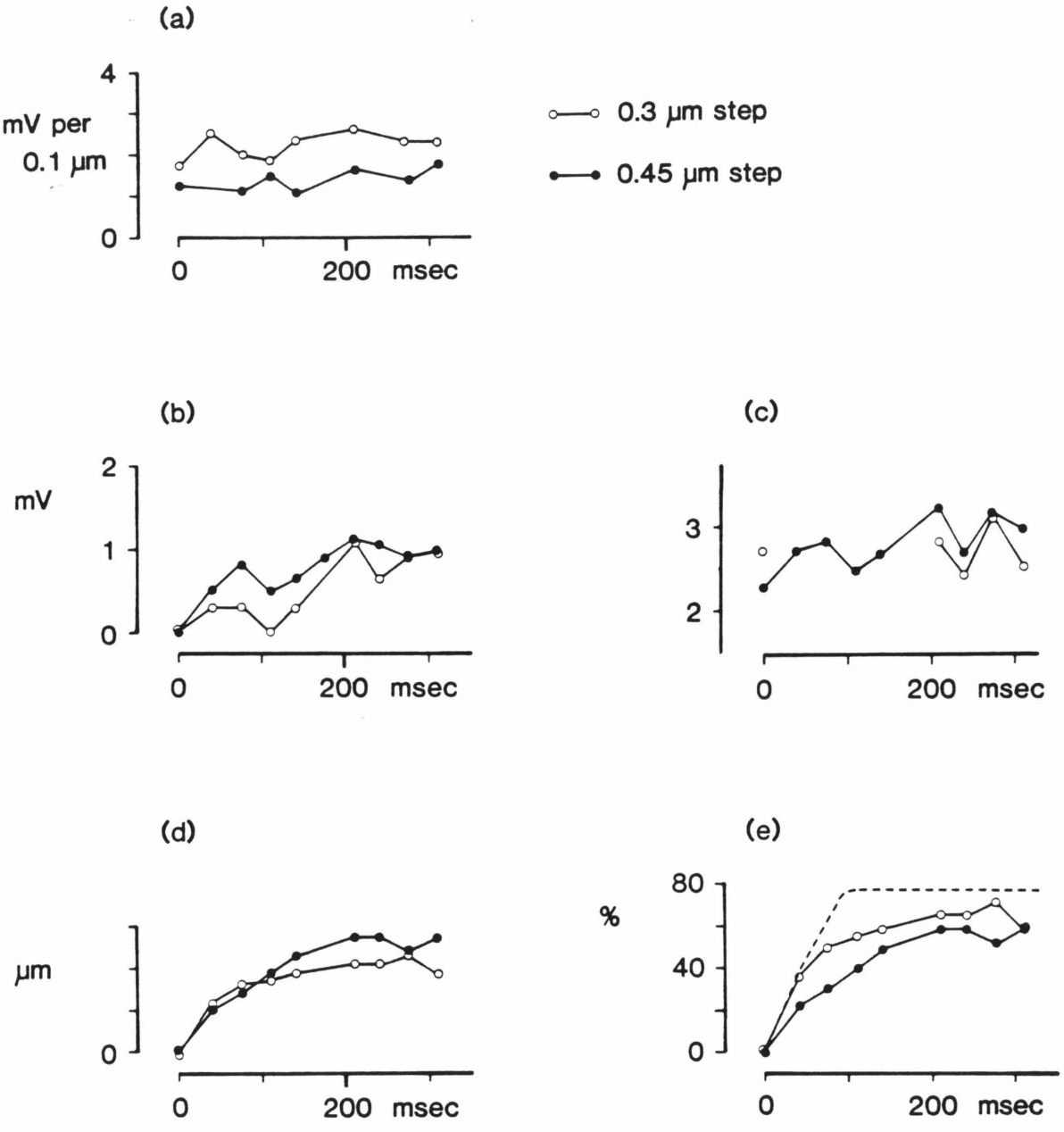
(a)
4
mV per
0.1 μm
0
0
200 msec
0.3 μm step
0.45 μm step
(b)
2
mV
1
0
0
200 msec
(c)
3
2
0
200 msec
(d)
μm
0
0
200 msec
(e)
80
%
40
0
0
200 msec

response range changed erratically during the adapting steps, suggesting that these features do not correlate in a simple manner to level of adaptation. Figure 8(b) indicates that the negative shift in response range was not a smooth function of time during the step. By contrast, the shift in operating range during the adapting steps increased relatively smoothly. The shift is plotted in microns in 8(c) and as percent of the adapting step in 8(d). Also shown in (d) is the time course of the decline in the receptor potential to the +0.3 μm step alone, expressed as percent of the peak response.

Figure 8 illustrates a number of features characteristic of adaptation in these cells. (1) The rate of operating range shift often closely parallels the rate of decline of the receptor potential, as in figure 8(d), although some discrepancy also is common. One source of discrepancy is suggested by a comparison of 8(b) and (c): the hyperpolarizing shift in reponse range when it occurs is not well correlated with the operating range shift, and enhances the rate of receptor potential decline relative to the rate of operating range shift. Also, if the adapting stimulus is supersaturating, the operating range may shift in the absence of any decline in the receptor potential. (2) The response range often shifts, always in the direction that will contribute to the adaptation of the step response. (3) There is no consistent change in the shape of the displacement-response curve during adaptation. (4) In terms of absolute displacement (figure 8c), the operating range shifts more for larger adapting steps.

The operating range shift is greater for larger steps even when the comparison is between steps that extend outside the cell's resting operating range (supersaturating steps). Figure 9 compares the response

Figure 9. Adaptation to saturatingly large steps of different amplitude. The data were recorded in a one-chamber bath containing high-$Ca^{++}$ perilymph. (A) shows the response of one cell to two different positive steps with a superimposed 20 Hz triangle wave stimulus. The steps were +0.45 μm (upper pair of traces) and +0.75 μm (lower pair). The triangle wave had a peak-to-peak amplitude of 0.3 μm in both cases. In (B), the same data are replotted as displacement-response curves. Taking the beginning of the rise of the step as time zero, the curves were taken over the following time windows: (1) 0-25 ms, (2) 37.5-62.5 ms, (3) 87.5-112.5 ms, (5) 187.5-212.5 ms. In (C), the operating range shift in μm is plotted as a function of time for each of the steps (open circles: +0.45 μm, filled circles: +0.75 μm). In (D), the same operating range shifts are plotted as percentage of the adapting step.

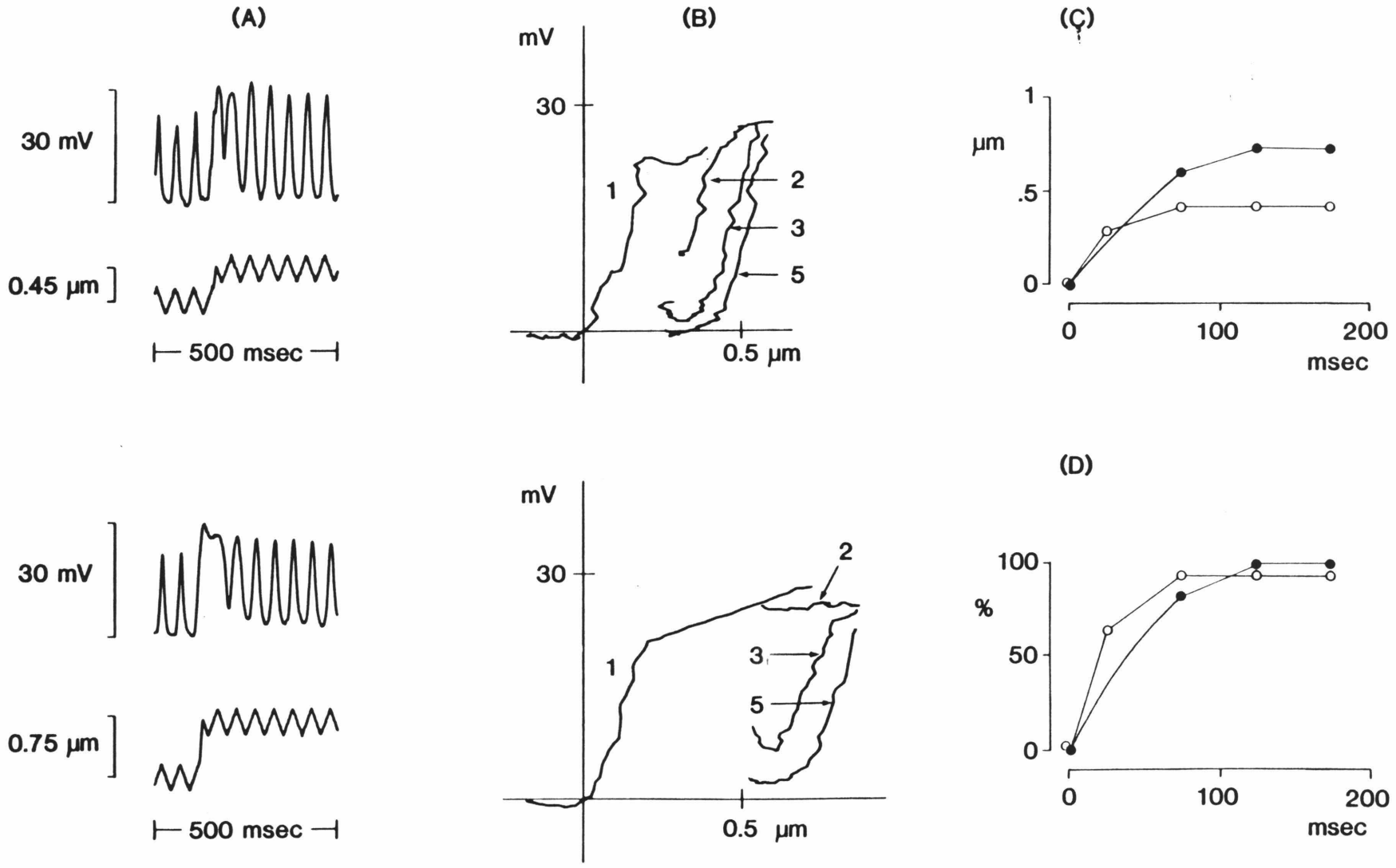
(A)
30 mV
0.45 µm
500 msec
(B)
mV
30
1
2
3
5
0.5 µm
(C)
µm
1
.5
0
0
100
200
msec
30 mV
0.75 µm
500 msec
mV
30
1
2
3
5
0.5 µm
(D)
%
100
50
0
0
100
200
msec

of a single cell to two steps, one +0.45 and the other +0.54 μm, with a superimposed 20 Hz triangle wave. As the initial displacement-response curves (9b) indicate, both steps were larger than the cell's resting operating range, approximately 0.2 μm. From figure 9(c), which plots the operating range shift, in microns, with time during each of the adapting steps, one can see that the shift caused by the larger step was faster (in μm/ms) and plateaued at a greater absolute value. If one replots the operating range shifts as percent of the adapting step (figure 9d), one finds that the equilibrium values reached were similar for the two steps: 93% for the 0.45 μm step and 98% for the 0.75 μm step. The operating range of the cell of figures 7 and 8 also shifted to a final position that was a constant percentage of step size, about 60%, for the two steps tested (figure 8d). In the 7 cells tested with positive steps of 2 or 3 different amplitudes, there was a tendency for the operating range shifts shown by a given cell to be similar proportions of step amplitude. That is, in 5 of the 7 cells, the operating range shifts expressed as percentage of step size were, for a given cell, within ±10% of the mean value for the cell. The variability between cells was greater; mean values varied between 30 and 100%.

Adaptive shifts in operating range also occur during negative steps, but at a lower rate. Figure 10 compares the effects of equal positive and negative steps in one cell. The -0.75 μm step (figure 10a, lower pair of traces) immediately followed the +0.75 μm step (upper pair of traces; this is the same cell and the same +0.75 μm step as in figure 9). There are four stimulus conditions in this sequence: the positive step and finally the positive step back to resting position. The first 200 ms of the positive step have been detailed in figure 9.

Figure 10. Adaptation to, and recovery from, positive and negative steps. The cell is the same as that in figure 9. (A) The same +0.75 μm step as in figure 9 is shown in its entirety followed by a -0.75 μm step. A 20 Hz triangle-wave, 0.3 μm in peak-to-peak amplitude, was presented continuously. At the offset of the positive step, the response to the triangle-wave was greatly reduced then gradually recovered. Although the negative step completely suppressed the triangle-wave response, the excitatory rebound following the step indicates that an adaptive shift occurred during the negative step. In (B) displacement-response curves are shown at various times relative to the positive step (upper plot) and to the negative step (lower plot). The curves, 1-8, correspond to the times labelled 1-8 in (A). Thus curve 1 was the displacement-response curve before either step; curve 2 was obtained towards the end of the positive step; curves 3, 4 and 5 were obtained at 25, 225 and 675 ms after the offset of the positive step; curve 6 was taken during the negative step; and curves 7 and 8 correspond to 25 and 75 ms after the offset of the negative step.

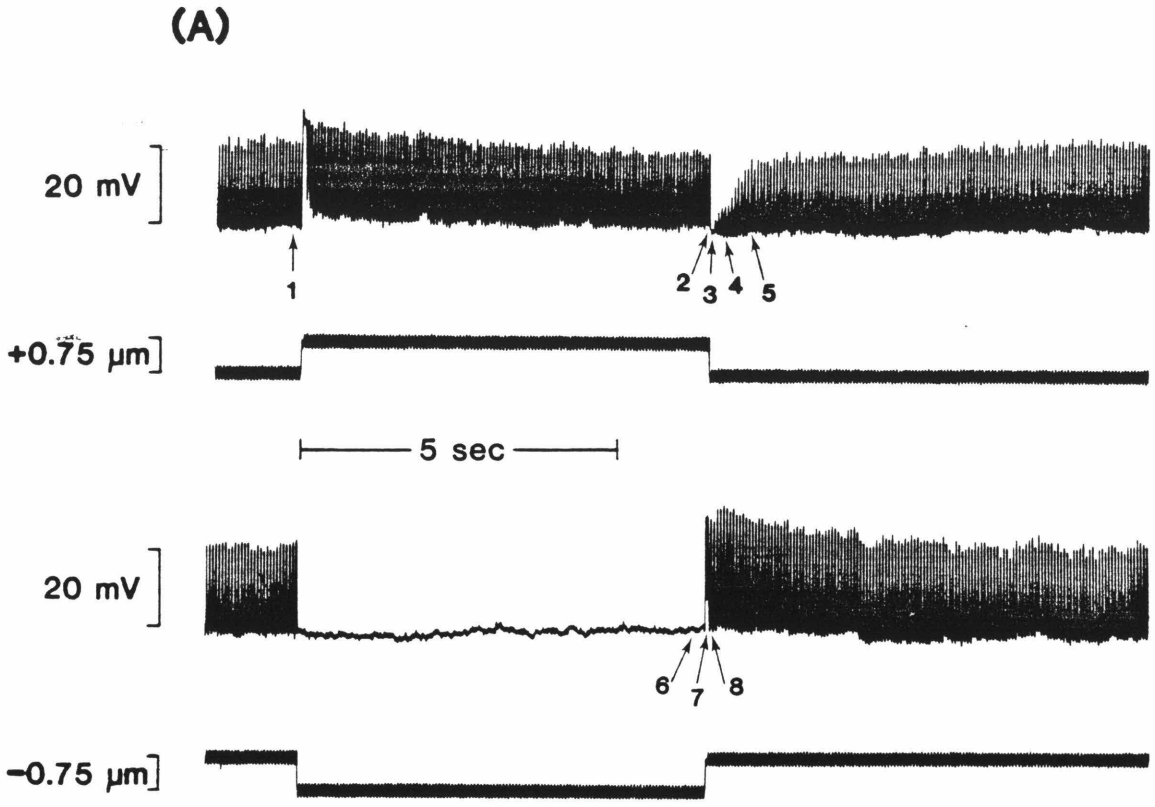
(A)
20 mV
1
2
3
4
5
+0.75 µm
5 sec
20 mV
6
7
8
−0.75 µm

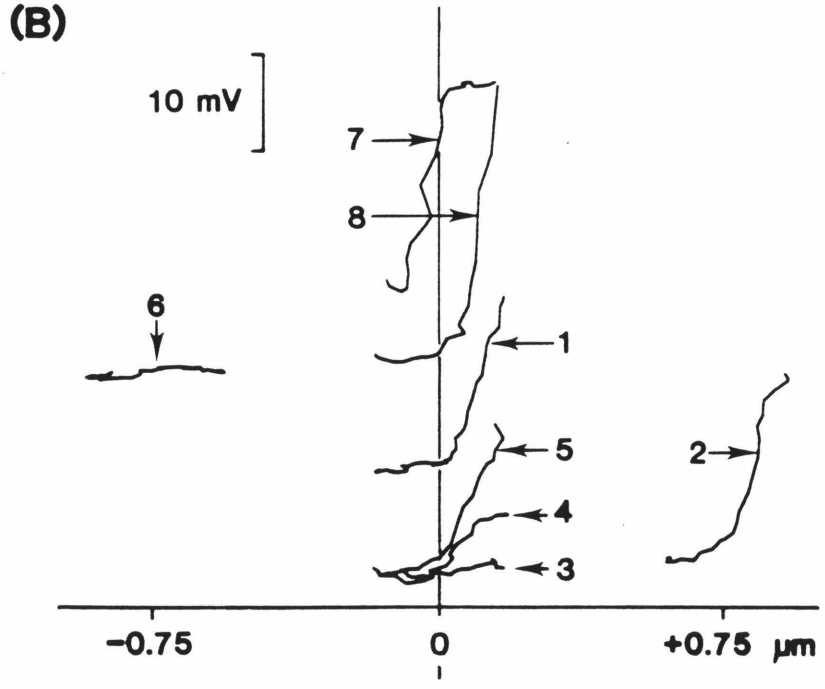
(B)
10 mV
7
8
6
1
5
2
4
3
−0.75
0
+0.75 µm

Looking at the positive step in its entirety, in figure 10(a), one can see that there are two phases in the response: an initial period of rapid change in both total receptor potential amplitude and triangle-wave response, lasting about 100 ms (see figure 9), and then a period of gradual change, lasting the duration of the step, during which the response range decreases by about 15% and shifts about 1 mV negative. At the offset of the positive step (the negative step back to rest), the response to the triangle wave initially was inhibited, then recovered to its pre-step amplitude. The recovery from inhibition, like the response to the positive step, featured a fast phase followed by a period of very gradual change. The rapid phase lasted about 700 ms, compared to about 100 ms at step onset. From the end of the rapid phase to the beginning of the negative step, about 6.5 s later, the amplitude of the triangle-wave response increased by about 15%, and the cell depolarized about 1 mV.

The fast and slow response phases following each transition are due to different processes. The rapid phase was the period over which the operating range shifted; this was demonstrated for the positive step in figure 9. Figure 10(b) compares displacement-response curves at various stages relative to the positive step: before (curve 1), just before the end of the step (curve 2), and after (curves 3-5). Together, figures 9 and 10 indicate the following sequence of operating range shifts. In the first 100 ms of the positive step, the operating range shifted virtually 100% of the step displacement and remained there for the duration of the step. Following the offset of the positive step, the operating range shifted back to its original position but took longer to do so (one can't determine precisely how long the shift back took

because the small size of the response at early times (e.g., curve 4, figure 10b) makes it hard to assess the operating range). By 600-700 ms, it was clear that the operating range had reached its pre-step position (compare curves 1 and 5 in figure 10b). It remained there until the negative step, 11 s later. Thus the fast phase of recovery also appears to have coincided with the period of operating range shift. During the slow phase of recovery, the triangle-wave response gradually increased by about 15%. Perhaps membrane currents not associated with transduction caused the slow change in response amplitude that occurred both during and after the positive step--e.g., ionic pumps might be stimulated by changes in ionic concentration due to the receptor current.

During the positive step, the cell's operating range shifted by nearly 100% of the step amplitude. One might expect that as a consequence the cell would not distinguish between the step back to the original, resting, position and a negative step of equal amplitude from the resting position. However, comparison of the recovery from the +0.75 μm step with the response to the -0.75 μm step (figure 10a) indicates that the cell did not see the two stimuli as equivalent. The triangle-wave response did not recover during the negative step. That the operating range did shift negatively during this step can be detected by comparing displacement-response curves from just before and just after the step (curves 1, 7, and 8 in figure 10b). Twenty-five ms after the offset of the step (curve 7), the operating range was 0.17 μm more negative than it was before the step; by 75 ms (curve 8), the operating range had returned to its rest position. Clearly, the operating range did not shift far enough to come into register with the

new hair bundle position, i.e., it did not shift as much as it had during the positive step and at the offset of the step. There are not enough intracellular data to indicate whether in general the equilibrium operating range shift is smaller for negative than for positive steps. The effects of positive and negative steps of equal amplitude can be compared in three other cells. In one case, the final operating range shift during a +0.3 μm step was about +0.21 μm (70%), compared to 0.15 μm (50%) during the -0.3 μm step. In a cell tested with ±0.9 μm steps, the equilibrium operating range shift was about 53% of the positive step and 35% of the negative step. But in another cell, the shifts during ±0.9 μm steps reached similar final values: 80% for the positive step and 76% for the negative step. Thus it remains to be determined whether there is an asymmetry in the amount that the operating range will shift. There does appear to be an asymmetry in the rate at which the operating range shifts. In the cell of figure 10, the operating range shifted faster after positive transitions (figure 9 and curves 7-8, figure 10) than after negative ones (figure 10, curves 3-5 and the -0.75 μm step). In general, it was found that the rate of operating range shift in the first 50-100 ms of a step was faster for positive than for negative displacements, whether the displacements were from the original bundle position or a different position.

Operating shifts occur during symmetric sinusoidal or triangle-wave displacement as well. If stimulated at ≥10 Hz with a gated sinusoidal or triangle-wave displacement that is symmetric about the resting hair bundle position, a cell shows a small but reliable positive shift in operating range during the first 2-3 stimulus cycles (figure 11). The positive shift occurred whether the initial half-cycle was negative or

Figure 11. Operating range shift in the receptor potential during symmetrical stimulation. The cell was in a one-chamber bath containing high-$Ca^{++}$ perilymph. (A) shows the receptor potential in response to a gated, 30 Hz sinusoidal stimulus. In (B), the responses to the positive-going sweeps of the first and second cycles are plotted against displacement. The curves have been fit by eye to the data points for each sweep. Displacement-response curves corresponding to the third and fourth cycles (not shown) are indistinguishable from curve 2.

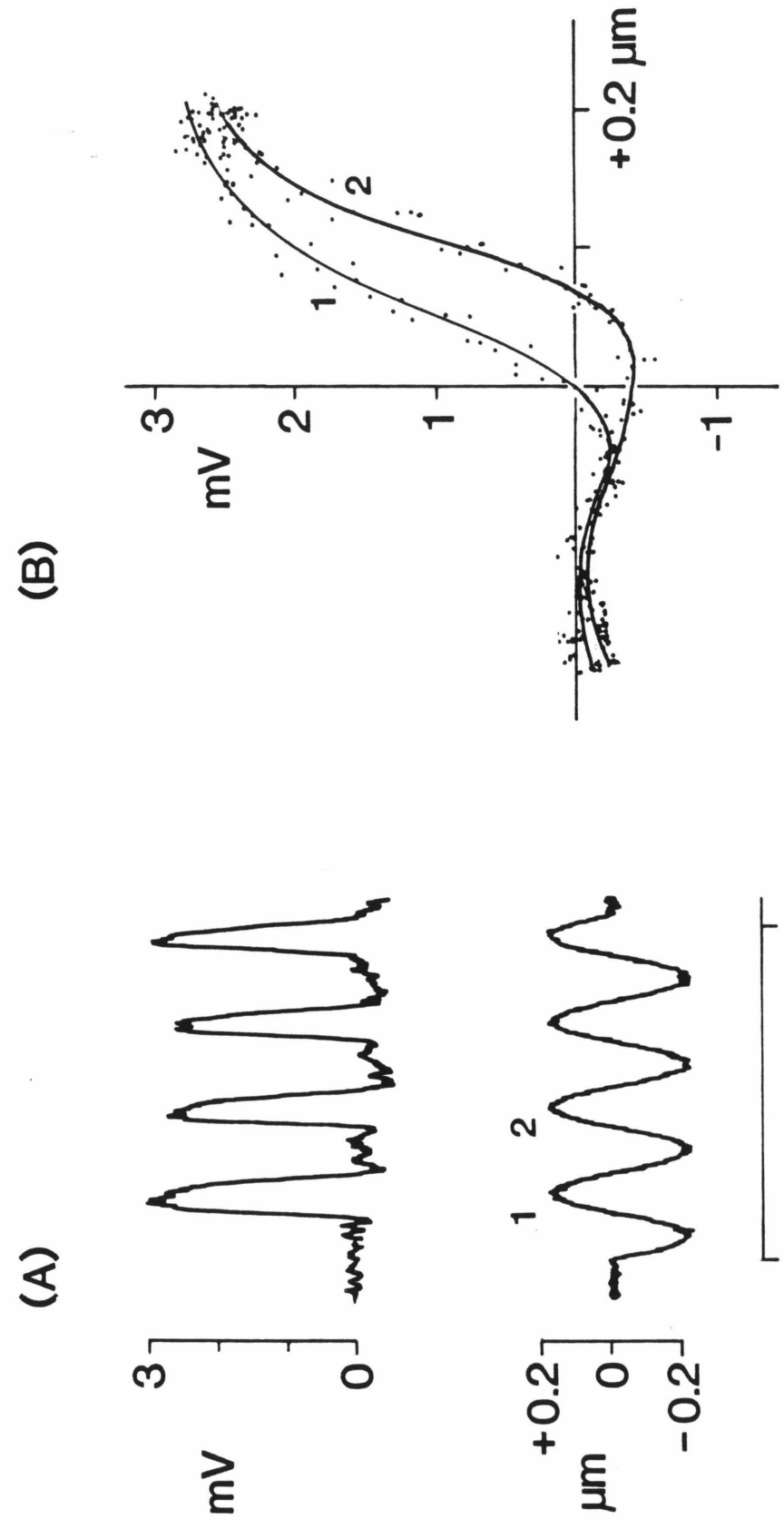
(A)
3
0
mV
+0.2
0
-0.2
μm
1
2
0
msec
200
(B)
3
2
1
mV
-1
+0.2 μm
1
2

positive. The operating range settled into a new position within 100 ms of the start of the stimulus; in the example of figure 11, it had stopped shifting by 60 ms. The shift may stop because of a kind of negative feedback: once the operating range shifted positively, the stimulus would no longer appear symmetric to the cell, but negatively biased.

One plausible hypothesis about the adaptive operating range shift, based upon the intracellular voltage data, is that it depends upon a voltage-sensitive process that responds to the receptor potential. However, the operating range shifts that have been described can occur when the membrane potential is clamped at its resting level, -50 to -70 mV, and the receptor current recorded. In the voltage-clamped cell of figure 12, robust operating range shifts occurred during both stimuli tested: a symmetric 30 Hz sine wave (a) and a negative step (b). Of the other four voltage-clamped cells, two showed some degree of adaptation to negative steps by rebounding at the offset of the step, as in figure 12(b). In one of these two it is clear that, as for the cell of figure 12, the major effect of the step on the displacement-response curve was to shift its operating range in the direction of the step. For the other cells, displacement-response curves are not available either because the data are too noisy or because the stimuli were not large enough to define the limits of the operating range. Figure 13 shows receptor current in response to +0.5 μm steps for two of these cells. In both cases, the inward currents decayed to approximately stable values within 50 ms. The stable values were about 40% and 67% o the peak value in (a) and (b) respectively.

Figure 12. Operating range shift in receptor current. The receptor current has been inverted so that an upward deflection signifies an inward current. Recordings were made in high-$Ca^{++}$ perilymph with a two-electrode voltage-clamp. The responses in (A) and (B) are from one cell and are averages of 10 and 20 trials, respectively. (A) shows the receptor current during a gated, 30 Hz sinusoidal stimulus. In (B), the stimulus was a -0.75 µm step. In (C), the response to the first two cycles of the gated sine wave (1,2) and to the offset of the negative step (3) are plotted against displacement.

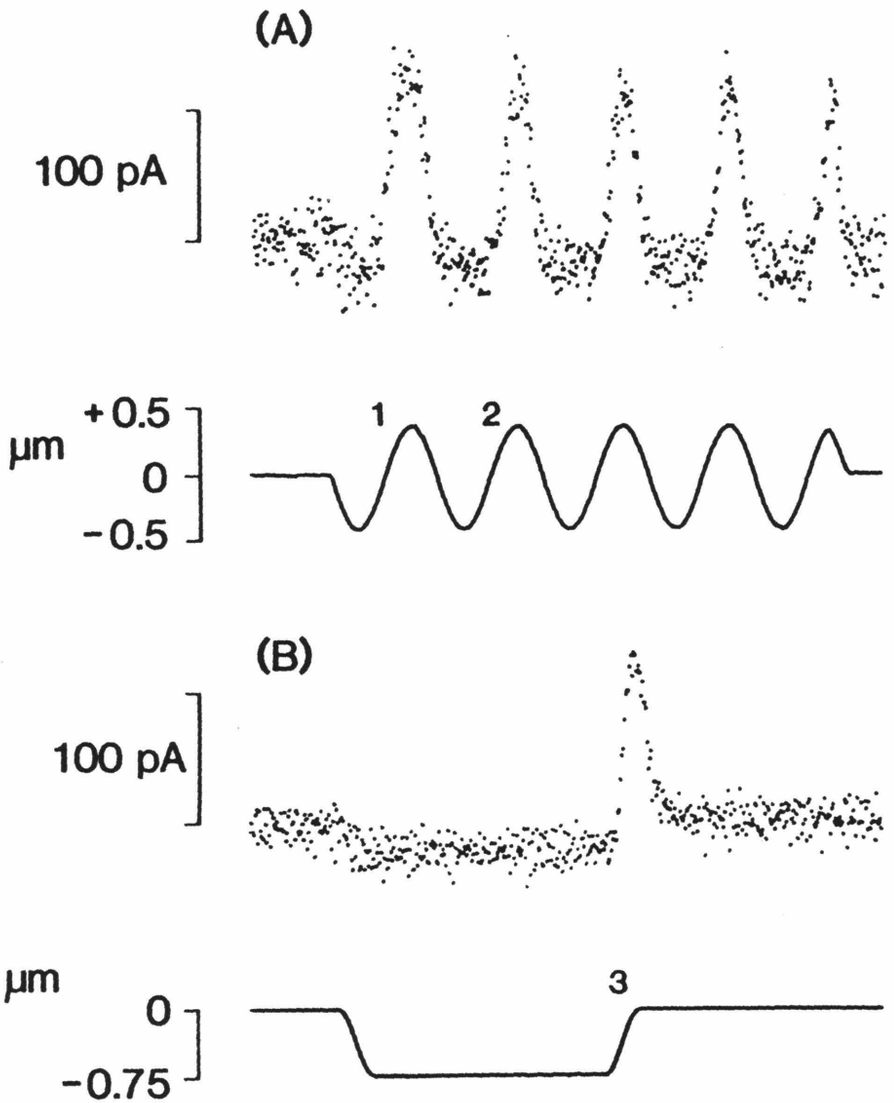
(A)
100 pA
µm
+0.5
0
-0.5
1
2
(B)
100 pA
µm
0
-0.75
3

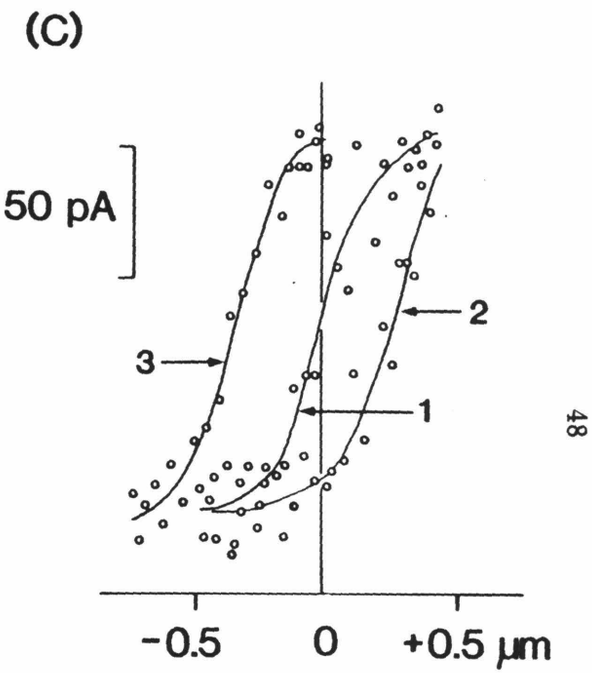
(C)
50 pA
3
2
1
-0.5
0
+0.5 µm

Figure 13. Receptor current in response to positive steps of hair bundle displacement. Again, the current traces are inverted. The upper and lower pairs of traces were obtained from two different cells, both in high-$Ca^{++}$ perilymph, and are averages of 25 and 20 trials, respectively.

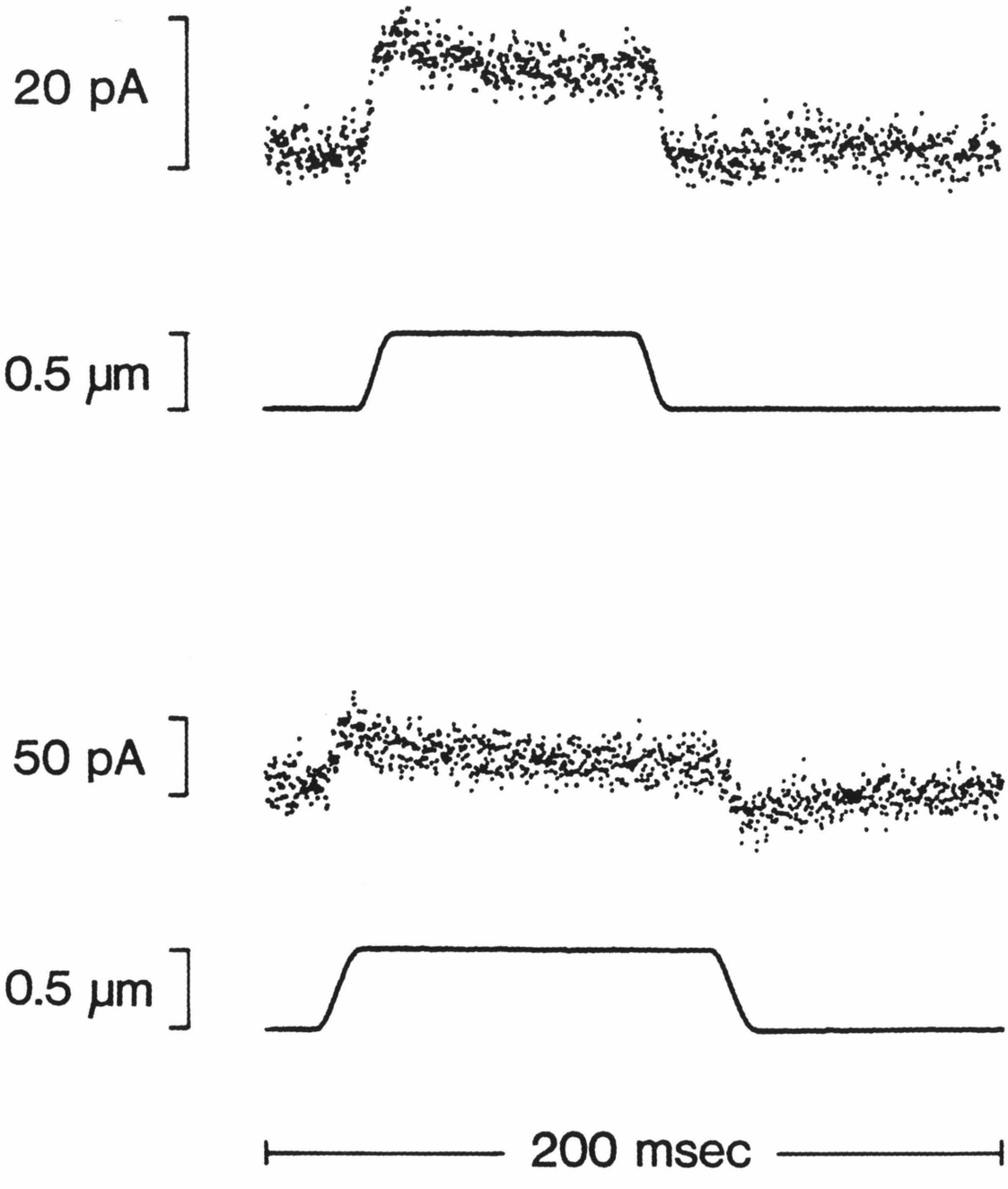
20 pA
0.5 µm
50 pA
0.5 µm
200 msec

**Calcium effects**

Corey (1980) observed that in the in vitro microphonic preparation of the bullfrog sacculus the rate of the operating range shift during an adapting step depended on the concentration of $Ca^{++}$ in the apical bath. I attempted to test this observation in single cells by changing extracellular $Ca^{++}$ levels while recording receptor potential. Changes in $Ca^{++}$ concentration were compensated for by varying $Mg^{++}$, $K^{+}$ or $Na^{+}$ in the other direction. In four experiments, the single-bath chamber was used, and both apical and basal surfaces of the hair cells were exposed to the changes in $Ca^{++}$. In one experiment, the double-bath chamber was used, so that $Ca^{++}$ level could be varied in the apical bath and kept constant in the lower bath. Eight cells were recorded from for long periods, up to an hour, while the different salines were perfused through the chamber. A recording from a cell was always begun in standard saline because elevated $Ca^{++}$ (4 mM) facilitates penetration of cell membranes with microelectrodes.

The operating range shifted negatively when $Ca^{++}$ was lowered, either in the whole bath or in the apical bath alone. To distinguish this shift from the stimulus-induced adaptive shift in operating range, I will refer to it as a shift in the static operating range. This effect was always gradual, continuing over many minutes, and irreversible; the position of the operating range did not recover when the $Ca^{++}$ concentration was changed from a low level (<4 mM) back to the standard level (4 mM) or higher (up to 8 mM). Upon first changing to low $Ca^{++}$, a negative shift could occur without any obvious change in the shape of the displacement-response curve. But with time in the low-$Ca^{++}$ saline, the negative shift would progress, the response range would

decrease, the operating range would increase and the slope sensitivity within the operating range would decrease.

Figure 14 illustrates some displacement-response curves obtained from a cell as the chamber was perfused with salines containing 4 mM $Ca^{++}$, then 0.5 mM $Ca^{++}$ and finally 8 mM $Ca^{++}$. Figure 14(a) compares curves obtained in the three different salines in response to triangle-wave stimuli without any step. After changing from standard 4 mM $Ca^{++}$ saline to 0.5 mM $Ca^{++}$, the cell's operating range shifted negatively and broadened, and the sensitivity and the response range decreased. These trends continued even after the saline was changed from 0.5 mM $Ca^{++}$ to 8 mM $Ca^{++}$. The operating range was about 20% broader in both 0.5 mM and 8 mM $Ca^{++}$ than in 4 mM $Ca^{++}$. In one cell in a double-bath chamber, the static operating range began to shift negatively while the cell was still in the starting saline conditions: 4 mM $Ca^{++}$ in the upper bath and artifical perilymph (1.36 mM $Ca^{++}$) in the lower bath.

The latter observation suggests that the negative shift of the static operating range may be tied somehow to the process of stimulating and recording. Although it is not possible to do the control--assess operating range without stimulating and recording--several observations suggest that lowering $Ca^{++}$ level causes a shift which is enhanced and made irreversible by the invasive intracellular stimulating and recording techniques. First, a similar but reversible effect is observed in the microphonic preparation (Corey, 1980). Second, cells that give robust responses do not show an obvious negative shift in static operating range in the absence of any change in $Ca^{++}$ level. The cell mentioned above, whose operating range shifted in 4 mM $Ca^{++}$, had small noisy responses. Third, cells that were not studied until after

Figure 14. Calcium effects on the displacement-response curve and the adaptive operating range shift. (A) and (B) are from one cell. The preparation was in a one-chamber bath, perfused with perilymphs of different calcium content. Changes in $Ca^{++}$ concentration were compensated by adjusting $K^{+}$. (A) shows displacement-response curves in 4 mM, 0.5 mM and 8 mM $Ca^{++}$. The upper and lower plots in (B) were obtained in 4 mM and 0.5 mM $Ca^{++}$, respectively. Each shows the cell's displacement-response curve at the onset of a +0.54 μm step (time zero) and 1 s later, just before the offset of the step.

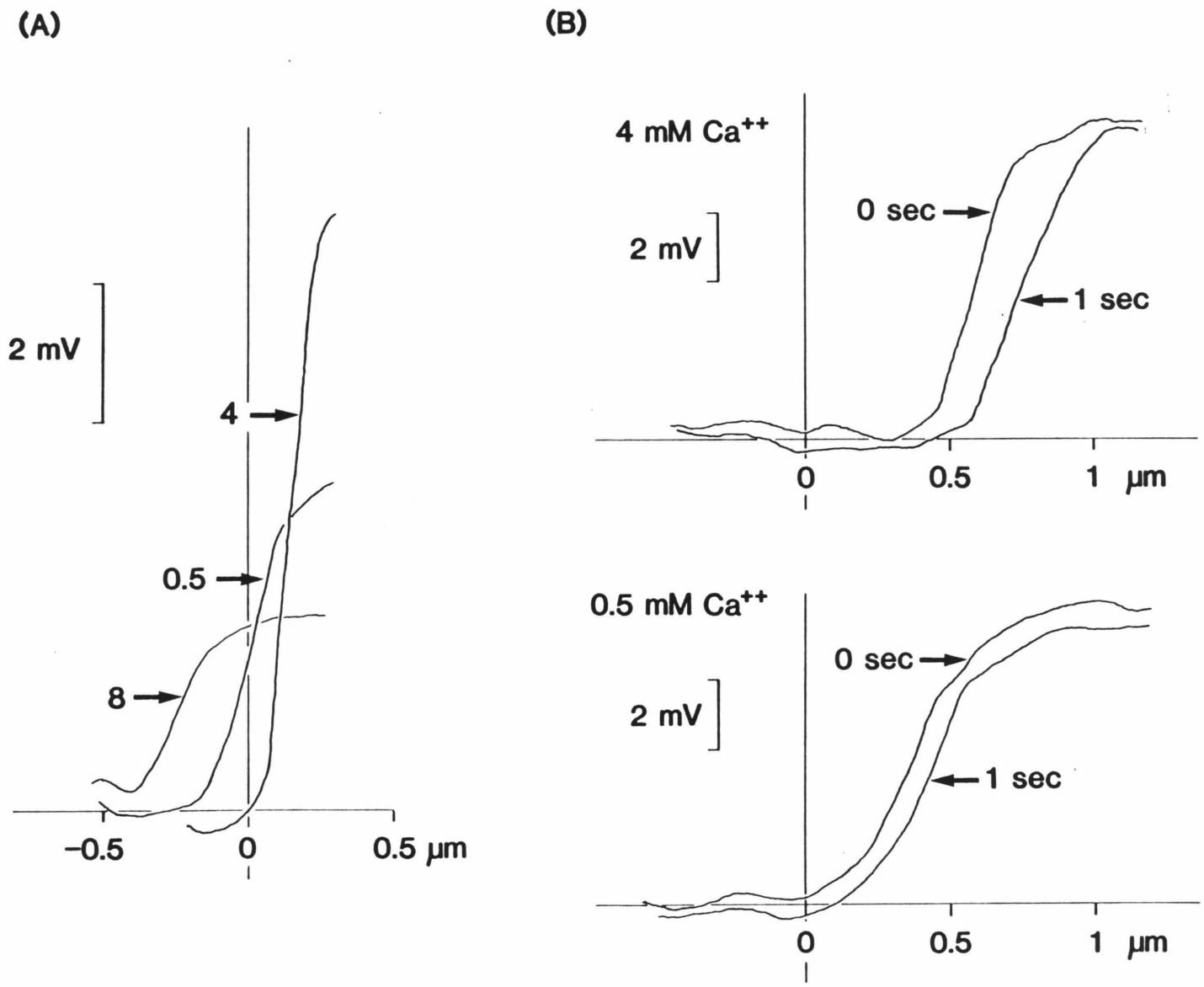
(A)
2 mV
4
0.5
8
−0.5
0
0.5 µm
(B)
4 mM Ca++
2 mV
0 sec
1 sec
0
0.5
1 µm
0.5 mM Ca++
2 mV
0 sec
1 sec
0
0.5
1 µm

the whole preparation had been through several changes of $Ca^{++}$ underwent negative shifts in static operating range when $Ca^{++}$ was lowered while they were being studied. Although their operating ranges may have been affected by $Ca^{++}$ changes that occurred before they were studied, the effects were either reversible or not saturating.

Lowering $Ca^{++}$ reduced the occurrence of adaptive operating range shifts but in an erratic and irreversible fashion. Figure 14(b) compares displacement-response curves obtained from the cell of 14(a) during +0.54 μm steps in 0.5 and 4 mM $Ca^{++}$ saline. The operating range shifted 36% of the step in 4 mM $Ca^{++}$ and not at all in 0.5 mM $Ca^{++}$. During a -0.54 μm step, the curve shifted 42% in 4 mM $Ca^{++}$ and 23% in 0.5 mM $Ca^{++}$. The positive operating shift during a gated triangle-wave stimulus was 76% greater in 4 mM $Ca^{++}$ than in 0.5 mM $Ca^{++}$. In another cell, positive shifts in operating range occurred during positive steps and at the onset of a triangle-wave stimulus in 4 mM $Ca^{++}$ but not after the calcium level was reduced to 0.1 mM. (Negative steps were not tested in this cell.) In a third cell, lowering $Ca^{++}$ from 4 mM to 2 mM did not affect the percentage shift during a negative step which was about 40%. However, the shift during a positive step decreased from 100% in 4 mM to about 50% in 2 mM $Ca^{++}$. This cell was in a double chamber so that only the apical $Ca^{++}$ level was changed.

# CHAPTER 2

## Adaptation in Hair Cell and Primary Neuron Responses *In Vivo*

### Methods

The experimental animals were young American bullfrogs, *Rana catesbeiana*, 75-150 g, as in the *in vitro* experiments. In 27 experiments, I recorded the *saccular microphonic potential*: a stimulus-evoked potential difference between the endolymphatic chamber of the sacculus, housing the otoconia, otolithic membrane and endolymph (figure 1), and an indifferent electrode inserted in tissue near the otic capsule. We assume that the stimulus-evoked potential results from currents flowing across the apical membranes of the saccular hair cells which face the endolymphatic compartment. This assumption is based on analogy with the microphonic potential recorded with equivalent techniques in other hair cell organs (Furukawa *et al.*, 1972; Dallos, 1973) and *in vitro* from the excised bullfrog sacculus (Corey, 1980). The currents underlying the microphonic potential are presumably the receptor currents and currents that arise secondarily due to voltage or ionic changes caused by the receptor currents. In 14 experiments, single-unit activity was recorded extracellularly from a total of 35 neurons in the saccular nerve. Intracellular recordings were made from 71 saccular nerve fibers in another 14 experiments. In three of the latter experiments, saccular microphonic potential was recorded as well.

Before surgery, the bullfrog was anaesthetized by immersion for about 30 min in a solution of tricaine methanesulfonate (trade name: MS-222) in water (1.5 g/l). During surgery and recording, the animal was periodically wetted with the tricaine solution. Often, it was

necessary to supplement the tricaine with intraperitoneal injections of between 0.03 and 0.08 ml of 50 mg/ml sodium pentobarbital (Nembutal); no more than 0.03 ml was administered at a time.

The most straightforward surgical approach to the sacculus and the saccular nerve is the ventral approach through the roof of the mouth. Because the electrode holder was mounted above the frog, ventral exposure of the the sacculus meant that the frog had to be upside-down during recording. As the otoconial mass lies dorsal to the sensory macula, we initially were concerned that responses recorded from an upside-down frog would differ from responses recorded from a frog in the more normal prone position. To check this possibility, a dorsal surgical approach was taken in 13 of the experiments on saccular microphonic potential and in nine of the experiments in which extracellular primary neuron activity was recorded. There was no obvious difference between results obtained with the ventral and dorsal approaches, so the data have been pooled. I will describe first the dorsal and then the ventral surgical approaches.

To expose the dorsal aspect of the sacculus for microphonic recording, muscle and bone overlying the otic capsule, about 1 cm lateral to the midline and at the rostro-caudal level of the eardrum, were removed. The large white otoconial mass of the sacculus was then visible, ventral to the horizontal semicircular canal. The membranes bounding the perilymphatic and endolymphatic compartments were perforated to allow passage of a microelectrode. The hole in the membrane enclosing the endolymphatic compartment was made as small as possible since too large a hole would result in an insignificant potential difference between the endolymph and the extracellular fluid

surrounding the indifferent electrode. The dorsal approach to the saccular nerve was about 5 mm lateral to the midline. Here the cranial bone had to be removed very carefully because immediately below it courses a large blood vessel associated with the endolymphatic sac. Retraction of the blood vessel exposed the central trunk of the eighth nerve and the medial wall of the otic capsule. The vestibular ganglia are located just medial to the otic capsule; distal to the ganglia, just before entering the otic capsule, the eighth nerve splits into an anterior and posterior ramus. The saccular branch is the most posterior division of the anterior ramus and is the first to split off from the ramus. The majority of saccular fibers split off first (most posteriorly) in a thin sheet; these are joined near the saccular macula by a small branchlet which separates from the main ramus a little more anteriorly. Recordings were made distal to the vestibular ganglia because the distal portion of the saccular nerve can be identified unambiguously while the central portion is part of the eighth nerve trunk (figure 3). To expose the distal saccular nerve, I removed the medial wall of the otic capsule.

In the ventral approach (figure 3), the lower jaw and muscle overlying the otic capsule were removed. To record microphonic potential, I opened the ventral wall of the capsule over the otoconial mass and, again, perforated the membranes surrounding the otoconia to facilitate insertion of microelectrodes. For extracellular recording from saccular fibers, the otic capsule was left intact over the otoconial mass and was opened just over the distal saccular nerve. To record intracellularly from saccular fibers near their terminals, I made

the opening over the saccular macula and the most distal third of the saccular branch.

During the experiment, the anaesthetized frog was secured to a small platform on an electromagnetic shaker (Ling Shaker Model 408) which provided accelerational stimuli along a vertical axis. Figure 15 shows the set-up for dorsal recording. In order to minimize uncontrolled accelerational stimuli to the frog, it was important that it be well-coupled to the shaker. Its head was held in place with three clamps, one on the snout and one on each side of the jaw. In experiments using the ventral approach, the head was pressed upside-down into a plasticine mold, clamped at the snout and further secured with tape. The body of the frog also was taped down. The electrode holder was mounted on posts attached to the platform and advanced by a simple hydraulic microdrive. Microelectrodes were glass, filled with 3 M KCl, and had resistances between 40 and 100 MΩ for intracellular recording from fibers and between 5 and 40 MΩ otherwise. Potentials were recorded with a high-impedance DC preamplifier (Grass Instruments, Model P18), amplified, and in most experiments, stored on magnetic tape with an FM tape recorder (Hewlett-Packard, Model 3968A; passband DC to 1.25 kHz). In some of the microphonic experiments, data were averaged on-line with a computer (Digital Equipment Corporation, Model PDP 11/34). The averaging program, written by J. H. R. Maunsell, had a resolution of 50 μs. I averaged tape-recorded microphonic data and post-synaptic potentials from saccular fibers with the same program. Impulse (spike) activity of the saccular fibers was analyzed with a peri-stimulus time histogram program written by A. Moiseff.

Figure 15. The set-up for dorsal recording of the saccular microphonic potential and primary neuron activity.

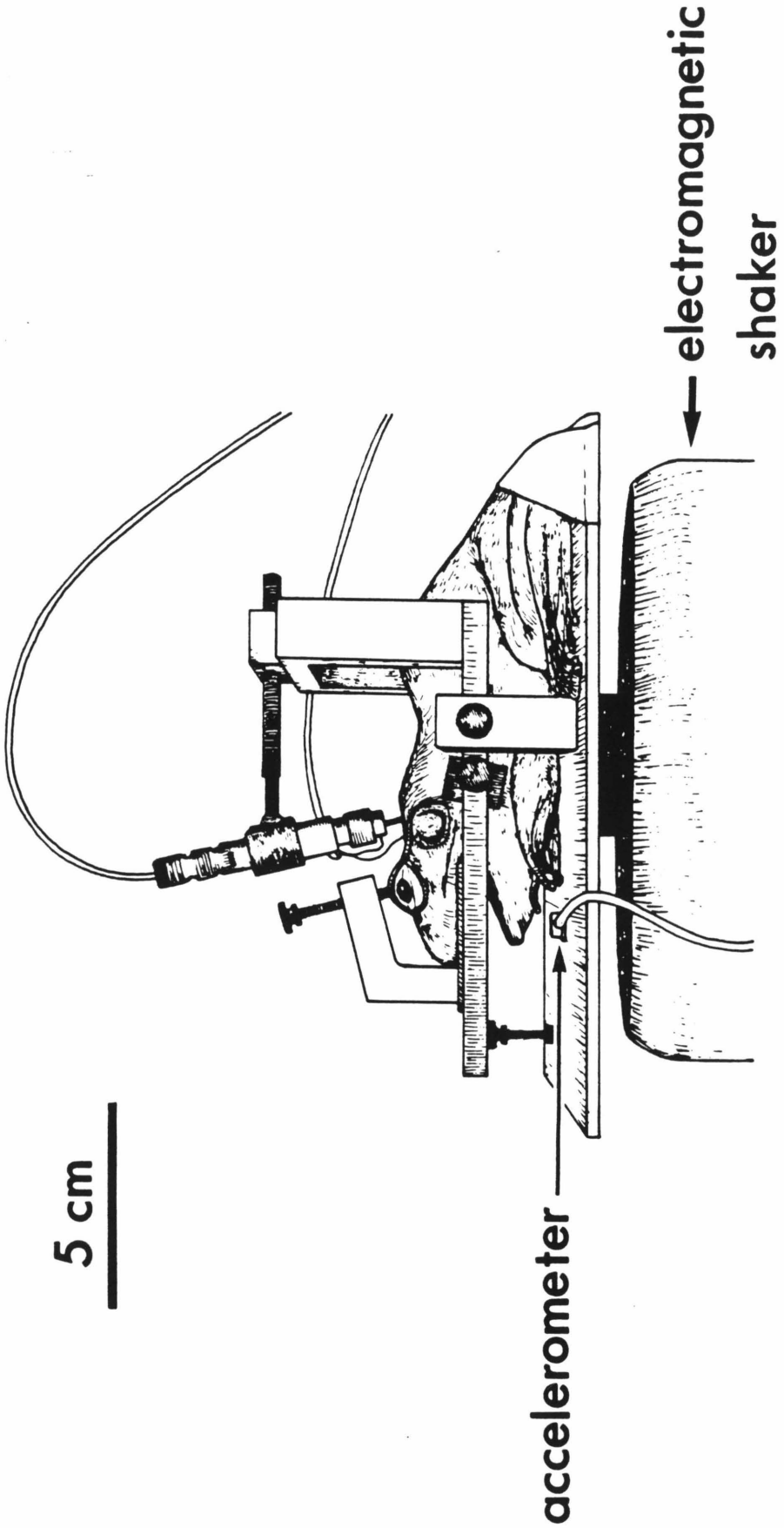
electromagnetic
shaker
accelerometer
5 cm

The shaker was driven with square waves (i.e., up-and-down steps) between 5 and 30 Hz or with sinusoids between 5 and 120 Hz. A miniature piezoresistive accelerometer (Endevco Model 2264-150) mounted on the platform with the frog monitored acceleration and provided feedback to the shaker driver to improve the response of the shaker to step (square-wave) inputs. Even so, step input to the shaker had to be filtered to prevent ringing at the transitions. As a result, the acceleration "steps" presented to the frog were not true steps but had rise times of 3-6 ms. Stimuli, expressed as the modulation of the steady-state acceleration due to gravity, were between 0.01 and 0.1 g in amplitude. The noise floor was quite high, about 0.003 g, which is well above the thresholds of the more sensitive saccular fibers (Lewis et al., 1982). Also, the plateau phases of individual steps often were not flat but showed nonsystematic noise above the 0.003 g level: transients and occasional rippling. Finally, turning up the accelerometer feedback to the shaker introduced a low-frequency drift, at about 0.2 Hz, in the position of the platform. Since none of these noise sources were stimulus-locked, their effects were minimized by averaging the recorded responses.

All surgery and experiments were done at room temperature, 22°C. In three microphonic experiments, I varied the temperature of the otic capsule by pipetting artificial perilymph of different temperatures between 10 and 40°C onto it. A Bailey Instruments digital thermometer (Model BAT-8) monitored temperature. In one experiment, the thermistor probe (Bailey Instruments, Model IT-1E: exposed sensory, 0.65 mm diameter) was placed in the ipsilateral middle ear cavity. In the other experiments, it was press-fit into a hole in the anterior wall of the

otic capsule, placing the exposed sensor within 0.5-1 mm of the sacculus.

**Results**

**(i) Saccular Microphonic Potential**

The stimulus-evoked potentials recorded inside the otoconial mass were small, in the range of .1 to 2 mV. The concern exists with such small potentials that they are partly or wholly artifactual. In particular, mechanical (bending) artifacts may be expected, given the combination of vibratory stimuli and flexible electrodes. Although bending artifacts occurred under certain conditions, several considerations make it unlikely that the potentials that have been analyzed were artifactual. First, they disappeared when the animal died. Second, if too large a hole was made in the membrane bounding the otoconia, no potential was detected even under intense stimulus conditions. This would be expected for a potential difference between the endolymphatic and perilymphatic compartments but not for an artifactual potential due to motion of the electrode tip. Third, the potentials were localized to the sacculus and were negative-going, as expected for excitatory responses recorded extracellularly from hair cells. (As will be discussed shortly, in vitro studies of hair cell responses predict that excitatory responses should dominate the microphonic potential.) Fourth, at least one feature of the recorded potentials had a thermal $Q_{10}$ of about 2, in common with many processes in living cells. Finally, sinusoidal stimulation evoked a kind of response which is characteristic of many hair-cell organs and cannot easily be explained as a stimulus artifact, commonly referred to as a "2f response".

In many hair cell organs, a sinusoidal stimulus evokes a microphonic potential which looks like a distorted sine wave at twice the input frequency, hence the term "2f response" (Flock, 1971). An example from the present study appears in figure 16(a). (In all figures in this report the microphonic potential is inverted, so that negative-going potentials, corresponding to net depolarization of the cells, are shown as upward. The relevant feature that 2f-producing organs have in common is hair cells that are not uniformly oriented. Organs whose hair cells all have the same orientation, such as the lateral line organ and the mammalian cochlea, produce a "1f" response, that is, the frequency of the microphonic potential equals that of the sinusoidal input. The 1f response reflects the fact that the orientation of a hair cell defines the directionality of its response. Thus, hair cells of similar orientation depolarize in response to the same stimulus set, hyperpolarize to a second set of stimuli, and are unaffected by all others (Shotwell et al., 1981). All hair cells in a uniformly-oriented organ depolarize during whatever portion of the sinusoidal stimulus has a component in the direction of their orientation vector (e.g., figure 11). Because the excitatory portion of the sine wave occurs once per cycle, the microphonic potential is 1f.

In the next most simple case, hair-cell organs are bidirectional, that is, have cells of two, opposing, orientations. The excitatory responses of the opposing hair cell populations to a sine wave are 180° out of phase with each other. In other words, the excitatory response of one population is in phase with the inhibitory response of the other population. If a sinusoidal stimulus is small enough to fall within the cell's operating ranges, at any given time it will evoke approximately

Figure 16. The "2f" saccular microphonic potential. (A) and (B) The averaged microphonic potential (upper trace in each pair) has been inverted to facilitate comparison with intracellular receptor potentials. The stimulus traces are the signal of the accelerometer, averaged over the same interval as the responses. The stimuli are (A) sinusoidal vertical acceleration, 35 Hz, and (B) vertical steps of acceleration. (A) and (B) were recorded in different animals. (C) Schematic illustration of the bullfrog saccular macula, showing hair cell orientations.

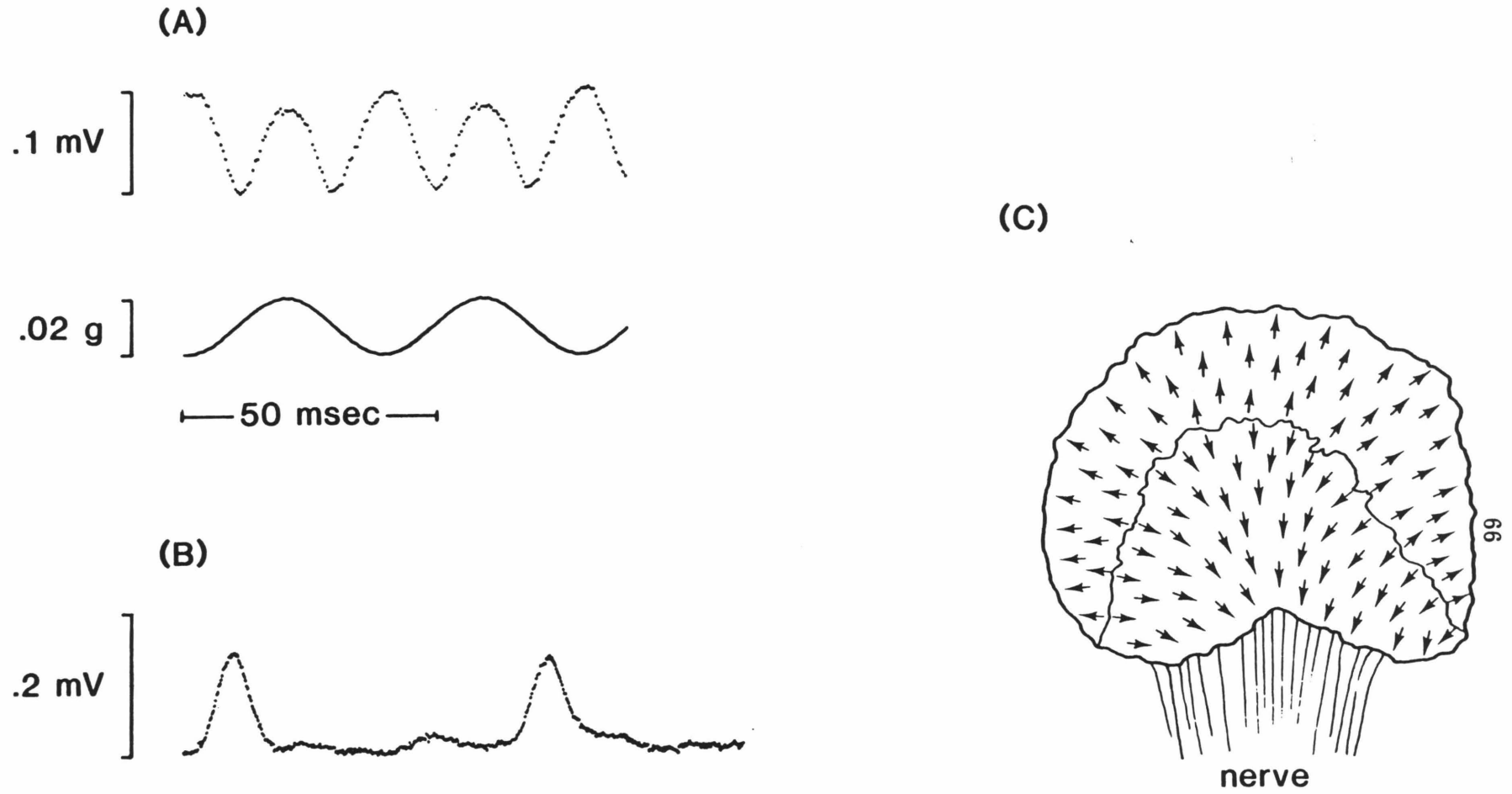
(A)
.1 mV
.02 g
50 msec
(B)
.2 mV
.02 g
50 msec
(C)
nerve
66

equal excitatory and inhibitory responses which will tend to cancel out the microphonic potential. But if the stimulus is saturatingly large, it evokes a greater excitatory than inhibitory response. Then net excitatory responses of the opposing orientations occur 180° out of phase, and a 2f microphonic potential is recorded. In any organ with opposing hair cell orientations, the extracellular excitatory response of one population is attenuated by the hyperpolarizing response of the inhibited cells. Microphonic data from hair cell organs usually are recorded in response to sinusoidal or impulsive stimuli, but one would expect that an effective alternating stimulus of any waveform, e.g., the square wave used in this study, would evoke a 1f or 2f response depending on the same considerations of hair cell geometry invoked above.

The bullfrog sacculus also produces a 2f response although it is not simply bidirectional. The array of orientations spans a full 360°, as illustrated schematically in figure 16(c). Hair cells of opposing orientations are arranged along a border sometimes called the striola. The 2f response arises because any stimulus with a component parallel to the plane of the macula, no matter what its orientation, will depolarize approximately as many cells as it hyperpolarizes. For example, a stimulus directed away from the nerve would hyperpolarize, to varying degrees, most cells on the neural (proximal) side of the striola and would depolarize all cells on the abneural (distal) side. If the stimulus saturates the cells' operating ranges, the net depolarization of the abneurally located cells exceeds the net hyperpolarization of the other population and a negative-going extracellular potential, the microphonic potential, ensues. Thus the microphonic potential recorded

from an organ with opposing hair cell orientations is attenuated by the hyperpolarizing response of the inhibited cells.

The primary objective of these experiments was to determine the response of saccular hair cells to a step of acceleration, for comparison with their *in vitro* responses to steps of hair bundle displacement. Figure 16(b) shows a representative record of averaged microphonic potential during one cycle of a square wave, effectively a positive step followed by a negative step. After the onset of either step, the response rose to a peak then during the step decayed smoothly. Usually the response decayed to, or undershot, the original potential. Often this was followed by low-frequency oscillations, particularly if the potential undershot its pre-step value. Thus the hair cells *adapt* 100% to a new constant level of acceleration. In other words, they detect the time derivative of acceleration or "jerk." The latency between stimulus and response onsets was on the order of 1-3 ms and the peak of the response lagged the end of the rising phase of the step by 2-4 ms. The response decline occurred over about 10-15 ms. Some factors that affect this time course have been identified, but first let us compare *in vivo* microphonic potential during an acceleration step with *in vitro* hair cell responses during step hair-bundle deflections.

Figure 17 compares (a) the microphonic potential during a +0.02 g step of acceleration with the intracellular receptor potential (b) and receptor current (c) during step displacements of the hair bundles. The rate of response decline is much faster in (a) and (c) than in (b). Adaptation of the microphonic potential was reliable and fast, usually complete within 10-20 ms. By contrast, the intracellular data were much

Figure 17. Comparison of in vivo and in vitro adaptation of hair cell responses. (A) shows the averaged saccular microphonic potential in response to a +.0.02 g step of acceleration. (B) is the receptor potential recorded in vitro in response to a +0.35 µm displacement of the hair bundle. (C) is the receptor current in response to the offset of a -0.75 µm step displacement of the hair bundle. (B) and (C) are the same data as in figures 5 and 12(B), respectively.

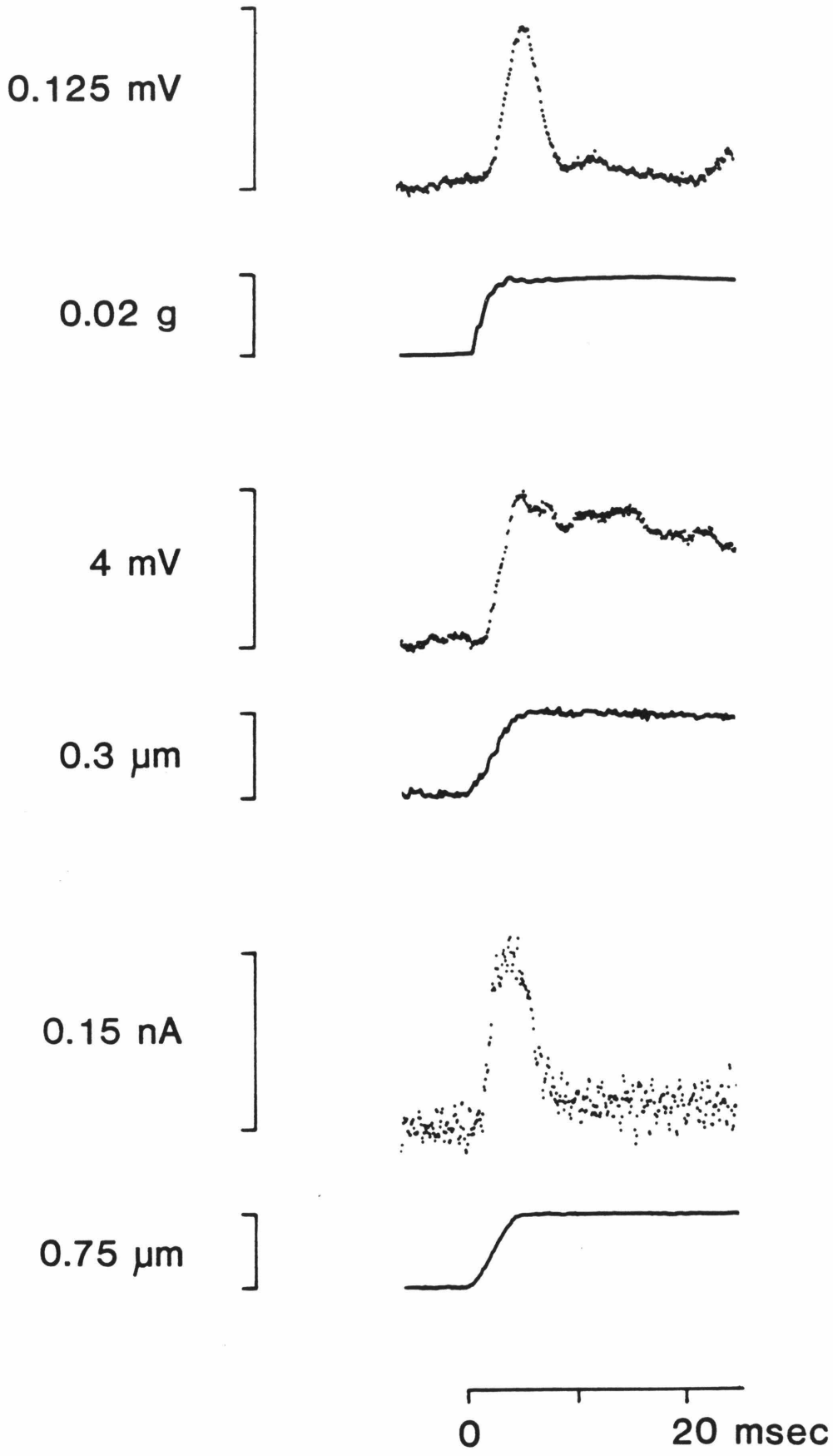
0.125 mV
0.02 g
4 mV
0.3 µm
0.15 nA
0.75 µm
0
20 msec

more variable and usually slower. The adaptation rate in (c) was the fastest in vitro rate observed. Another difference is that in my hands the intracellular responses did not tend to ring, although by optimizing recording techniques, ringing can frequently be seen in vitro (Lewis and Hudspeth, 1983a,b). Finally, the latency of the response to acceleration was on the order of a few ms, whereas that of the in vitro microphonic current to displacement of the otolithic membrane is in the range of a few tens of μs (Corey and Hudspeth, 1979a). Potential factors in the differences can be grouped into three main classes: (1) the mechanisms (processes) underlying the observed response declines, (2) experimental techniques and conditions, and (3) the physiological states of the cells. If differences in the third category occur, they presumably arise because of differences in the second category, some of which are known.

Does the cellular adaptation described in vitro, involving a shift in operating range, contribute to the adaptation of the microphonic potential? The differences between the two preparations limit our ability to answer this question. In vivo we cannot define the operating range directly in terms of hair bundle displacement, but must be content to measure the range of accelerations to which the hair cells are sensitive ("effective" accelerations). My approach has been to determine whether, during an acceleration step, the microphonic potential undergoes an adaptive shift in the range of effective accelerations (to avoid confusion, I will use "operating range" only in reference to hair bundle displacement in vitro, not to acceleration stimuli). A positive result is necessary but not sufficient to show that the decline of the microphonic potential is due to the adaptive mechanism observed

*in vitro*. A shift in the range of effective accelerations could have a noncellular origin, i.e., could result from mechanical relaxation of the input to the hair bundles rather than a shift in the operating range of hair bundle displacement. Despite these problems, it was worthwhile to look for an adaptive shift of the microphonic potential because a negative result would cast doubt upon the functional significance of the *in vitro* operating range.

To test for an adaptive shift in the range of effective accelerations, I applied a comparatively brief test step at various times relative to the onset of a longer adapting step. The response of the population of cells excited by the test step was observed during adapting steps that were either excitatory or inhibitory for that population. As was observed *in vitro*, the rate of adaptive shift was slower during an inhibitory adapting step than during an excitatory step of equal amplitude. In the experiment of figure 18(a), an upward test step was applied at various times during an adapting step of downward acceleration. The response (of the cells that depolarize during upward acceleration) to the test step gradually increased. In 18(b), the time courses of the adaptive shift in figure 18(a) and of the rate of response decline to an excitatory adapting step of equal amplitude are normalized and graphed together.

Another way in which the adaptive shift of the microphonic potential is similar to that of the *in vitro* response is that it is proportional to stimulus amplitude. Figure 19 compares the microphonic potentials recorded during four acceleration steps of different amplitude. The normalized responses decay with similar time courses. Since the adaptive shift closely parallels the response decline

Figure 18. Adaptive shift in the range of effective accelerations during an inhibitory adapting step. (A) Excitatory test steps were superimposed on an inhibitory adapting step (-.007 g) at different times relative to the onset of the adapting step. (B) The time course of the changes in the response to the test step during the adapting step (open circles) is expressed as percent of the test response with no adapting step. The solid curve is the time course of the response decline during an excitatory adapting step that was also .007 g.

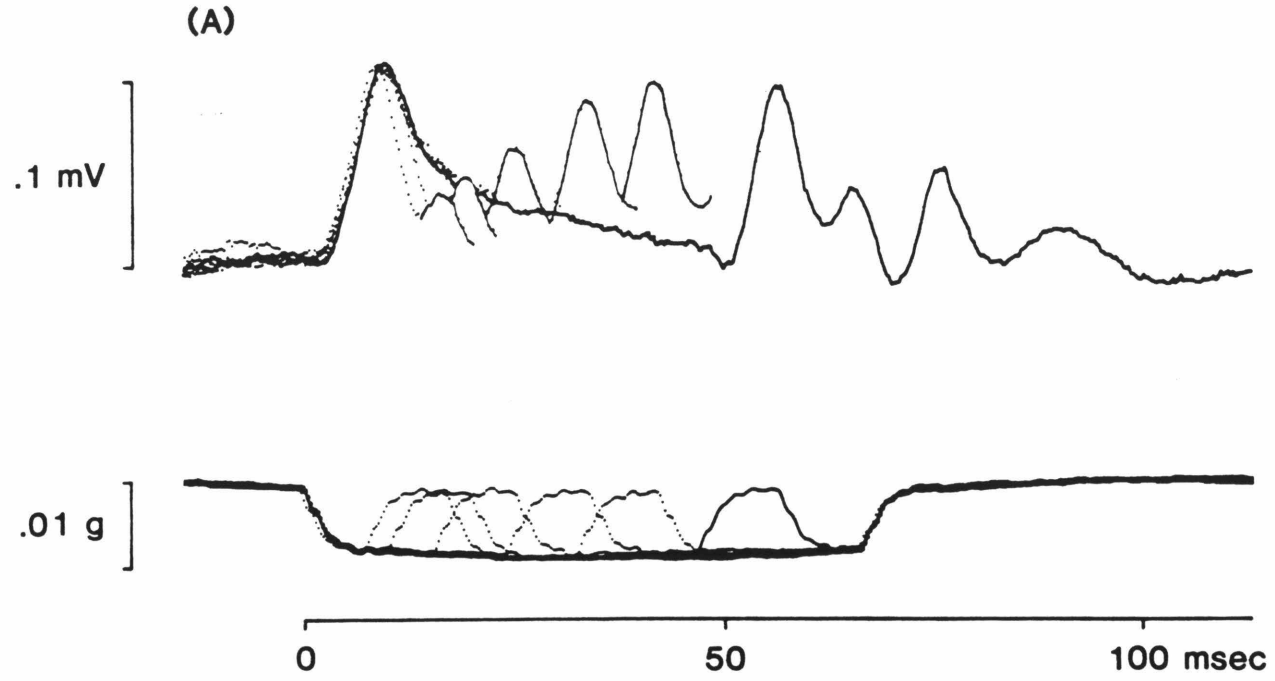
(A)
.1 mV
.01 g
0
50
100 msec

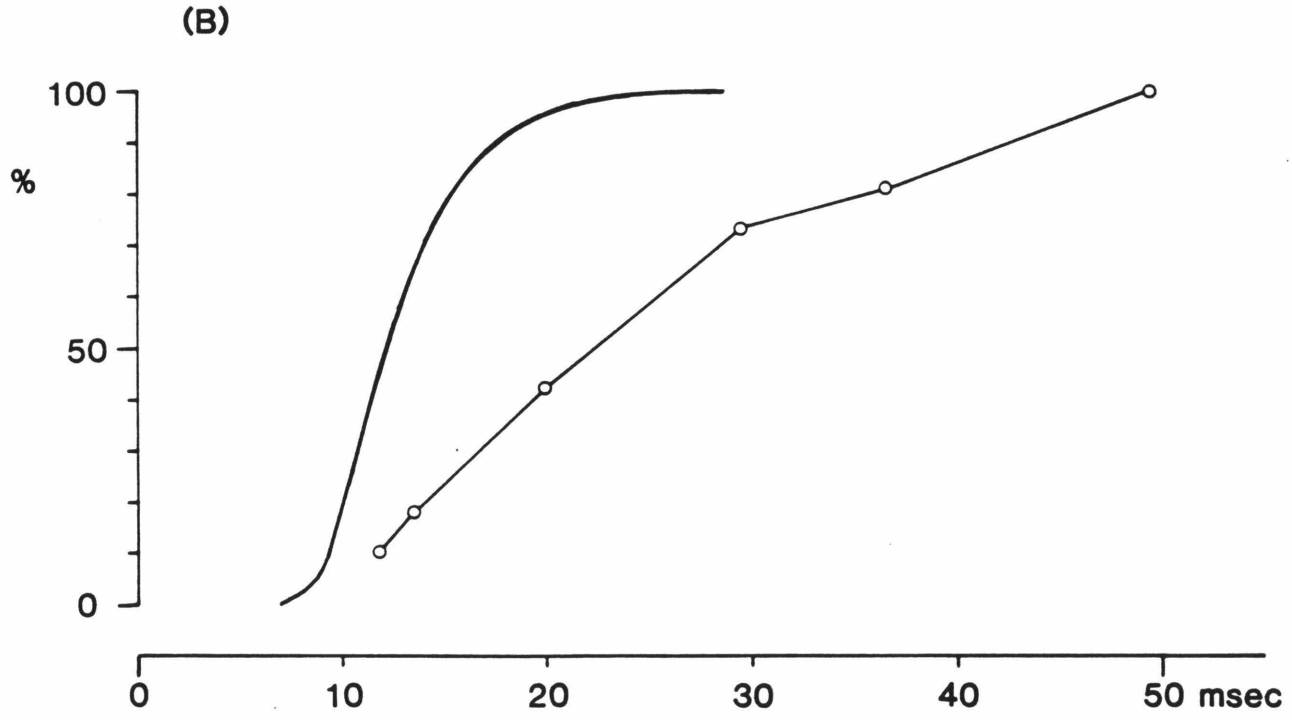
(B)
100
%
50
0
0
10
20
30
40
50 msec

Figure 19. Adaptation of the saccular microphonic potential to acceleration steps of different amplitude. (A) The responses are presented in order of increasing stimulus amplitude, from top to bottom. The stimuli, superimposed below the response traces, were .011 g, .019 g, .022 g, and .032 g (total amplitude of each transition). (B) The responses to each positive step in (A) (the second response in each trace in (A)) have been normalized to the same height. The responses to the three largest steps (solid lines) virtually superimpose when normalized; the response to the smallest step (dots) diverged slightly from the others. Taking the beginning of the step as time zero, the response decayed to 1/e of its peak value in 14.2 ms for the smallest step and 13.6 ms for the other three.

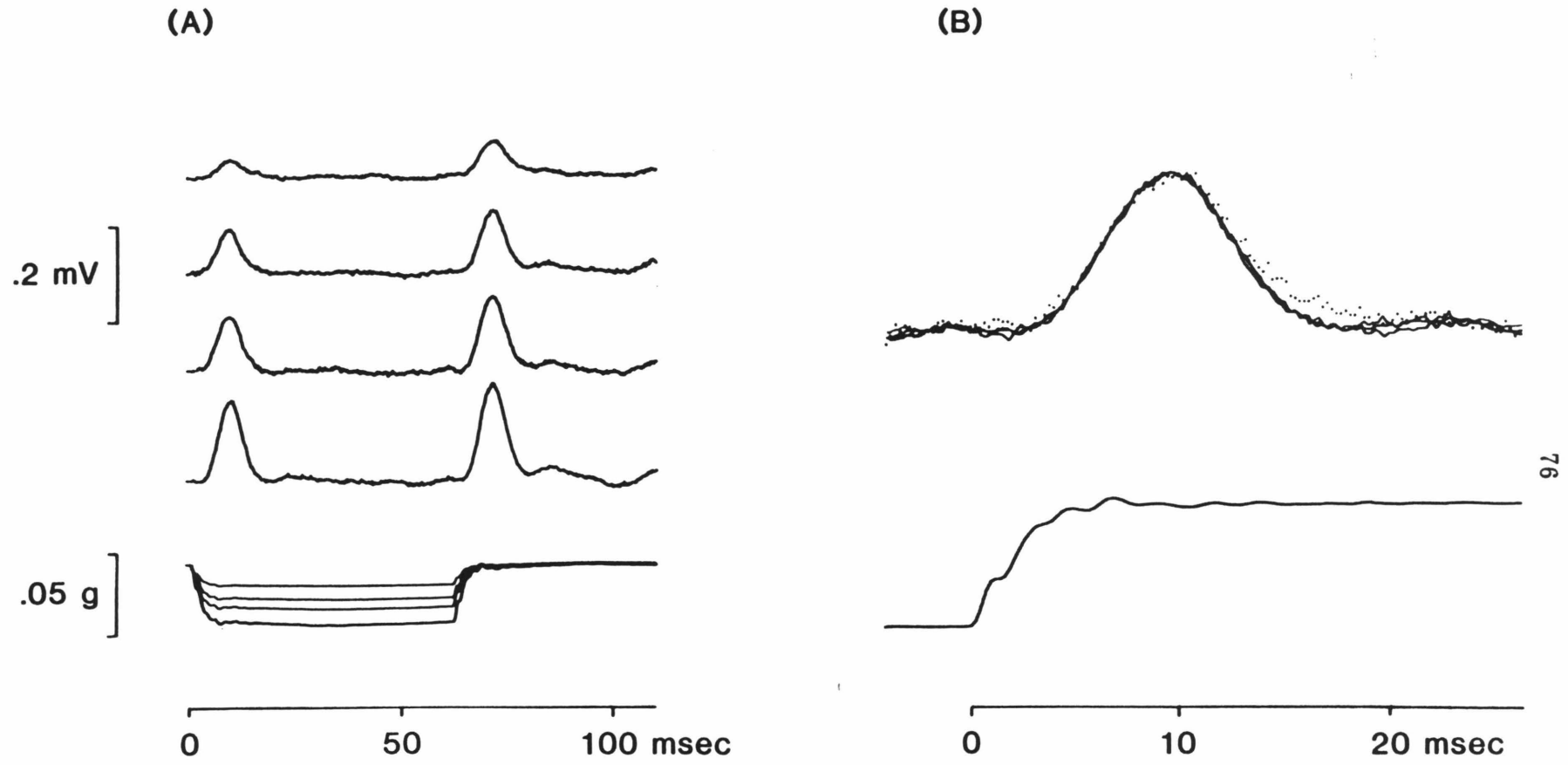
(A)
.2 mV
.05 g
0
50
100 msec
(B)
0
10
20 msec
76

(figure 18), the rate of adaptive shift in absolute (not normalized) units varies linearly with stimulus amplitude.

The temperature dependence of the decay of the microphonic potential during an acceleration step was examined in three experiments. While warm or cool saline was pipetted onto the otic capsule, temperature was monitored in the ipsilateral middle ear in one experiment, in the otic capsule in one, and in both places in the third. The effect of temperature change on the rate of adaptation of the microphonic potential was somewhat variable, suggesting that the temperature being monitored was an unreliable indicator of the temperature at the site of adaptation. In the experiment in which temperature was monitored in both the middle ear and the otic capsule, within 0.5 mm of the sacculus, an effort was made to record data only after temperature stabilized at a new level. Probably the most reliable temperature series obtained in this experiment is shown in figure 10. To estimate thermal $Q_{10}$ values from these data, the time between step onset and the decay of the response to 1/e of its peak value was determined and its reciprocal taken as an estimate of adaptation rate. The rate of one record was then compared with the rate of the next record in the sequence to obtain one $Q_{10}$ value. For the series of figure 20, $Q_{10}$ values ranged from 1.16 to 2.96, with a mean value of 1.97 (standard error = 0.65). This value is comparable to the $Q_{10}$ of between 2 and 3 estimated for the rate of adaptation of the _in vitro_ microphonic current (Corey, 1980).

To recapitulate, the adaptation of the microphonic potential appears analogous to the cellular adaptation described _in vitro_ by four criteria: (1) the response decline (adaptation) to a constant stimulus

Figure 20. Temperature dependence of the adaptation of the microphonic potential during acceleration steps. Temperature was monitored inside both the otic capsule and the ipsilateral middle ear. The averages are presented, from top to bottom, in the order in which they were taken. The number of trials averaged at each temperature was between 50 and 100; the entire series took about 30 minutes.

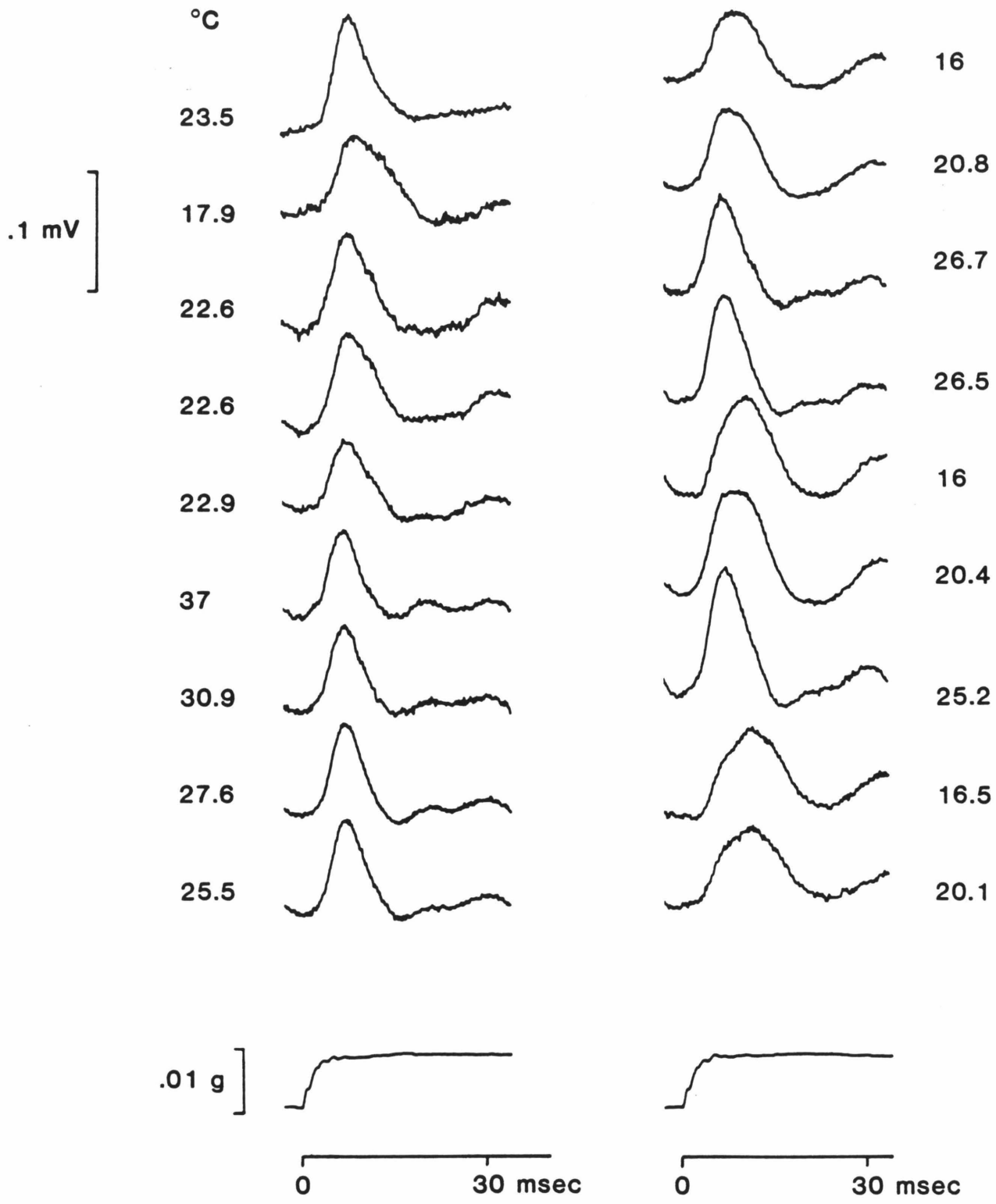
°C
23.5
17.9
22.6
22.6
22.9
37
30.9
27.6
25.5
16
20.8
26.7
26.5
16
20.4
25.2
16.5
20.1
.1 mV
.01 g
0
30 msec
0
30 msec

can be attributed largely to the adaptive shift; (2) the shift during a negative stimulus is initially slower than that during a positive stimulus; (3) the rate of adaptive shift (in absolute stimulus units) for stimuli of a given polarity is approximately proportional to stimulus amplitude; (4) the temperature dependence of the rate of shift appears to be greater than 1.5.

**(ii) Primary Neuron Recordings**

The microphonic potential data indicate that adaptation is a prominent feature of the averaged response of the saccular hair cell population. How variable is this feature within the population? This question was addressed by recording from primary saccular neurons, which sample from subsets of the hair cell population. One possibility was that some neurons would not adapt to acceleration steps; this would allow us to make some inferences about the gross motion of the sacculus, and would be of great interest in terms of hair cell heterogeneity within the sacculus. Primary neuron data also allow us to assess the importance of adaptation, especially of the adaptive shift in stimulus range, in the output of the organ. For example, it was plausible that the shift in effective acceleration range observed at the hair level would be overwhelmed at higher levels by other adaptation mechanisms, such as synaptic adaptation or refractoriness of spike-generating processes.

The primary neuron experiments fall into two categories, both in terms of what was recorded and the kinds of questions answered. In the first experiments that I will discuss, graded postsynaptic responses of primary neurons were recorded in order to look at information transfer

across the synapse. Averaging the response of a single neuron to an acceleration step over many trials provided a record that could be compared to the microphonic potential data. The comparison is of rates of response decline (adaptation) during a step. The second kind of experiment looked for adaptive shifts in postsynaptic responses by recording extracellular spike activity of single neurons during combinations of adapting and test steps.

The intracellular activity recorded near the terminals of TTx-treated saccular neurons is characterized by frequent depolarizing events (excitatory postsynaptic potentials, epsp's) or variable amplitude. Depending on the extent of the TTx block, the larger events might develop into regenerative responses. The activity in a single fiber during acceleration steps is shown in figure 21(a). By averaging together sweeps in which no regenerative activity could be discerned, a probability profile of the graded postsynaptic activity during a step is obtained; that is, when the average has a high value, there is a high probability of an epsp at that time relative to the stimulus. Averaging revealed that, in general, the afferent terminals depolarized during steps of one or the other polarity, not both. Like the microphonic potential, the averaged postsynaptic potential during an excitatory step always rose to a peak, then adapted (figure 21b). Oscillations, lower in amplitude and slower than the initial (onset) response, often followed it (figure 21b). The rate of decay of the onset response was proportional to stimulus amplitude, at least for stimuli within the linear working range of the neuron (figure 22).

The averaged postsynaptic data also revealed hyperpolarizing responses to acceleration steps. In some averages, a comparatively

Figure 21. Graded postsyaptic activity in a saccular nerve fiber during acceleration steps. Over a period of an hour prior to these records, 0.15 ml of a solution of tetrodotoxin (TTx) in artificial perilymph ($10^{-5}$ g/l) had been applied topically to the nerve, in three aliquots. (A) shows a single sweep. (B) is an average of 100 sweeps like that shown in (A). No spikes occurred during the averaging interval.

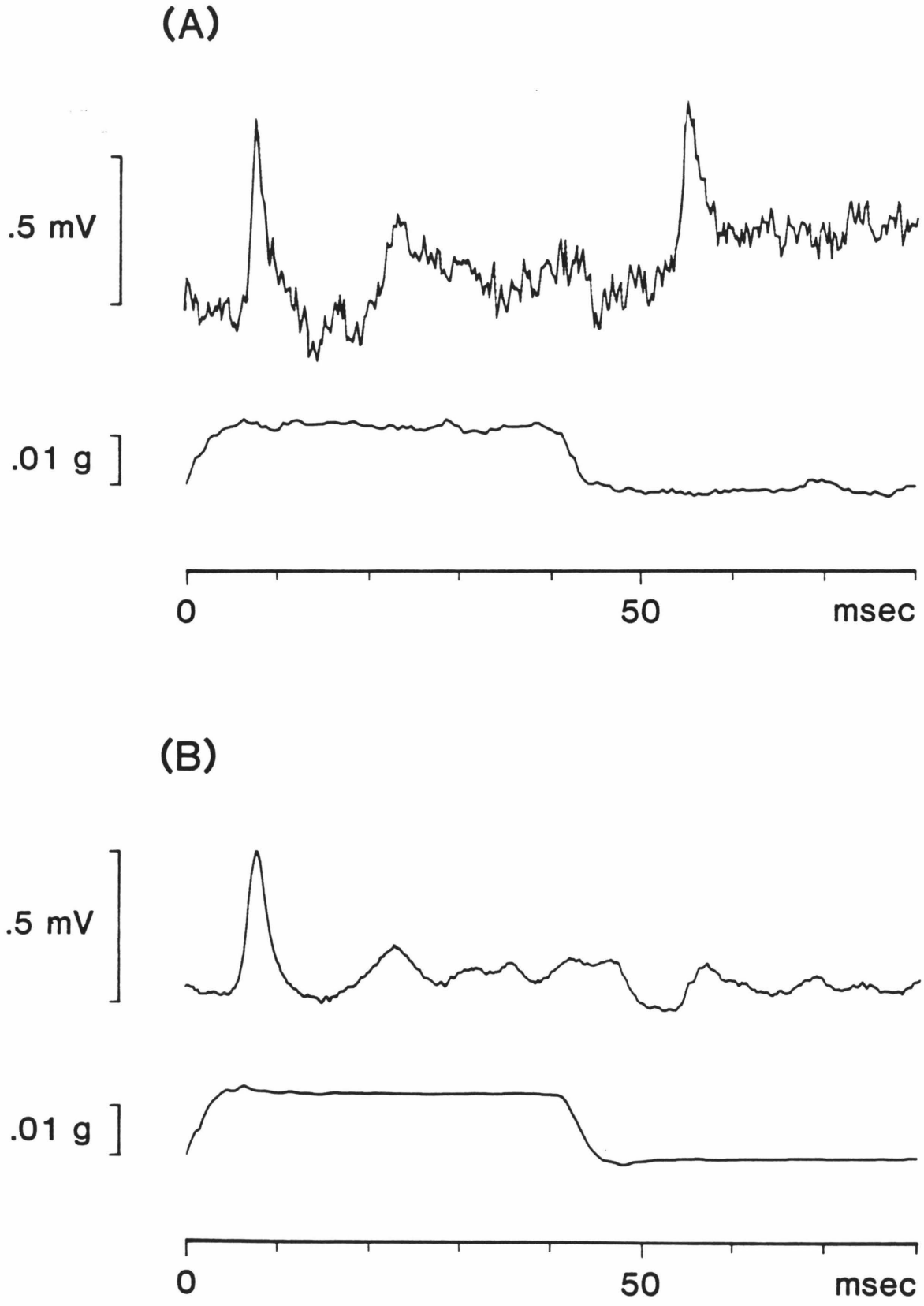
(A)
.5 mV
.01 g
0
50
msec
(B)
.5 mV
.01 g
0
50
msec

Figure 22. Adaptation of the averaged postsynaptic potential in a TTx-treated saccular nerve fiber to acceleration steps of different amplitude. The steps were +0.0042 g and +0.009 g. The responses are reproduced at different scales for comparison; the response to the smaller step is uppermost in the figure. Taking the beginning of the rise of the step as time zero, the responses to the small and large steps had decayed to 1/e of their peak values by 13.1 and 12.7 ms, respectively. Not shown is the response of the same fiber to a +0.0075 g step, which decayed to 1/e of its peak value by 12 ms.

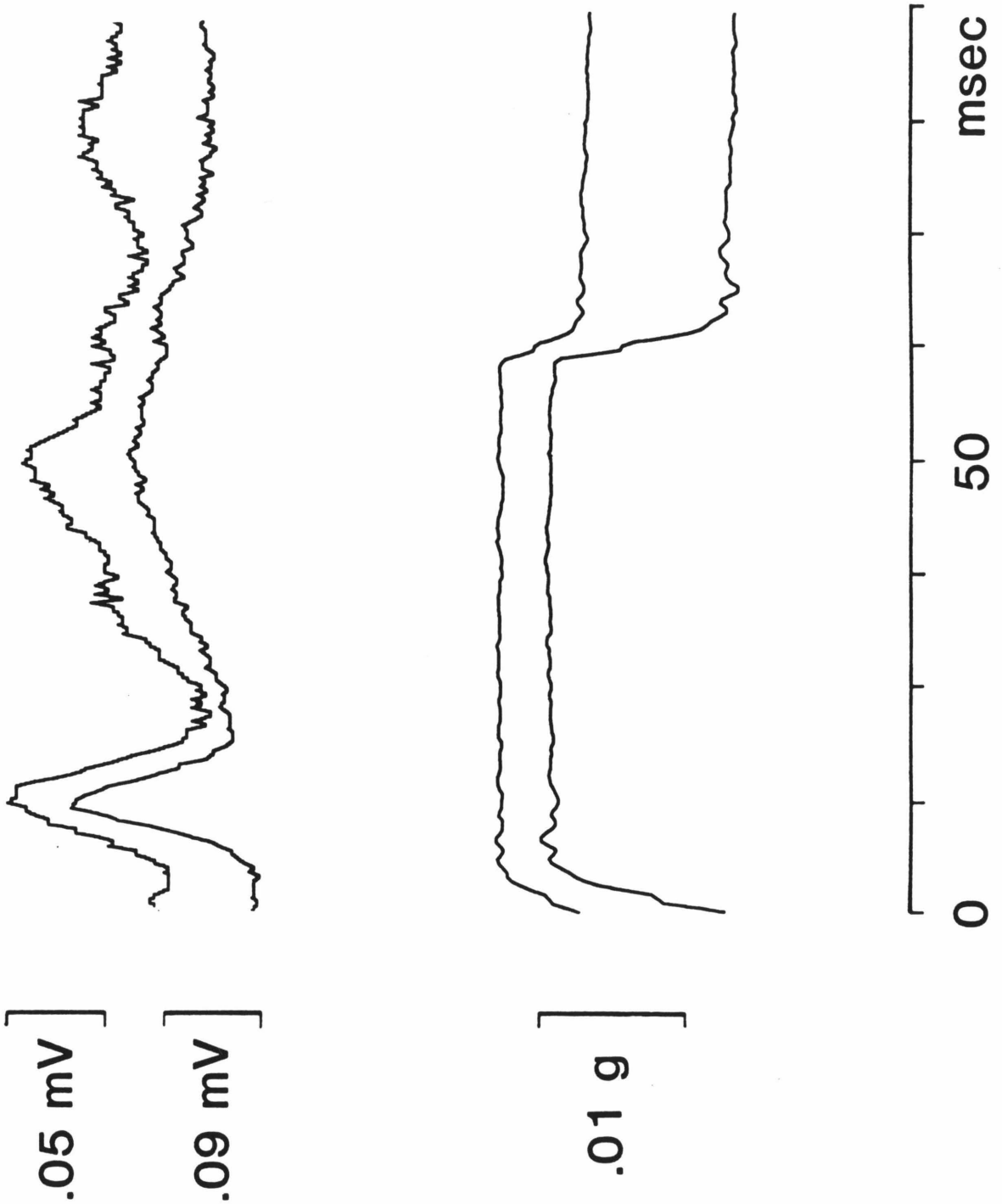
.05 mV
.09 mV
.01 g
0
50
msec

small hyperpolarizing potential occurred near the onset of a step opposite in direction to the excitatory direction for the cell (figure 23a). This is also evident in the neuron of figure 22(b) but not in the neuron of figure 22. The potential was due to small hyperpolarizing events that are obscured by noise in single response sweeps (figure 23b), rather than to infrequent large events. The latency to peak of the averaged hyperpolarizing potential was characteristically longer, by 0.5-4 ms, than that of the averaged epsp in the same neuron. Like the averaged epsp, the averaged hyperpolarizing potential declined during the step. Sometimes it was followed by a depolarizing potential of equal or greater amplitude.

Comparison of intracellular postsynaptic and microphonic averages suggests that adaptation to acceleration steps is not greatly enhanced by synaptic processes. The best evidence for this comes from three experiments in which postsynaptic potentials and microphonic potential were recorded in response to the same acceleration steps, though not simultaneously (figure 24). Postsynaptic responses were obtained before and after the microphonic potential, to control for any irreversible changes due to the invasive technique used in recording microphonic potential. A simple indicator of the rate of adaptation of a response such as those in figure 24 is the time between the onset of the step and the decay of the onset response to 1/e of its peak value. Based on this value, the adaptation rates of the averaged postsynaptic potentials of figure 24 varied from 0.7 to 1.4 times the rate of the corresponding microphonic potential. These few data cannot tell us the distribution of postsynaptic rates relative to the microphonic (presynaptic) rates, but do suggest that the differences are not great.

Figure 23. Hyperpolarizing postsynaptic potentials in a TTx-treated saccular nerve fiber in response to acceleration steps. In (A), 183 sweeps have been averaged. Two single sweeps are shown in (B).

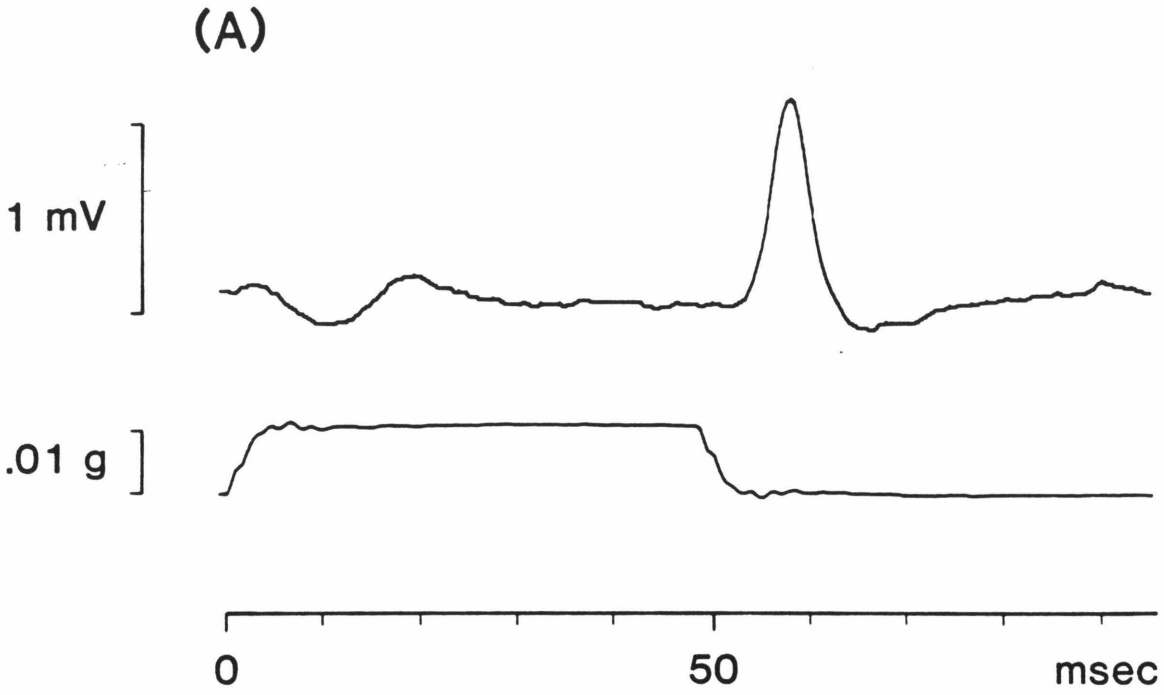
(A)
1 mV
.01 g
0
50
msec

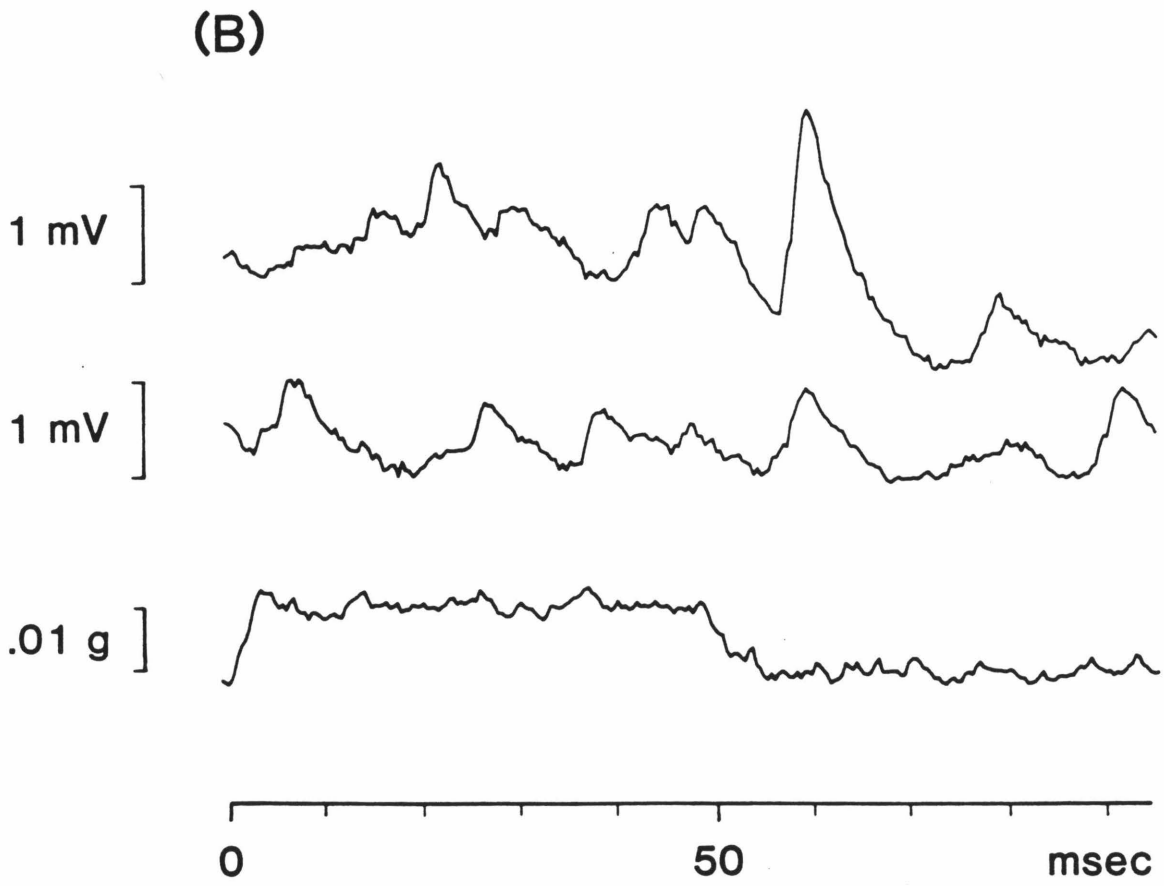
(B)
1 mV
1 mV
.01 g
0
50
msec

Figure 24. Comparison of adaptation in averaged postsynaptic potentials and the saccular microphonic potential. (A) and (B) are data from two different experiments. In each case, the microphonic potential (upper traces) was recorded in between the two records of averaged postsynaptic potential (lower pairs of traces). The postsynaptic potentials are from different neurons.

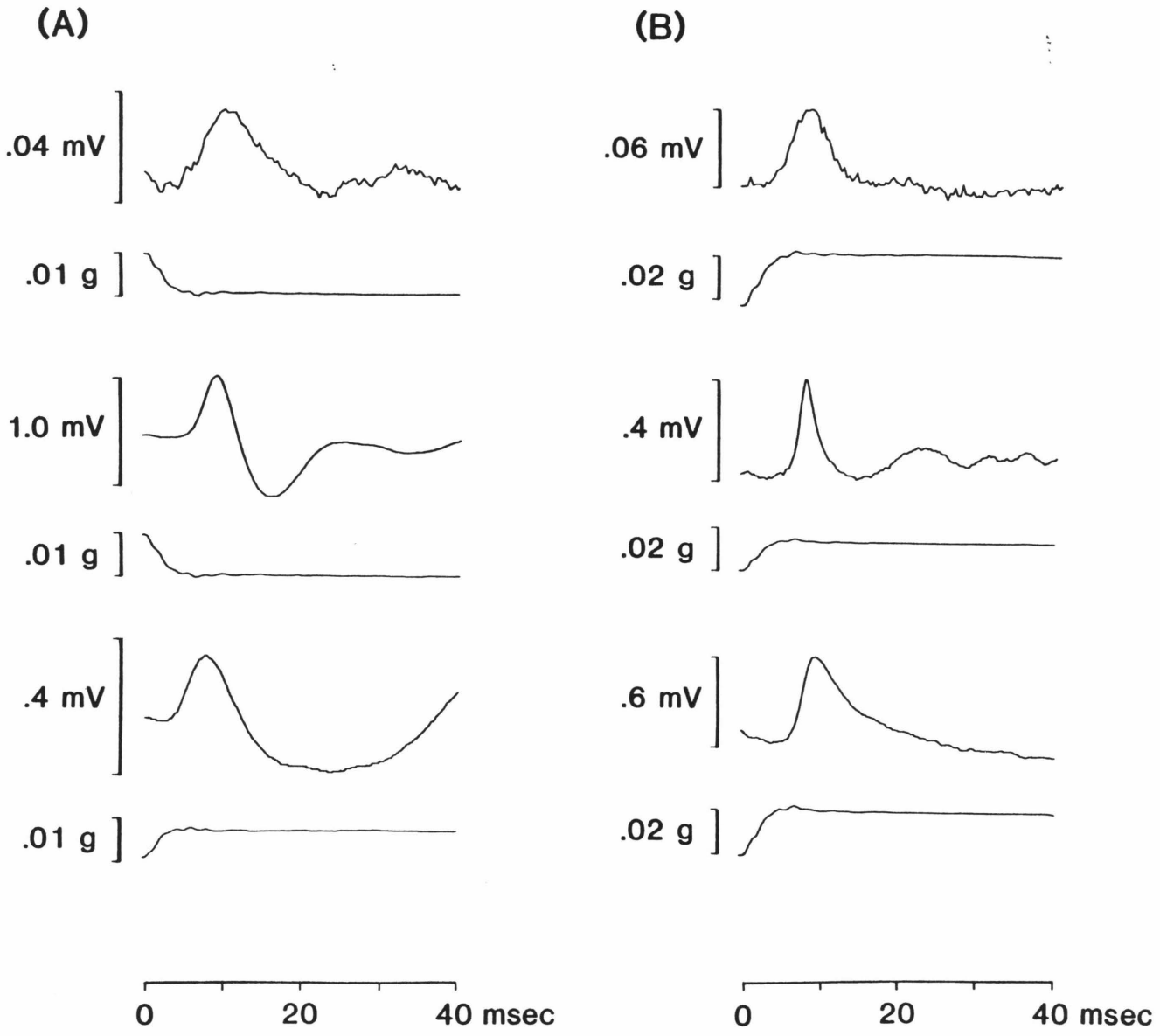
(A)
.04 mV
.01 g
1.0 mV
.01 g
.4 mV
.01 g
0
20
40 msec
(B)
.06 mV
.02 g
.4 mV
.02 g
.6 mV
.02 g
0
20
40 msec

The pattern of spike activity in saccular neurons closely follows the behavior of the graded postsynaptic potentials. This was seen by recording from fibers whose activity was partially blocked by TTx, and comparing patterns of spike activity and postsynaptic potentials over the same time interval. As with the graded potentials, the pattern of spike activity in many neurons cannot be discerned from the responses to single stimuli. (The variability of individual responses depends in part on spike rate and stimulus level. Units with low spike rates tended to have more variable responses. In all units, variability in the timing of spikes relative to the stimulus decreased as stimulus level was increased.) The firing pattern of a neuron is revealed by a peri-stimulus time (PST) histogram of its spike activity. A PST histogram is a display of spike number vs. time relative to the stimulus, obtained by recording the times at which spikes occur over many stimulus trials. The PST histogram and averaged postsynaptic potential obtained over the same time interval from a TTx-treated neuron are shown in figure 25. The patterns are similar. During the positive acceleration step, spike activity was reduced and the averaged potential showed hyperpolarization. At the onset of the negative step, the averaged epsp and the spike rate rose and decayed with similar time courses.

The results of the intracellular experiments on saccular neurons can be summarized as follows. First, all neurons showed pronounced adaptation to steps of acceleration. This result is supported by the extracellular data from saccular neurons, as will be described. Thus, in answer to the question posed at the beginning section, adaptation appears to be a fairly uniform feature of the responses of saccular neurons; there is no indication of a class of neurons that do not

Figure 25. Comparison of graded postsynaptic potentials and spike activity in a single TTx-treated saccular nerve fiber. (A), (B) and (C) are, respectively, a peri-stimulus time (PST) histogram, the averaged postsynaptic potential and a single response trace. All three were obtained within the same time interval in response to the same acceleration step, an average of which is shown in the lowermost trace.

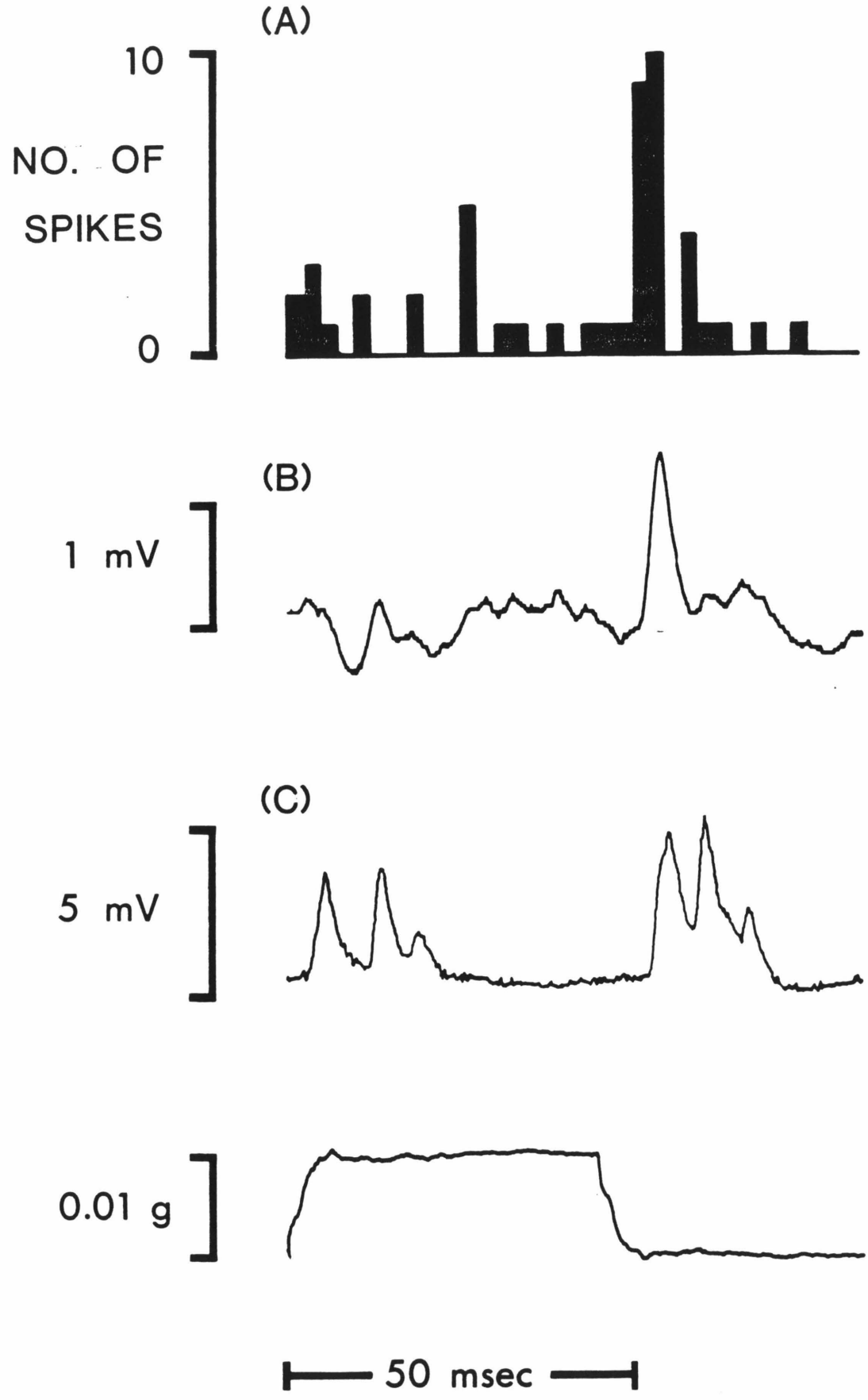
(A)
10
NO. OF
SPIKES
0
(B)
1 mV
(C)
5 mV
0.01 g
50 msec

adapt. Second, the rates of adaptation estimated from the averaged postsynaptic potentials were in the same range as those of the saccular microphonic potential. Third, neurons were typically excited by stimuli of one polarity and often inhibited by stimuli of the opposite polarity. Again, the extracellular data substantiate this observation. Fourth, the pattern of spike activity, the output of the sacculus, is closely related to the pattern of postsynaptic potentials.

The major finding of the extracellular experiments was that, as was observed for the microphonic potential, primary neurons undergo an adaptive shift in the range of effective stimuli (working range) during an acceleration step. This can be seen by comparing PST histograms of the responses of a single neuron to various combinations of adapting and test steps. For example, by superimposing excitatory test steps on an adapting step of opposite polarity, an inhibitory adapting step, one can show that the effective range of acceleration stimuli shifts in the direction of the adapting step. In the example of figure 26, the neuron fired in response to positive (upward) accelerations. Downward accelerations were inhibitory, as can be seen by comparing the response to a +.007 g test step alone (26a) with the response to the same test step superimposed on a -.009 g adapting step (26b). The adapting step reduced the response to the test step to 17% of its value in the absence of the adapting step, the control value. When the interval between the onset of the adapting step and the test step was increased from 8 ms (26b) to 39 ms (26c), the response to the test step increased to 67% of the control value. These data are interpreted to indicate that during the downward adapting step, the range of effective accelerations shifted in the direction of the step. In other words, the downward step may

Figure 26. Patterns of extracellular spike activity from a neuron in the saccular nerve in response to adapting and test steps. In this experiment, the eighth nerve was transected just lateral to the medulla. Thus the observed adaptation and adaptive shifts in the range of effective stimulus occurred in the absence of central efferents. Spike activity was summed over 100 trials to obtain each histogram. See text for details.

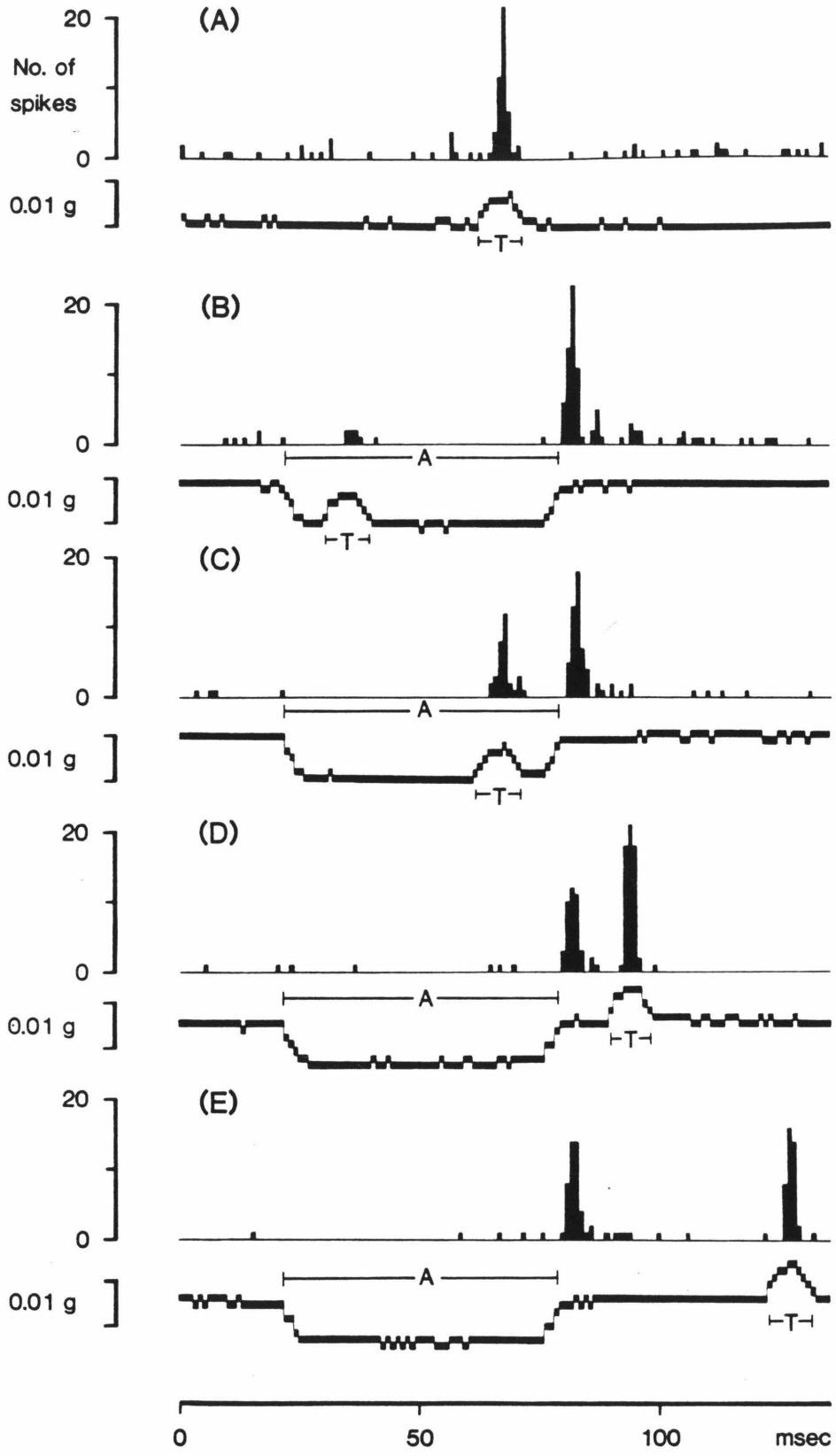
20
No. of spikes
0
0.01 g
(A)
T
20
0
(B)
A
0.01 g
T
20
0
(C)
A
0.01 g
T
20
0
(D)
A
0.01 g
T
20
0
(E)
A
0.01 g
T
0
50
100
msec

have initially saturated the neuron in the negative direction, but with time its working range shifted negatively. This interpretation also explains the responses to the offset of the negative adapting step and to a test step presented at different intervals after the adapting step. In (d) and (e), the +.008 g test step was presented at 12.5 and 46 ms, respectively, after the offest of a -.009 g adapting step. At 12.5 ms, the reponse was 125% of the control response (in (a)); by 46 ms after the offset of the step, the response had fallen to 83% of control. Thus the test step was more effective immediately after an adapting step of opposite polarity, suggesting that the neuron's working range was still somewhat negatively shifted so that the test step seemed more positive than normal. In contrast, the effectiveness of a test step was reduced if it were immediately preceded by an adapting step of the same polarity. In 27(a) and (b), a +.007 g test step was presented 11 and 42 ms, respectively, after a +.008 g adapting step. The response at 11 ms was 37% of the response at 42 ms (a control response to the test step alone was not obtained in this case). By themselves, these results are consistent with either an adpative shift or densensitization. But figure 27(c) shows that the response decline during an excitatory step is not due to a decrease in sensitivity. Ten ms after the onset of a +.008 g adapting step, when the response to it had almost fully decayed, a +.008 g test step evoked a large response. This result suggests that by 10 ms the neuron's working range had shifted positively. Similarly, the progressive increase in sensitivity to the test step during an inhibitory adapting step (figure 26b and c) is not compatible with a desensitizating mechanism. Similar evidence for

Figure 27. Patterns of extracellular spike activity from a neuron in the saccular nerve in response to adapting and test steps. These PST histograms are from the neuron of figure 26, and were obtained under similar conditions.

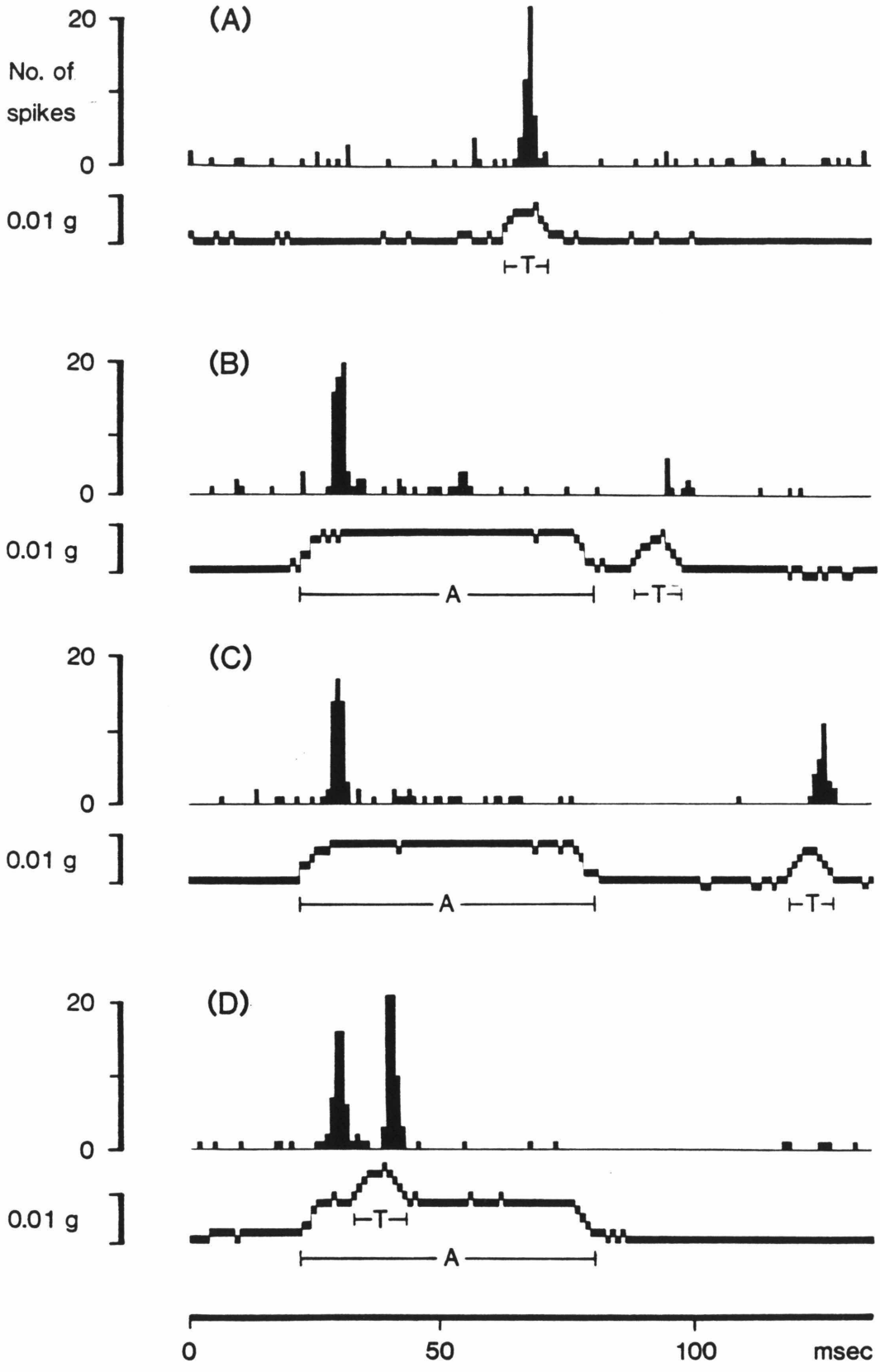
(A)
20
No. of
spikes
0
0.01 g
T
(B)
20
0
0.01 g
A
T
(C)
20
0
0.01 g
A
T
(D)
20
0
0.01 g
T
A
0
50
100
msec

adaptive shifts was obtained from all saccular neurons tested in this manner (n=30).

As was observed for the microphonic potential, the rate of response decline during a step is proportional to step size (figure 28). Here the response decline is a decrease in the probability that a spike will occur.

The features that varied most obviously among units, when tested with the limited set of stimuli used in these experiments, were threshold, response latency and firing rate. No effort was made to determine thresholds in the more sensitive units because of the high noise floor (.003 g); however, thresholds of the less sensitive units varied from .004 - .05 g. Response latencies, measured from the end of step risetime to the peak of the response, varied from 2 to 16 ms, with a mean value of 4.44 ms (standard error = 2.71 ms). The latencies of most cells (54 of 69, 78%) were between 2 and 5 ms, a range that fits well with the 2-3 ms latency of the microphonic potential. Neurons with greater latencies, particularly latencies of 10 ms or more, may not have been saccular afferents, but efferent fibers of afferents from the lagena or utriculus. In the experiments in which intracellular recordings were made near the saccular macula, so that it was clear that one was recording from the saccular nerve, latencies of all 34 neurons were in the 2-5 ms range, with a mean value of 3.17 ms (standard error = 0.9 ms). Eleven of the 15 neurons with latencies greater that 5 ms were from nerves that had been exposed using the dorsal approach. In such experiments, recording sites were in the vicinity of the branch point of the saccular nerve and the rest of the anterior ramus; recordings made proximal (medial) to the fork may have included some non-saccular

Figure 28. Adaptation to acceleration steps of different amplitude. Shown is a series of PST histograms of the extracellular activity of a single neuron in the saccular nerve, in response to adapting steps of increasing amplitude. The response to a test step applied after each of the different adapting steps indicates that the larger the adapting step, the greater its effectiveness at reducing the test response.

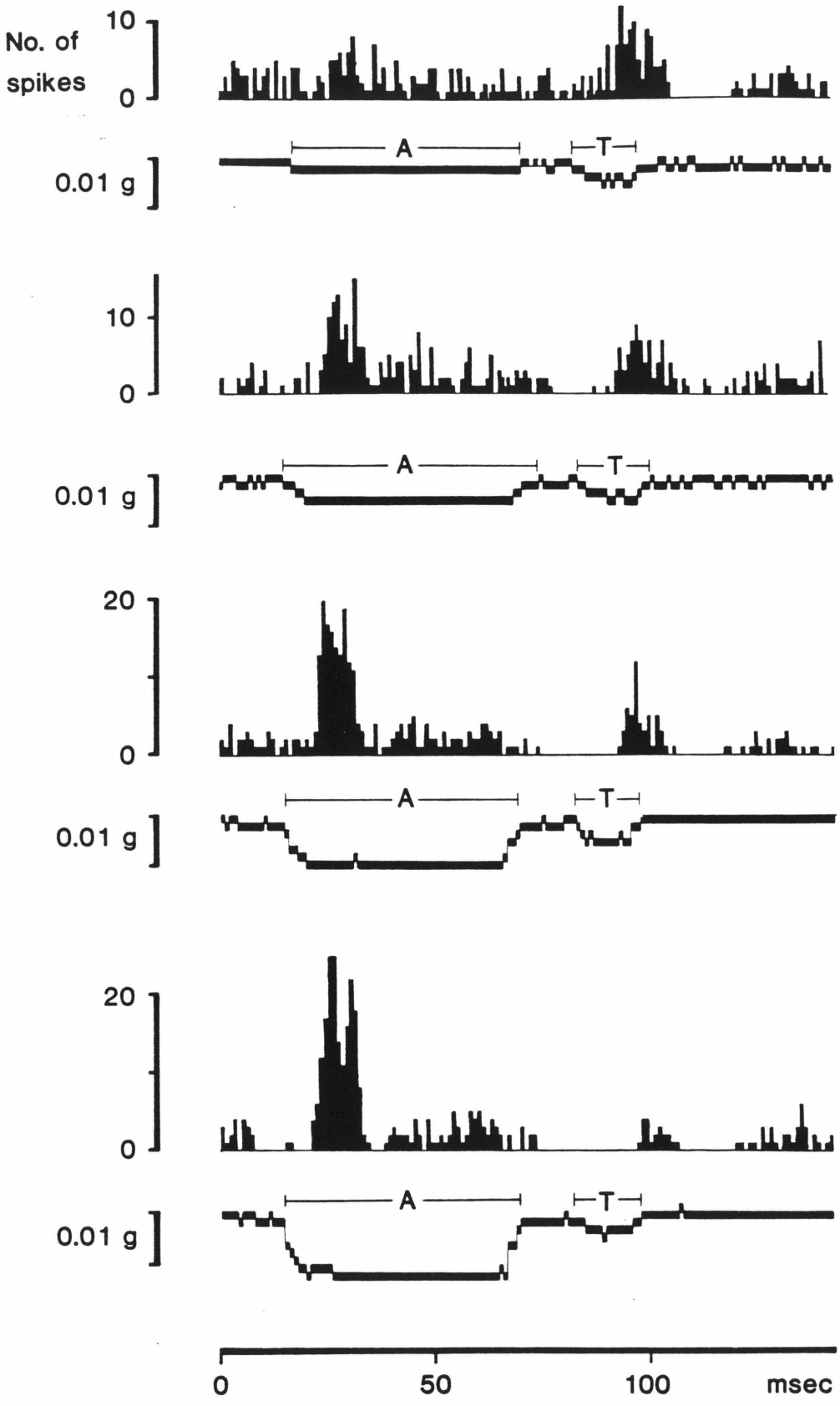
No. of spikes
10
0
A
T
0.01 g
10
0
A
T
0.01 g
20
0
A
T
0.01 g
20
0
A
T
0.01 g
0
50
100
msec

neurons. The ventral approach afforded easier access to the saccular nerve, even when the sacculus was not exposed in the region of the macula. Still, it is possible that the four long-latency neurons recorded with this approach were not sacculuar afferents, since recording site was not verified histologically. For example, electrode penetrations may have angled into regions where fibers of different origin mingle.

The one neuron with a latency greater than 12 ms also was unique in terms of its response. At the lower stimulus levels to which is was sensitive, it responsed tonically, without adapting, to acceleration steps. At high stimulus intensities, >.02 g, the response did show adaptation. The long latency suggests that this neuron was either an efferent or an afferent from a vestibular organ whose mechanical response is more damped than that of the sacculus, causing it to respond more slowly to a change in acceleration. For our purposes, the tonic response of the neuron to .009 - .02 g steps is useful because it implies that reasonably flat acceleration steps were being delivered to the inner ear.

Although efferents may have been recorded from on occasion, they do not play an obligatory role in the observed adaptation. In two experiments, four neurons were recorded after the transection of the eighth nerve just medial to its entry into the medulla. These neurons underwent response declines and adaptive shifts during steps that were similar to those observed in neurons prior to the transections. The neuron of figures 26 and 27 was one of the four obtained after the eighth nerve was cut. The latencies of the four neurons were all 5 ms

or less, which says very little except that it is still possible that the long-latency neurons were efferents.

Firing rate affected response pattern. Neurons with very low rates fired only at the onset of an acceleration step of one polarity (figure 29). Such response are purely phasic, in the terminology of sensory physiology. Although these neurons did not respond to steps of opposite polarity, they were inhibited by them; when an excitatory step was superimposed on a step of opposite polarity, its effectiveness was reduced. In neurons with higher rates, the response to a step was superimposed on a tonic level of activity. Responses to excitatory and inhibitory steps appeared as increases and decreases, respectively, relative to the tonic rate (figures 26-28). Such changes also had a phasic quality to them, since they decayed while the stimulus was maintained. Sometimes they decayed to the background rate, in which case the response was phasic. Sometimes the response did not decay (adapt) fully, but to a level above or below background, depending on whether the steps were excitatory or inhibitory. Such responses are both phasic and tonic.

In some neurons, acceleration steps evoked an onset (phasic) response followed by ringing in the range of 30-60 Hz. Ringing occurred in some neurons but not others in a given preparation. In the example in figure 30(a), the initial response to an excitatory step was followed by a smaller peak 26.5 ms later, followed by a third peak about 30 ms later. These intervals correspond to instantaneous frequencies of 38 and 33 Hz, respectively, suggesting a slowly-damped resonance at about 40 Hz. At the beginning of the downward step, activity was suppressed and then rebounded. The interval between the suppression of activity

Figure 29. Phasic responses to acceleration steps from a neuron in the saccular nerve. Each histogram is spike activity summed over 200 trials. As the adapting step was increased, the response to a test step, presented 10 ms after the offset of the adapting step, was reduced.

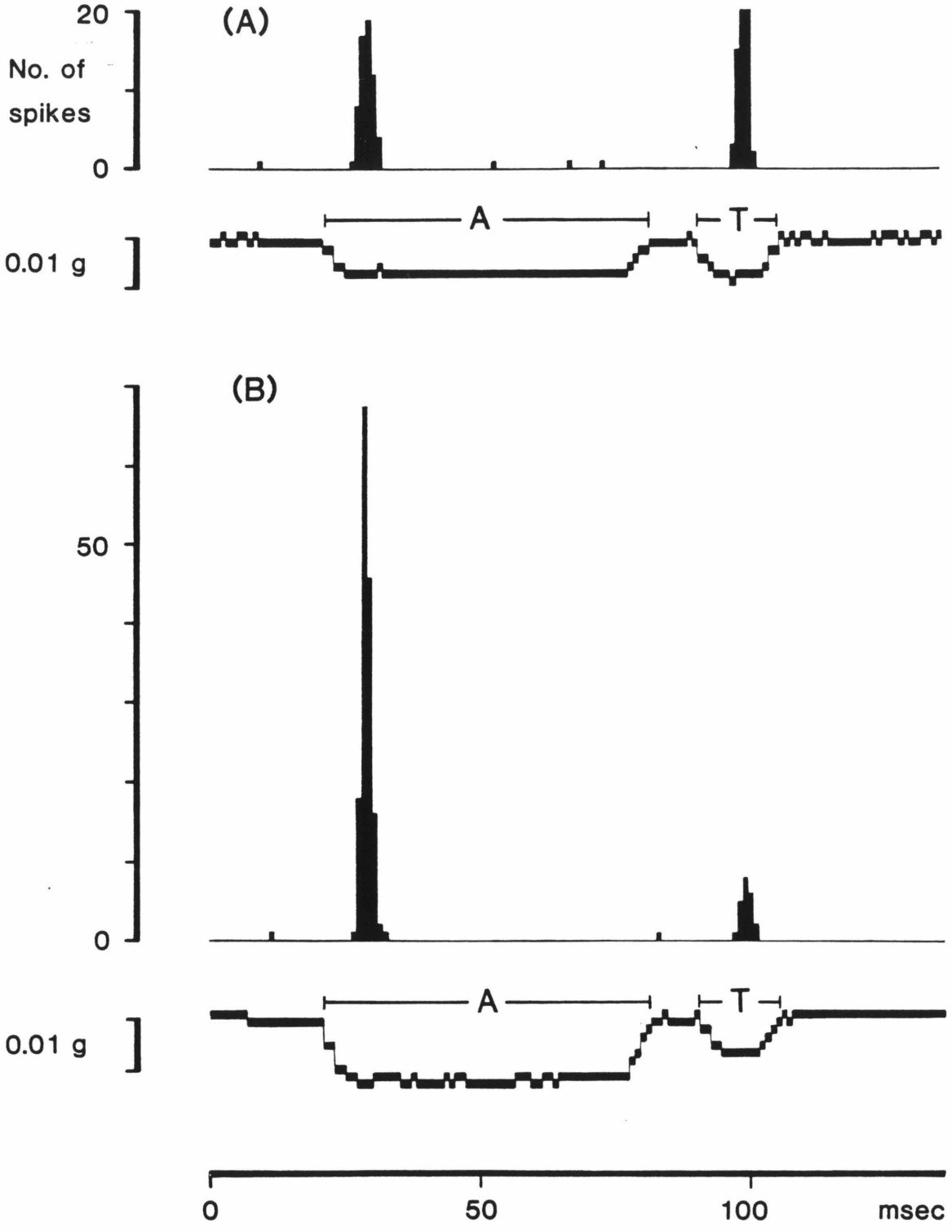
20
No. of
spikes
0
(A)
A
T
0.01 g
(B)
50
0
A
T
0.01 g
0
50
100
msec

Figure 30. (A) Ringing in the response of a neuron in the saccular nerve to acceleration steps. (B) An "iso-level" tuning curve from the same neuron. The number of spikes per cycle of a sinusoidal stimulus, .02 g in peak-to-peak amplitude, was determined at each of the frequencies shown.

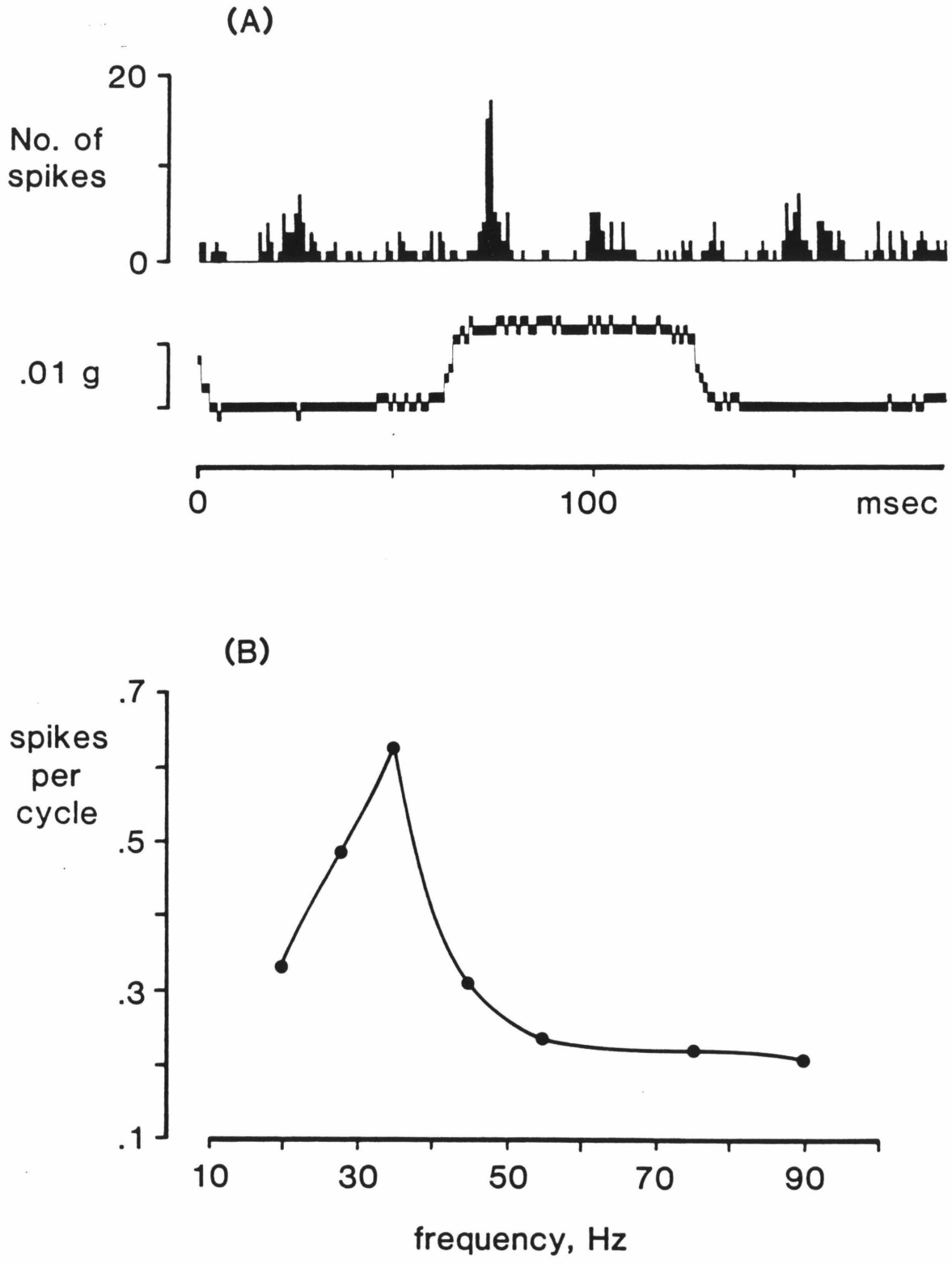
(A)
20
No. of spikes
0
.01 g
0
100
msec
(B)
.7
spikes per cycle
.5
.3
.1
10
30
50
70
90
frequency, Hz

and the peak of the rebound (about 16 ms) is the half-period of ringing in response to the inhibitory step, and indicates a ringing frequency of about 31 Hz. When tested with sinusoidal stimuli between 10 and 100 Hz, the neuron responded most vigorously around 35 Hz (figure 30b).

# CHAPTER 3

## Discussion

Hair cells of the bullfrog sacculus adapt in vitro to direct and maintained deflections of their hair bundles, and in vivo to constant acceleration stimuli. In both cases, the adaptation process entails a shift in the range of stimuli to which the cells are sensitive. The responses of primary saccular neurons appear to reproduce rather faithfully the features of the hair cell response that have been observed both in vitro and in vivo. In particular, one need not invoke extra stages of processing to explain the adaptation of afferent neurons to the acceleration steps used in this study.

The primary neuron responses to acceleration steps can be explained by a simple model which makes use of the information obtained directly from hair cells in the in vitro preparation (figure 31a). A brief overview of the model follows. It consists of three sequential stages, the mechanical response of the organ, the electrical response of the hair cells, and the spike activity of the primary neurons. Mechanically, the organ is modelled as a damped harmonic oscillator which responds to a step of force (acceleration) with a displacement that rises slowly to a new steady value. This displacement is the input to the hair cells. We shall restrict our attention to stimuli that fall within the nearly linear operating ranges of the hair cells, and model the cells as simple band-pass filters. The high-pass and low-pass behaviors of these filters are due to the adaptation process and passive membrane properties, respectively. The high-pass feature dominates in the cells' response to the relatively slow displacement stimulus. Thus, the hair

Figure 31. (A) A model of saccular processing of acceleration steps. Three stages are proposed: (1) The acceleration step (a) is transduced to a displacement (x) of the otoconial mass with respect to the macula. The mechanical behavior is assumed to be that of an harmonic oscillator (see (B)) near critical damping, on the over-damped side. The low-pass frequency behavior of such a system, depicted in box (1), slows down the rise of the displacement response. This mechanical response is the input to the hair cells (box 2), which are assumed to be in the linear portion (operating range) of their displacement-response curves. For the purposes of this simple model, they are represented only in terms of their adaptation process, as high-pass filters. Their output in response to the displacement step has the characteristic shape of the saccular microphonic potential during an acceleration step. Finally, the spike-generating mechanisms (box 3) translate the graded potential into firing patterns. (B) The mechanical analogue of the bullfrog sacculus as modelled in (A) (box 1). M: mass.

(A)

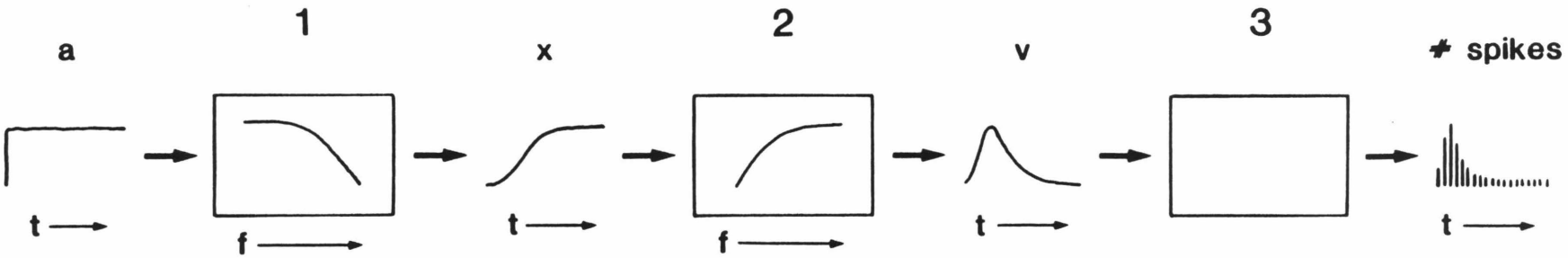




(B)

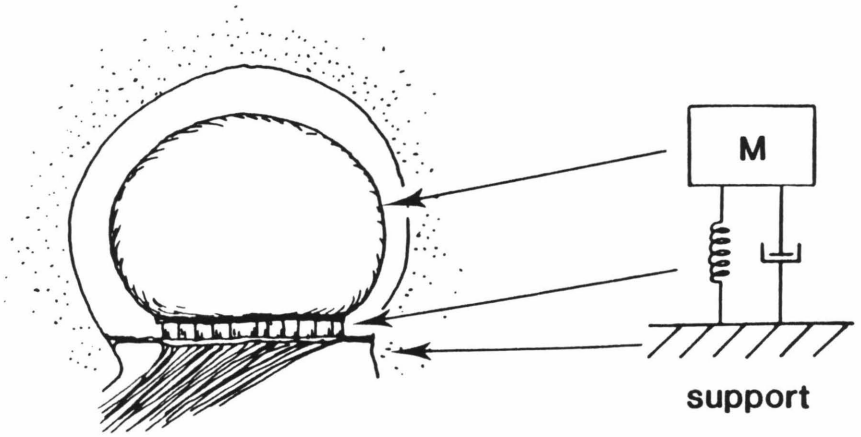

cell response rises to a peak which leads the displacement signal, then decays to zero (adapts fully). Assuming faithful information transfer across the afferent synapse, this is the signal transmitted to the third stage of the model, comprising the spike-generating mechanisms of the primary neuron. This stage converts membrane potential into spike rate, such that a large depolarization corresponds to a high instantaneous spike rate.

Alternatively, one could model the stimulus-induced adaptive shift in saccular neurons by introducing an adaptation term (high-pass feature) into the mechanical response of the organ. Mayne (1966) has proposed that relaxation of the otolith displacement (due to equilibration of perilymph in the organ with perilymph in other inner ear spaces) may account for a relatively slow adaptation process in mammalian otolith organs. The advantages of the model proposed here are that it is compatible with most models of the mechanical behavior of otolith organs and is the simplest way of relating the in vitro and in vivo observations. However, it is possible that the in vivo adaptive shift is due to other mechanisms in addition to, or instead of, the cellular adaptation described in vitro. With these alternatives in mind, a more detailed discussion of what is known and conjectured about the stages in saccular processing of acceleration stimuli follows.

What evidence supports the proposal that the organ behaves mechnically like a damped harmonic oscillator? Basically, the evidence is that otolith afferents are sensitive to linear acceleration, and the organs are physically reminiscent of differential-density accelerometers (de Vries, 1950; Trincker, 1962; Young, 1969; Corriea and Guedry, 1978). The latter are harmonic oscillators suspended in a fluid dense

enough that it influences the mechanics of the system--e.g., water rather than air. A mechanical harmonic oscillator is simply a mass coupled by a spring to a fixed support; in real systems, frictional or damping forces, represented by a dashpot, must be included (figure 31b). In an otolith organ, the load object that undergoes motion is the otolith. Because it is immersed in perilymph, the mass of the system is not the otolith mass but the difference between the otolith mass and the mass of an equal volume of perilymph (the "displaced" fluid). The fixed support comprises all tissues to which the otolith is coupled and which are more firmly anchored in the body than is the otolith. The spring represents all elastic connections between the otolith and the fixed support; such connections will act to restore the otolith to its original position following a movement.

In the bullfrog sacculus, the otoconial mass, or otolith, is coupled by the otolithic membrane and hair bundles to the fixed support, the macula (figure 31b). If we assume that the hair bundles are free to pivot but rigid, then the elasticity in the system is confined to the bonds between hair bundles and the otolithic membrane (figure 2) and the fine strands of otolithic membrane material secreted by the supporting cells and extending up to the membrane proper (A. J. Hudspeth and R. Jacobs, unpublished observations). The epithelium containing the sensory macula is anchored to the wall of the membranous labyrinth by 10-20 capillary-bearing "pillars" or "struts," and also has a sturdy connection to the brain, the saccular nerve.

Direct observations of otolith motion during linear acceleration were made by de Vries (1950) on the teleost sacculus. He showed that centrifugal or vibrational accelerations (both linear) cause displace-

ment of the otolith relative to the macula and parallel to the plane of the macula--i.e., in the appropriate plane for stimulation of the hair cells. He substituted his displacement measurements into the equation of motion for an harmonic oscillator, on the assumption that this is the appropriate model for the sacculus, and arrived at estimates for the parameters in the equation. In particular, he concluded that the relative motion between otolith and macula had a natural frequency of about 40 Hz, and was critically damped or nearly so. These estimates have important functional implications. As de Vries noted, critical damping is the optimal solution if one is designing an accelerometer to give a signal proportional to acceleration as quickly as possible after a change in acceleration. Underdamping would result in a resonant oscillator which would ring at or near the resonant frequency before settling to a steady-state level, while overdamping slows the rise of the mechanical response. De Vries estimated the risetime of response to a step change in acceleration as 20 ms and 5 ms for the sacculus and smaller utriculus, respectively. These times, which are rather slow for a sensory system, are obtained with near-critical damping. One might expect slower risetimes to be disadvantageous, and therefore that otolith organs would not be greatly over-damped. In the frequency domain, de Vries' calculations imply that the mechanical behavior of the teleost sacculus is that of a low-pass filter with half-power frequency around 40 Hz.

In general, otolith organs are modelled as being critically damped or over-damped (Mayne, 1966; Young and Meiry, 1968; Fernandez and Goldberg, 1976c). Although these workers do not defend this choice, it may have been based in part on optimal design considerations. Another

reason may have been the lack of evidence for ringing in studies of otolith afferents or in human psychophysical studies, although fast step changes in acceleration were not typically given. Certainly, de Vries' conclusions have had some impact, as his was the only study in which otolith mechanics were examined directly during dynamic (sinusoidal) as well as static stimuli. Fernandez and Goldberg (1976c) extrapolated from de Vries' data to mammalian otolith organs by correcting for the smaller volume of the mammalian otoith, and suggested that the latter might have a natural frequency of 400 Hz and also be critically damped. However, simple extrapolations from de Vries' data on teleosts to the otolith organs of other animals should not be taken too seriously, as teleost otoliths are structurally distinct from all others. Teleost otoliths are large single stones, whereas in all other animals, the "otolith" is like that of the frog, a large number of very small deposits of calcium carbonate (otoconia) held together in an organic gel (Carlstrom, 1963). These differences may have important consequences for the mechanical behavior of the organs. It seems safe to assume that the teleost saccular otolith moves as a unit, but the same cannot be said for the bags of otoconia in other otolith organs. Local deformations within the otoconial aggregate may occur, causing more complex stimulation pattens over the underlying macula than the unidirectional shear implied by the damped harmonic oscillator model (Vidal et al., 1971). This is not a popular notion in the literature. For instance, when Fernandez and Goldberg (1976c) developed a mathematical model of the responses of otolith afferents in the squirrel monkey, an implicit assumption was that variability among afferents within an animal was due to non-mechanical factors, or in other words,

that the mechanical input to the hair cells was uniform across the organ.

Another reason to exercise caution in pooling observations among otolith organs is that they do not all serve the same function. The teleost sacculus is an auditory organ, sensitive to frequencies up to 2 kHz (Fay, 1978). The sacculus and utriculus of the squirrel monkey detect very low frequency linear accelerations, <2 Hz, and respond to new steady levels of linear acceleration with varying degrees of adaptation (Fernandez and Goldberg, 1976a,b). Loe, Tomko and Werner (1973) identified a population of otolith afferents in the cat that is sensitive to head position--i.e., is tonically sensitive to changes in the gravity force acting to displace the otolith relative to the macula. The possibility that these neurons might respond phasically to fast changes in head position was not examined. In the bullfrog, the sacculus is a vibration detector (<300 Hz), while the utricle and lagena apparently have both tonic gravitational (positional) and vibratory sensitivity, localized to different regions in the maculae (Lewis et al., 1982). Positional and vibrational sensitivity in different areas of the same macula also have been seen in the sacculus and utriculus of the ray (Lowenstein and Roberts, 1950, 1951). The occurrence of functionally distinct regions in one organ does not necessarily imply non-uniform motion of the otolith; these regions often have distinguishing morphological features that could be the source of the functional differences (Lewis and Li, 1975; Platt, 1977). The morphological features include hair bundle geometry and whether the otolith actually extends over the region of the macula or not. Although there may be a compelling correlation between a morphological feature

and a particular effective stimulus within an organ or among organs in the same species, the correlations do not always extend to different species. In reviewing the morphologies of otolith organs in a variety of animals, Platt (1977) was unable to uncover any simple rules by which one could predict the function of a given macula or macular region. It seems as though a variety of morphological solutions provide adequate sensitivity to vibration and head position.

The mechanics of the bullfrog sacculus have not been directly studied, but some inferences can be made from the electrophysiological data. The onset of the saccular microphonic potential response to a step of acceleration lags the step onset by 1.5 - 3 ms. The latency of the hair cell response to a direct displacement of the otolithic membrane is on the order of tens of microseconds (Corey and Hudspeth, 1979), suggesting that the lag observed in the in vivo microphonic potential occurs in the delivery of the stimulus to the otolithic membrane. This in turn implies low-pass filtering in the mechanical response of the otoconial mass to acceleration.

Oscillations ("ringing") in the range 20 - 100 Hz sometimes were observed in the step response of the microphonic potential and of primary neurons. Primary neurons innervating the same sacculus had different tendencies to ring. When oscillations did occur, in either the microphonic potential or afferent activity, their amplitude varied with stimulus level. The ringing could have a mechanical or a cellular source. If the otolith motion were underdamped, it might oscillate after transitions in acceleration. The ringing frequencies observed are in the range of de Vries' estimates of the natural frequency of otolith motion in the teleost sacculus. Also, the between-animal variability in

the ringing tendency of the saccular microphonic potential is rather easily explained if one assumes that the ringing has a mechanical basis. Suppose that normally the otolith motion is critically damped or slightly over- or under-damped. One might expect that opening the perilymphatic chamber housing the otoconial mass in order to record microphonic potential would reduce damping in a somewhat capricious fashion, depending on the size and location of the surgical hole, etc. But the disturbance presumably would always tend to reduce damping and increase the probability of ringing.

Alternatively, the oscillations may originate in the hair cell membrane. Lewis and Hudspeth (1983a, b) have observed voltage oscillations at frequencies ranging from 20 to 200 Hz in hair cells in in vitro preparations of the bullfrog sacculus. In some cells, oscillations occur at the onset and offset of injected square pulses of current. A subset of these cells oscillate in the absence of injected current or mechanical stimulation. Two observations suggest that the oscillations are a labile phenomenon. First, in intracellular records, oscillations are more likely to occur if very high-impedance (≥300 MΩ) microelectrodes are used. Second, in recording from a single cell, one observes that the frequency and amplitude of the oscillations decrease with time. The lability of the phenomenon suggests either that it is characteristic of healthly cells--i.e., that many in vitro records are from somewhat damaged cells--or that it is an artifact of in vitro conditions. If the former possibility is the case, then in vivo the receptor currents evoked by acceleration steps may cause ringing of the hair cell membrane potential.

Whatever its source, damped ringing of the hair cell response would enhance the apparent rate of adaptation to a step, since the initial response would be brought back down by the oscillations. In the absence of an adaptation mechanism, the response would damp out to a steady value, a tonic indicator of the step amplitude. Usually, however, the microphonic and afferent responses decayed fully, so that we need to invoke an adaptation process. The hair cell adaptation described in vitro, which I will call cellular adaptation, is an obvious candidate, and in the simple model of figure 31, I have proposed that it is responsible for the adaptation of saccular responses in vivo. However, since the motion of the hair bundles is neither directly controlled nor monitored in vivo, one cannot conclusively localize the in vivo adaptation to the hair cell. Ignoring the in vitro evidence for the moment, what are the options in vivo? Given that the microphonic potential adapts, the adaptation must occur in the mechanical response to acceleration, or in the cellular response, or in both. My proposal is based on a circumstantial line of reasoning: that the cellular and in vivo adaptations are comparable and therefore the simplest interpretation is that they are manifestations of the same process in different experimental conditions. A summary of the similarities between the two sets of observations follows.

Perhaps the most important comparisons are of the time courses of adaptation (the response decline during a constant stimulus) and of the associated changes in the stimulus-response relation. Adaptation in vitro occurred at variable rates, but was usually substantially over by 100 ms. The adaptation of the in vivo microphonic potential was more reliable and faster, taking about 10-20 ms to go to completion. A case

can be made that this discrepancy is not large, given the technical differences between the two sets of experiments. As noted above, ringing may enhance the in vivo response decline during an acceleration step. One of the most likely sources of discrepancy is the relative health of the cells. This is a well-established factor in the variability in adaptation rates in vitro: cells that appear to be healthy by other criteria (e.g., appearance of nucleus and hair bundle, resting potential, response amplitude) adapt more rapidly, and more, than unhealthy looking cells. The rate of adaptation in a cell often deteriorated with recording time, indicating that the invasive stimulating and recording techniques damage the adaptation process. In the voltage-clamped cell of figure 12, for instance, the rebound at the offset of the negative step gradually disappeared, leaving only the square outward current during the step. This cell is interesting because its rebound response to the step offset adapted as quickly as the in vivo adaptation, as shown in figure 17, suggesting that either the slower in vitro rates were artifactually low or the rates of individual cells vary over an order of magnitude.

Both in vivo and in vitro, the response decline during a constant stimulus results largely from an adaptive shift in the cells' working range. In vitro, the range of membrane potentials corresponding to the operating range--the "response range"--often shifted in such a way as to contribute to the response decline to the step. The information available on hair cell conductances predicts some contribution from conductances not involved in transduction. In particular, when the receptor current in response to a positive step depolarizes the membrane, a voltage-sensitive $Ca^{++}$ conductance in the basolateral

membrane will be activated. The ensuing influx of $Ca^{++}$ will in turn activate a $Ca^{++}$-activated $K^+$ conductance, and the outward $K^+$ current through this conductance will tend to repolarize the membrane (Lewis and Hudspeth, 1983a, b). This conductance is presumed responsible for a fast repolarizing phase in the microphonic potential recorded *in vitro* from the saccular macula during a positive step displacement of the otolithic membrane (Corey and Hudspeth, 1983).

The rate of adaptation of the *in vitro* receptor potential, the *in vivo* microphonic potential and afferent responses was proportional to stimulus amplitude. The adaptation and adaptive operating range shift of the receptor potential varied with stimulus amplitude even when the comparison was between supersaturating amplitudes. Corey (1980) made this observation while recording microphonic current from the saccular macula *in vitro*, and noted that since the adaptation process has a broader operating range than the transduction process, adaptation does not succeed transduction in the chain of events leading to the afferent response. Thus, this finding rules out a simple form of negative feedback from the transduction mechanism onto itself, such as would occur if an ion entering through the transduction channel were to activate the adaptation process. It does not rule out the possibility that some feedback is mediated through the transduction channel. If the adaptation process were regulated intracellularly by an ion that passes through the transduction channel--e.g., $Ca^{++}$ or $H^+$--then the flux of that ion through the channel may feed into the adaptation process.

Both *in vivo* and *in vitro* the hair cells adapt faster to excitatory than to inhibitory stimuli. Again, the results in this study support earlier observations on the microphonic current recorded *in vitro* from

the saccular hair cells (Corey, 1980). Corey suggested that on the basis of this asymmetry one would predict the positive operating range shift that occurs during symmetrical stimuli such as a sine wave.

Finally, the thermal $Q_{10}$'s of the rate of adaptation in the in vitro microphonic current (Corey, 1980) and the in vivo microphonic potential both appear to be about 2, in the usual range for biological processes and higher than expected for mechanical processes--e.g., deformations in tissues or acellular structures. Thus the $Q^{10}$ value provides some support for the notion that the in vivo adaptation at least involves a cellular process, although it doesn't rule out a mechanical contribution.

In summary, the in vitro and in vivo adaptation processes behave similarly under a number of test conditions. In the absence of any telling evidence to the contrary, the hypothesis that attributes the adaptation of the in vivo saccular responses to hair cell adaptation is the simplest and most conservative.

The primary neuron data demonstrated that adaptation to constant acceleration is a fundamental feature of the information sent from the sacculus to the brain. In addition, comparison of the microphonic potential and primary neuron activity suggests that hair cell adaptation accounts in large measure for the prominent adaptation of afferent responses. This raises the possibility that the adaptation in neurons innervating other inner ear organs ensues at least in part from the kind of hair cell adaptation described here. Alternatively, different adaptive strategies may have evolved in different organs. In this respect, the effects of $Ca^{++}$ on adaptation rate of the in vitro microphonic current (Corey, 1980) are particularly interesting. Corey

observed that a 10-fold increase in extracellular $Ca^{++}$ caused about a 4-fold increase in adaptation rate. Extrapolating down to the very low $Ca^{++}$ levels in mammalian cochlear endolymph (about 30 μM) he suggested that cellular adaptation might be negligible in cochleae because of the low $Ca^{++}$, but also noted that it might be unnecessary because cochleae possess a mechanical high-pass filter, the heliocotrema.

Hair cell adaptation in the frog sacculus may be crucial to its role as a sensitive detector of vibrations. As the frog tilts its head, the component of gravity acting in the direction to cause otolith displacement changes and the otoliths assume new positions relative to the underlying sensory epithelia. Thus unless the sacculus has active physical restoring mechanisms, its hair bundles are subjected to static deflections. The adaptation process described here may preserve the cells' sensitivity to vibrations by aligning their narrow operating ranges with the static positions of their hair bundles.

## References

Blanks, R. H. I., and W. Precht (1976) Functional characterization of primary vestibular afferents in the frog. Exp. Brain Res. 25: 369-390.

Carlstrom, D. (1963) A crystallogravic study of vertebrate otolith organs. Biol. Bull. 125: 441-463.

Caston, J., Precht, W., and R. H. I. Blanks (1977) Response characteristics of frog's lagena afferents to natural stimulation. J. Comp. Physiol. 118: 273-289.

Corey, D. P. (1980) A biophysical approach to sensory transduction by vertebrate hair cells. Ph.D. thesis, California Institute of Technology.

Corey, D. P., and A. J. Hudspeth (1979a) Response latency of vertebrate hair cells. Biophys. J. 26: 499-506.

Corey, D. P., and A. J. Hudspeth (1979b) Ionic basis of the receptor potential in a vertebrate hair cell. Nature 281: 675-677.

Corey, D. P., and A. J. Hudspeth (1980) Mechanical stimulation and micromanipulation with piezoelectric bimorph elements. J. Neurosci. Methods 3: 183-202.

Corey, D. P., and A. J. Hudspeth (1983) Analysis of the microphonic potential of the bullfrog's sacculus. J. Neurosci. 3: 942-961.

Correia, M. J., and F. E. Guedry, Jr. (1978) The vestibular system: basic biophysical and physiological mechanisms. In Handbook of Behavioral Neurobiology, v. 1: Sensory Integration, R. B. Masterson, ed., pp. 311-351, Plenum Press, New York.

Dallos, P. (1973) The Auditory Periphery, Academic Press, New York.

Eatock, R. A. (1983) Adaptation in a vestibular organ of the bullfrog. Association for Research in Otolaryngology Abst. 6: 91.

Eatock, R. A., and A. J. Hudspeth (1981) Adaptation in hair cells: In vitro intracellular responses and in vivo microphonic potentials from a vestibular organ. Soc. Neurosci. Abst. 7: 62.

Eatock, R. A., Corey, D. P., and A. J. Hudspeth (1979) Adaptation in a vertebrate hair cell: Stimulus-induced shift of the operating range. Soc. Neurosci. Abst. 5: 19.

Fay, R. R. (1978) Coding of information in single auditory-nerve fibers of the goldfish. J. Acoust. Soc. Am. 63: 136-146.

Fernandez, C., and J. M. Goldberg (1976a) Physiology of peripheral neurons innervating otolith organs of the squirrel monkey. I. Response to static tilts and to long-duration centrifugal force. J. Neurophysiol. 39: 970-984.

Fernandez, C., and J. M. Goldberg (1976b) Physiology of peripheral neurons innervating otolith organs of the squirrel monkey. II. Directional selectivity and force-response relations. J. Neurophysiol. 39: 985-995.

Fernandez, C., and J. M. Goldberg (1976c) Physiology of peripheral neurons innervating otolith organs of the squirrel monkey. III. Response dynamics. J. Neurophysiol. 39: 996-1008.

Flock, A. (1971) Sensory tranduction in hair cells. In Handbook of Sensory Physiology, v. 1: Principles of Receptor Physiology, W. R. Loewenstein, ed., pp. 396-441, Springer-Verlag, Berlin.

Furukawa, T., and S. Matsuura (1978) Adaptive rundown of excitatory post-synaptic potentials at synapses between hair cells and eighth nerve fibres in the goldfish. J. Physiol. 276: 193-209.

Furukawa, T., Ishii, Y., and S. Matsuura (1972) An analysis of microphonic potentials of the sacculus of the goldfish. Jap. J. Physiol. 22: 603-616.

Goldberg, J. M., and C. Fernandez (1971) Physiology of peripheral neurons innervating semicircular canals of the squirrel monkey. I. Resting discharge and response to constant angular accelerations. J. Neurophysiol. 34: 635-684.

Goldberg, J. M., and C. Fernandez (1975) Vestibular mechanisms. Ann. Rev. Physiol. 37: 129-162.

Hudspeth, A. J. (1982) Extracellular current flow and the site of transduction by vertebrate hair cells. J. Neurosci. 2: 1-10.

Hudspeth, A. J., and D. P. Corey (1977) Sensitivity, polarity and conductance change in the response of vertebrate hair cells to controlled mechanical stimuli. Proc. Natn. Acad. Sci. U.S.A. 74: 2407-2411.

Hudspeth, A. J., and D. P. Corey (1978) Controlled bending of high-resistance glass microelectrodes. Am. J. Physiol. 234: C56-C57.

Landolt, J. P., and M. J. Correia (1980) Neurodynamic response analysis of anterior semicircular canal afferents in the pigeon. J. Neurophysiol. 43: 1746-1770.

Lewis, E. R., Baird, R. A., Leverenz, E. L., and H. Koyama (1982) Inner ear: dye injection reveals peripheral origins of specific sensitivities. Science 215: 1641-1643.

Lewis, E. R., and C. W. Li (1975) Hair cell types and distributions in the otolithic and auditory organs of the bullfrog. Brain Res. 83: 35-50.

Lewis, R. S., and A. J. Hudspeth (1983a) Frequency tuning and ionic conductances in hair cells of the bullfrog's sacculus. In Symposium on Hearing--Physiological Bases and Psychophysics, in press.

Lewis, R. S., and A. J. Hudspeth (1983b) Voltage- and ion-dependent conductances in vertebrate hair cells. Submitted for publication.

Loe, P. R., Tomko, D. L., and G. Werner (1973) The neural signal of angular head position in primary afferent vestibular nerve axons. J. Physiol. 230: 29-50.

Lowenstein, O., and T. D. M. Roberts (1951) The localization and analysis of the responses to vibration from the isolated elasmobranch labyrinth. A contribution to the evolution of hearing in vertebrates. J. Physiol. 114: 471-489.

Lowenstein, O., and T. D. M. Roberts (1950) The equilibrium function of the otolith organs of the Thornback Ray (Raja clavata). J. Physiol. 110: 392-415.

Macadar, O., Wolfe, G. E., O'Leary, D. P., and J. P. Segundo (1975) Response of the elasmobranch utricle to maintained spatial orientation, transitions and jitter. Exp. Brain Res. 22: 1-12.

Mayne, R. (1966) The function and operating principles of the otolith organs. II. The mechanics of the otolith organs. Goodyear Aerospace Corp. Report GERA-1112.

McNally, W. J., and J. Tait (1925) Ablation experiments on the labyrinth of the frog. J. Physiol. 75: 155-179.

Megela, A. L., and R. R. Capranica (1981) Response patterns to tone bursts in the peripheral auditory system of anurans. J. Neurophysiol. 46: 465-477.

Platt, C. (1977) Hair cell distribution and orientation in goldfish otolith organs. J. Comp. Neurol. 172: 283-298.

Precht, W., Llinas, R., and M. Clarke (1971) Physiological responses of frog vestibular fibers to horizontal angular acceleration. Exp. Brain Res. 13: 378-407.

Shotwell, S. L., Hudspeth, A. J., and R. Jacobs (1981) Directional sensitivity of individual vertebrate hair cells to controlled defection of their hair bundles. Ann. N. Y. Acad. Sci. 374: 1-10.

Smith, R. L. (1979) Adaptation, saturation, and physiological masking in single auditory-nerve fibers. J. Acoust. Soc. Am. 65: 166-178.

Trincker, D. (1962) The transformation of mechanical stimulus into nervous excitation by the labyrinthine receptors. Symp. Soc. Exp. Biol. 16: 289-316.

Vidal, J., Jeannerod, M., Lifschitz, W., Levitan, H., Rosenberg, J., and J. P. Segundo (1971) Static and dynamic properties of gravity-sensitive receptors in the cat vestibular system. Kybernetik 9: 205-215.

Vries, H. L. de (1950) The mechanics of the labyrinth otoliths. Acta oto-laryngol. 38: 262-273.

Young, L. R. (1969) The current status of vestibular system models. Automatica 5: 369-383.

Young, L. R., and J. L. Meiry (1968) A revised dynamic otolith model. NASA SP-152: 363-368.

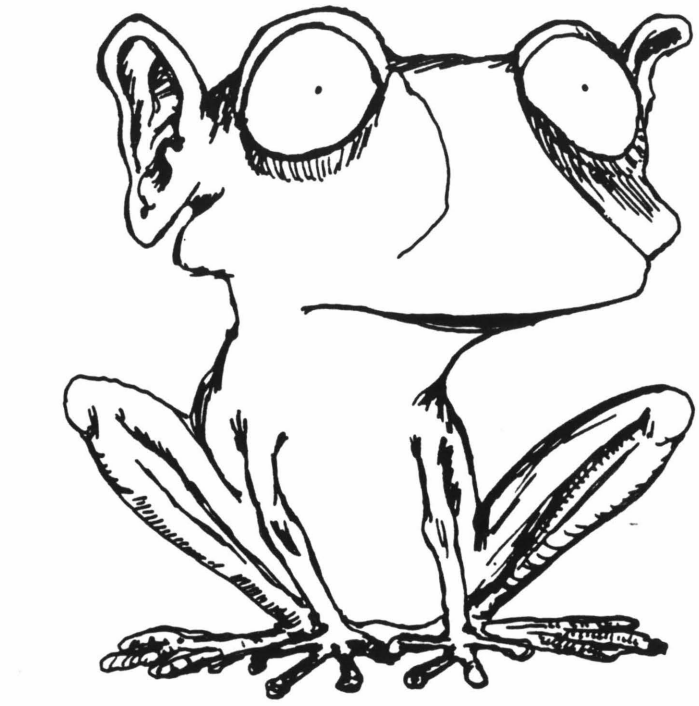


10 cm